

TI Designs

Automotive 1-kW 48-V BLDC Motor Drive Reference Design



Design Overview

This TI Design is a 3-Phase Brushless DC Motor Drive designed to operate in 48-V automotive applications. The board is designed to drive motors in the 1-kW range and can handle currents up to 30-A. The design includes analog circuits working in conjunction with a C2000 LaunchPad™ to spin a 3-Phase BLDC motor without the need for position feedback from Hall Effect sensors or quadrature encoder.

Design Resources

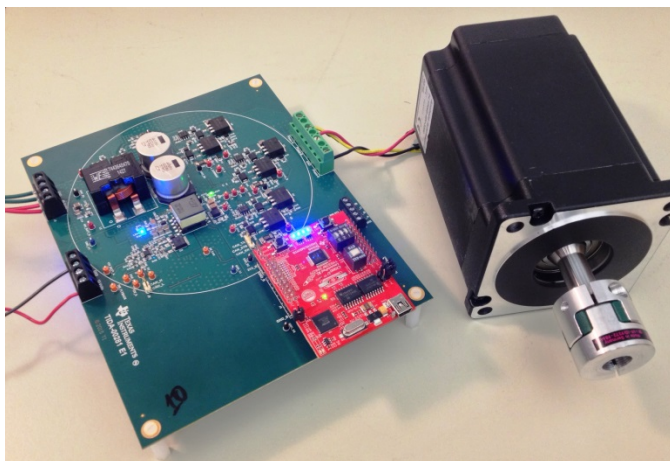
TIDA-00281	Design Folder
ccstudio	Tool Folder
MOTORWARE	Tool Folder
UCC27201A-Q1	Product Folder
TPS40210-Q1	Product Folder
TPS62152-Q1	Product Folder
LM5060-Q1	Product Folder
LM74610-Q1	Product Folder
HVDA553-Q1	Product Folder
OPA2365-Q1	Product Folder
LMT86-Q1	Product Folder
DRV5013-Q1	Product Folder

Design Features

- Speed Control of 3-Phase Brushless DC (BLDC) Motors With no Position Sensors Needed
- Phase Voltage and Current Sensing Scaled and Filtered Feedback for Control of 3-Phase Power
- Operates Over Wide Range of Voltages From 48-V Battery System
- Protection Against Overvoltage, Undervoltage, Overtemperature, Overcurrent, and Transient Faults
- Reverse Polarity Protection on 12-V Battery
- Isolated CAN Interface Connects to Automotive Networks on 12-V Battery System
- Critical Components Fit in a 5-inch Diameter Circular PCB
- Components Selected for Automotive Temperature and Quality
- Test Points Provide Easy Access to Key Motor Signals

Featured Applications

- Water Pump
- eTurbo
- Radiator Fan
- HVAC Blower
- Oil Pump



Contents

1	Key System Specifications.....	5
2	System Description	6
3	Block Diagram.....	7
3.1	Highlighted Products.....	7
3.1.1	UCC27201A-Q1.....	8
3.1.2	TPS40210-Q1	9
3.1.3	TPS62152-Q1	10
3.1.4	LM5060-Q1.....	11
3.1.5	LM74610-Q1	12
3.1.6	HVDA553-Q1	13
3.1.7	OPA365-Q1 and OPA2365-Q1	14
3.1.8	LMT86-Q1.....	15
4	System Design and Component Selection.....	15
4.1	PCB / Form Factor	15
4.2	Overall Considerations for Component Selection	16
4.3	12-V Input Protection	17
4.3.1	TVS Diodes.....	17
4.3.2	Reverse Battery Protection	18
4.3.3	12-V Input filtering.....	19
4.4	Power Supplies.....	19
4.4.1	Flyback Supply.....	20
4.4.2	3.3-V Step-down (Buck) Regulator.....	21
4.5	48-V Protection	22
4.5.1	48-V Filtering.....	23
4.5.2	48-V Switching.....	23
4.6	Motor Drive	24
4.7	Motor Control Feedback.....	25
4.7.1	Motor Current Feedback.....	25
4.7.2	Motor Voltage Feedback.....	26
4.7.3	Motor Drive Temperature Feedback	28
4.7.4	Motor Position Feedback (Hall effect sensors).....	28
4.8	LaunchPad	29
4.9	Isolated CAN	30

5	Getting Started Hardware	32
5.1	Install LaunchPad	32
5.2	Power Connection.....	33
5.2.1	12V Supply Connection	33
5.2.2	48V Supply Connection	34
5.3	Motor Connection.....	34
5.3.1	Motor Phase Connection	34
5.3.2	Motor Commutation Feedback Connection	35
6	Getting Started Software.....	35
6.1	Download and Install Code Composer Studio™.....	35
6.2	Download and Install Motorware™	35
6.3	Run the Example Software.....	36
7	Testing	41
7.1	Power Supplies.....	41
7.1.1	12V supply range of operation.....	41
7.1.2	Flyback efficiency	42
7.1.3	3.3V Buck Efficiency	43
7.1.4	48V switching.....	44
7.2	Motor Operation.....	44
7.2.1	Motor Operation Test Set-Up	44
7.2.2	Motor no-load speed and current versus 48V supply voltage.....	46
7.2.3	Motor speed versus constant load	47
7.3	Motor Current Feedback	50
7.4	Motor Phase Voltages and Feedback Signals.....	54
7.5	Response to Speed Ramp Commands	58
7.6	Response to Load Torque Steps.....	60
7.6.1	Load Torque Step Test Set-up.....	60
7.6.2	Load Torque Step Test Results	60
7.7	Dead-time Settings and PWM Signals.....	63
7.8	Motor Identification Algorithm Testing.....	66
7.9	CAN transceiver.....	67
7.9.1	CAN transceiver test set-up	67
7.9.2	CAN transmitter test results	68
7.9.3	CAN receiver test results.....	69
7.10	Thermal images.....	70
8	Design Files.....	72

8.1	Electrical Schematics.....	72
8.2	Bill of Materials	78
8.3	PCB Layout Recommendations	84
8.3.1	General Notes on Noise Sensitive Traces and Components	84
8.3.2	PCB Layering recommendations	85
8.3.3	General Power Supply Considerations.....	85
8.3.4	12V Protection Circuitry.....	87
8.3.5	Separation of 12V and 48V power	88
8.3.6	48V power protection	89
8.3.7	48V Power Routing	89
8.3.8	Motor Drive Circuit	91
8.3.9	Differential Signals	91
8.4	Layout Prints	92
8.5	Altium Project & Gerber files	97
9	Software Files	97
10	References	97
11	Terminology.....	98
12	About the Authors.....	98
13	Appendix.....	99
13.1	TINA Simulation Models.....	99

1 Key System Specifications

Table 1 System Specifications

PARAMETER	COMMENTS	MIN	TYP	MAX	UNIT		
$V_{IN(12V)}$	Input voltage	12-V battery voltage range (DC)		4.5	12	30	V
$I_{IN(12V)}$	Input current	9 V < $V_{IN(12V)}$ < 16 V				0.2	A
$V_{IN(12V)REV}$	Input voltage reverse	Reverse battery range		-15			V
$V_{IN(48V)}$	Input voltage	48-V battery voltage range (DC)		24	48	60	V
$I_{IN(48V)}$	Input current	Motor at full load				30	A
f_{PWM}	PWM frequency	Motor switching frequency		15		50	kHz
V_{PHASE}	Motor phase voltage					100	V
I_{PHASE}	Motor phase current					30	A
$I_{3.3V}$	3.3V supply current	to LaunchPad through connectors J5, J6, J9				250	mA
$Eff_{flyback}$	Flyback efficiency	12-V input to 12-V output, 100-mA output current		75%			
Eff_{buck}	Buck efficiency	12-V input to 3.3-V output, 300-mA output current		50%			
	CAN transmitter rate	Signaling rate with < 3% duty cycle distortion		500			kbps
	CAN receiver rate	Signaling rate with < 3% duty cycle distortion		500			kbps
	Motor current feedback gain				20		mV/A
	Motor current feedback bandwidth			1			MHz

2 System Description

TIDA-00281 is intended as a brushless DC motor drive design for automotive applications like electric pumps, cooling fan, turbo compressor, and so forth. The design goal was a motor drive design that could work with the emerging 48-V and 12-V battery systems in industry. The motor drive design uses the 48-V battery only to drive the motor and is isolated from the 12-V battery. All other devices on this design receive power from the 12-V battery. All analog components critical for the motor drive design are placed in a circular footprint (5-inch diameter) to replicate the typical motor drive board form factor.

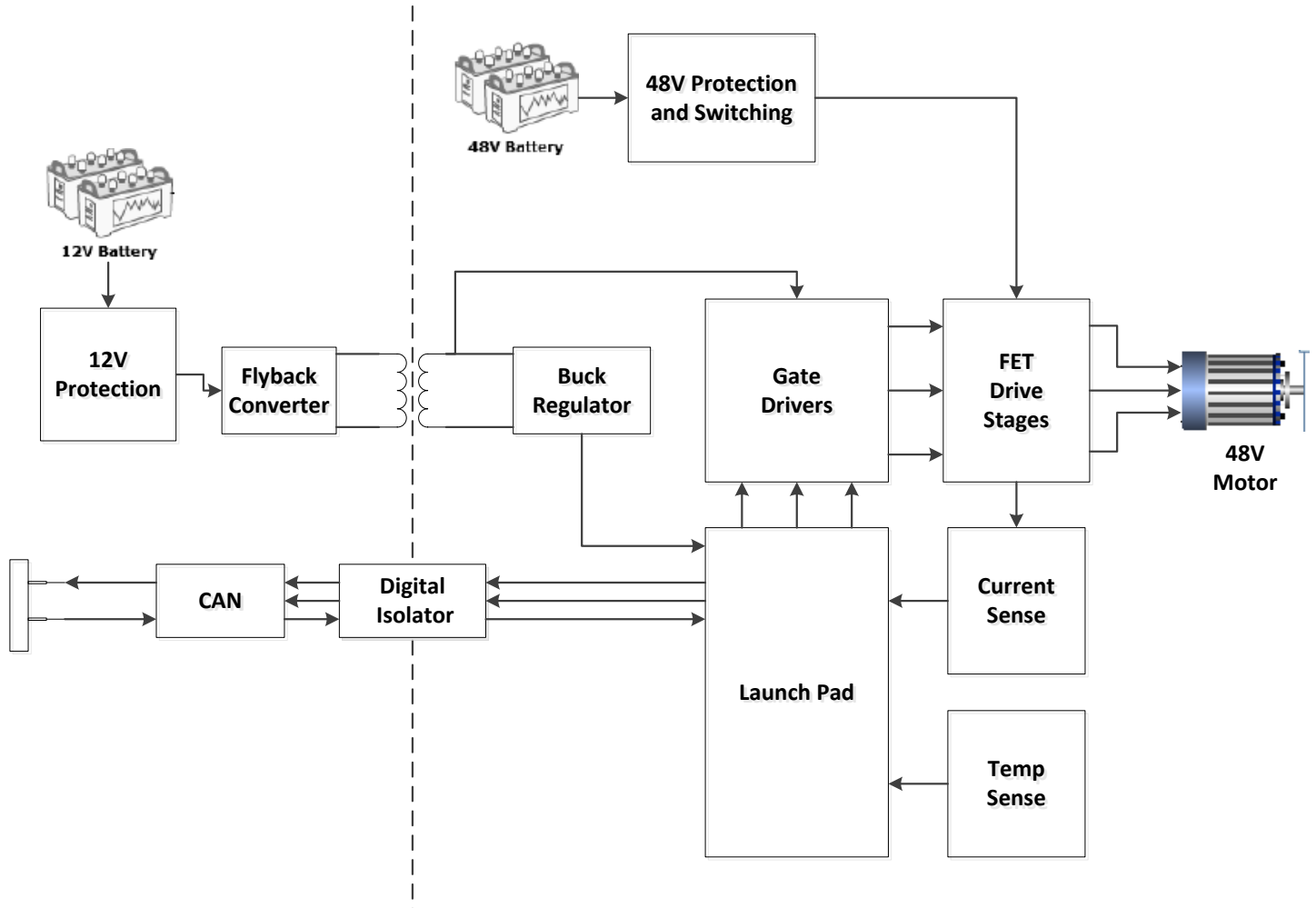


Figure 1: Overview of Application

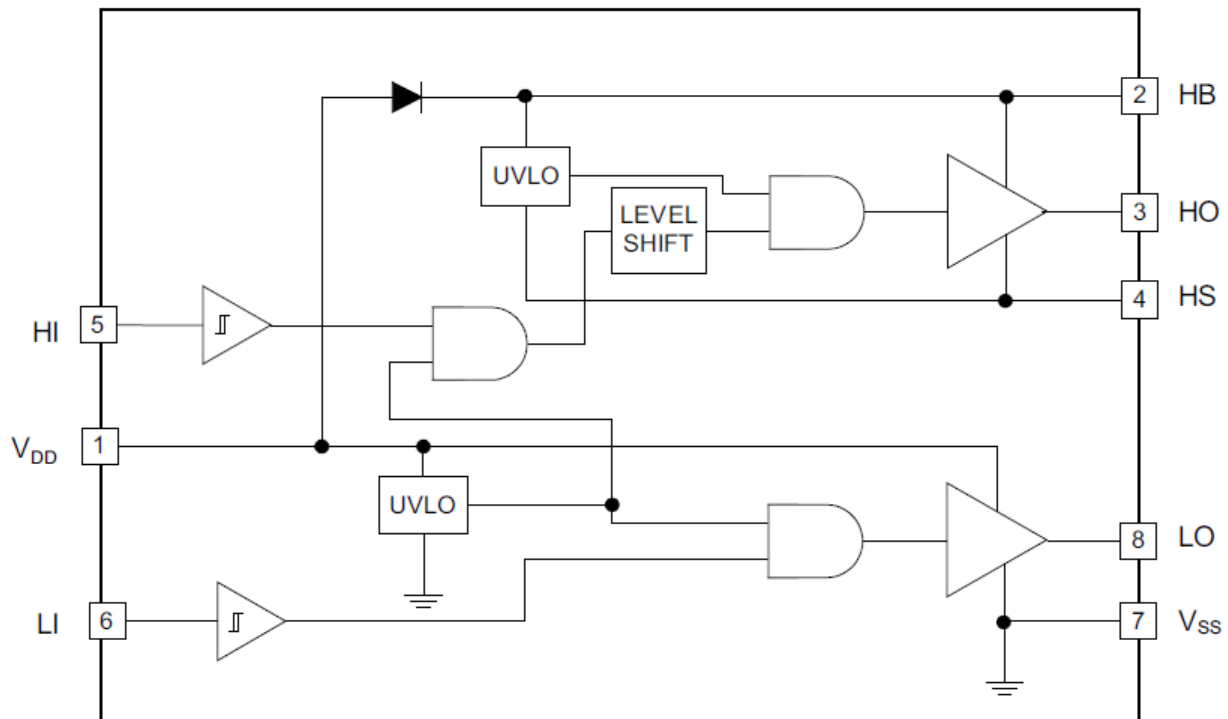


Figure 3 UCC27201A-Q1 120-V High-side and Low-side Gate Driver

- The device has a maximum boot voltage of 120 V, allowing operation with the 48-V supply under all conditions covered by the LV148 specification, including overvoltage conditions.
- The device drives two N-channel FETs in high-side and low side (half-bridge) configurations, so that one device can be used for each of the three BLDC motor phases.
- The device has 3-A sink and 3-A source output current capability, suitable for rapid charging and discharging of the gates of the drive stage FETs. The large output current means that the gate capacitance can be charged and discharged in a small fraction of the PWM switching time, allowing high efficiency.
- The device has rapid rise and fall time (8 ns rise, 7 ns fall with 1000-pF load) and precise (1 ns typical) delay matching between rise and fall times. This means that a small dead-time is possible between the alternating phases while still assuring no shoot-through current in the high-side and low-side FETs. This precision timing allows maximum use of the PWM duty cycle with high efficiency.
- An on-chip bootstrap diode eliminates the need for external discrete diodes.
- Undervoltage lockout is provided for both the high-side and the low-side drivers, thus forcing the outputs low if the drive voltage is below the specified threshold.
- The device is qualified to AEC-Q100 temperature grade 1, which allows for operation in automotive applications with a temperature range from -40°C to $+140^{\circ}\text{C}$.

3.1.2 TPS40210-Q1

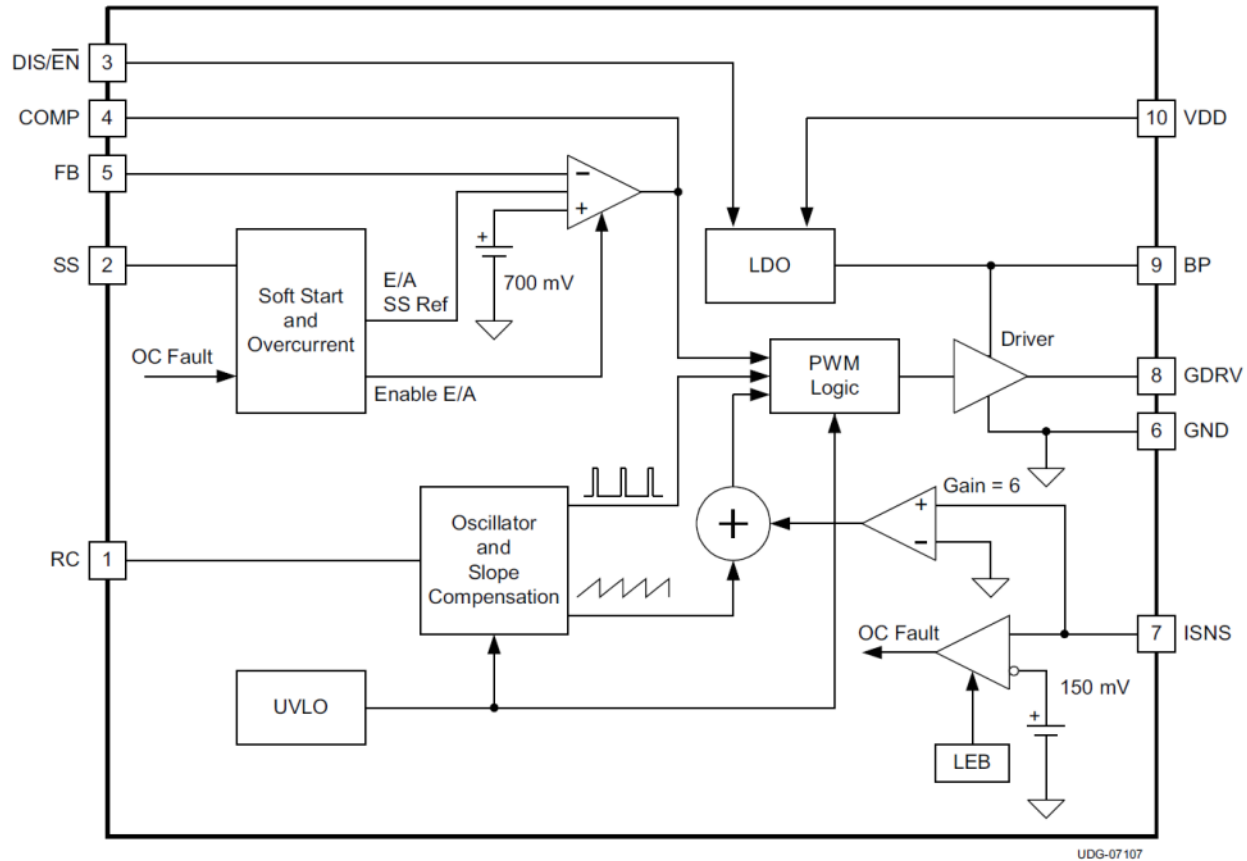


Figure 4: TPS40210-Q1 Current Mode Boost Controller

- This device has a wide input range (4.5 V to 52 V) which meets the requirements for the voltage range of the automotive 12-V battery system.
- The device is suitable for the flyback configuration with a grounded-source N-channel FET, which will be used to supply the isolated secondary for biasing the components on the 48-V side of the design.
- The device has a resistor-programmable oscillator frequency, which allows selection of the optimum switching frequency up to 1 MHz.
- The device incorporates current-mode control, which provides improved transient response and simplified loop compensation.
- The small package size (3 x 3 mm), internal slope compensation, and integrated low-side driver allow for a compact solution.
- The device is qualified to AEC-Q100 temperature grade 1, which allows for operation in automotive applications with a temperature range from -40°C to $+125^{\circ}\text{C}$.

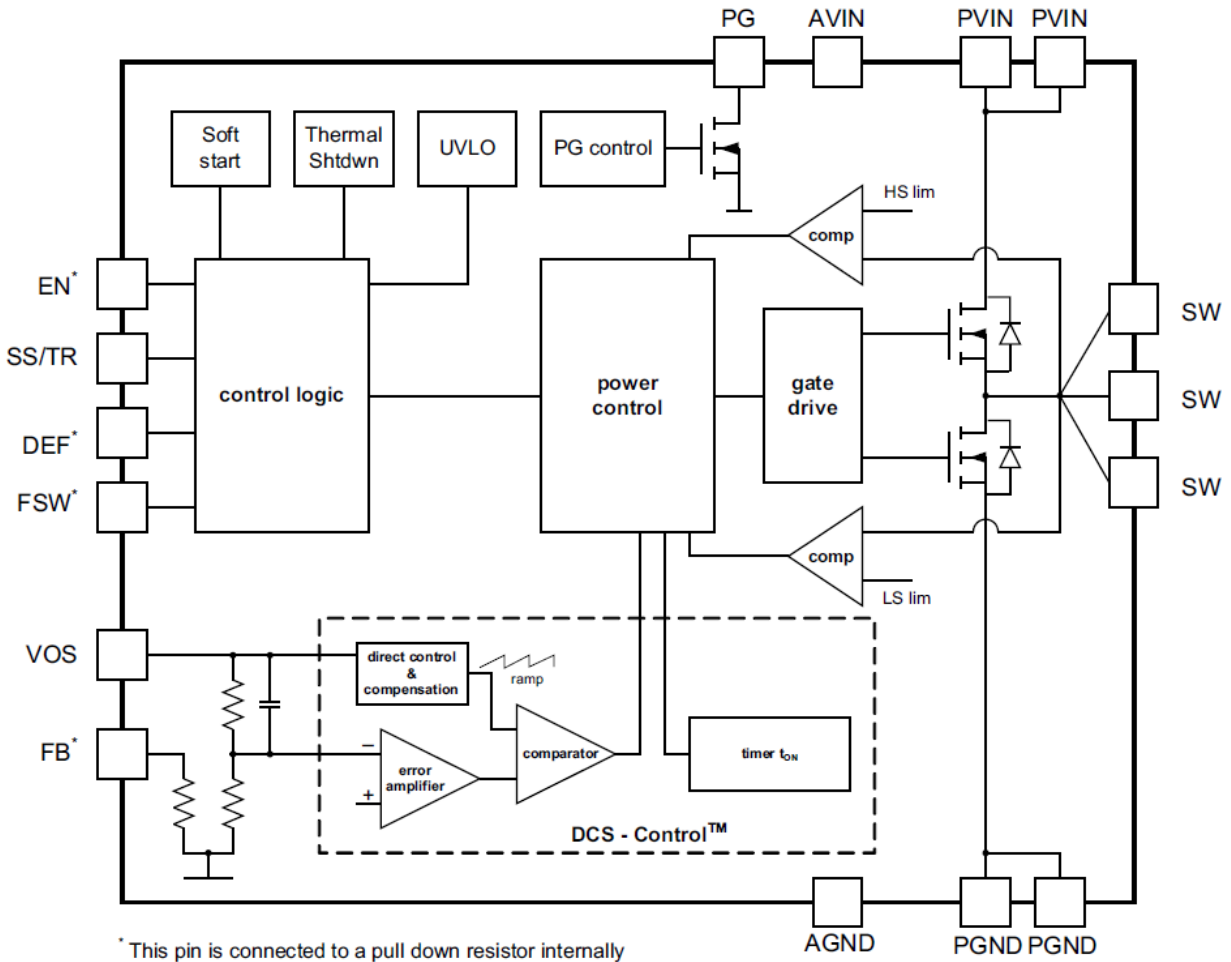


Figure 5: TPS62152-Q1 Automotive 3.3-V Output Step-Down Converter

- The device has an input voltage range from 4 V to 17 V, allowing significant variation of the secondary 12-V supply coming from the flyback controller.
- The device has a high switching frequency of 2.5 MHz (typical) which allows for the use of small inductors and provides fast transient response, as well as high output-voltage accuracy by use of the DCS-Control topology. This switching frequency is also well above the AM radio band, thus reducing EMI concerns.
- The device has an internal current limit of 1 A, which protects against high-current faults, while providing the necessary 3.3-V supply of about 250 mA (maximum) for the LaunchPad and ancillary control circuits.
- The device is qualified to AEC-Q100 temperature grade 1, which allows for operation in automotive applications with a temperature range from -40°C to $+125^{\circ}\text{C}$.

3.1.4 LM5060-Q1

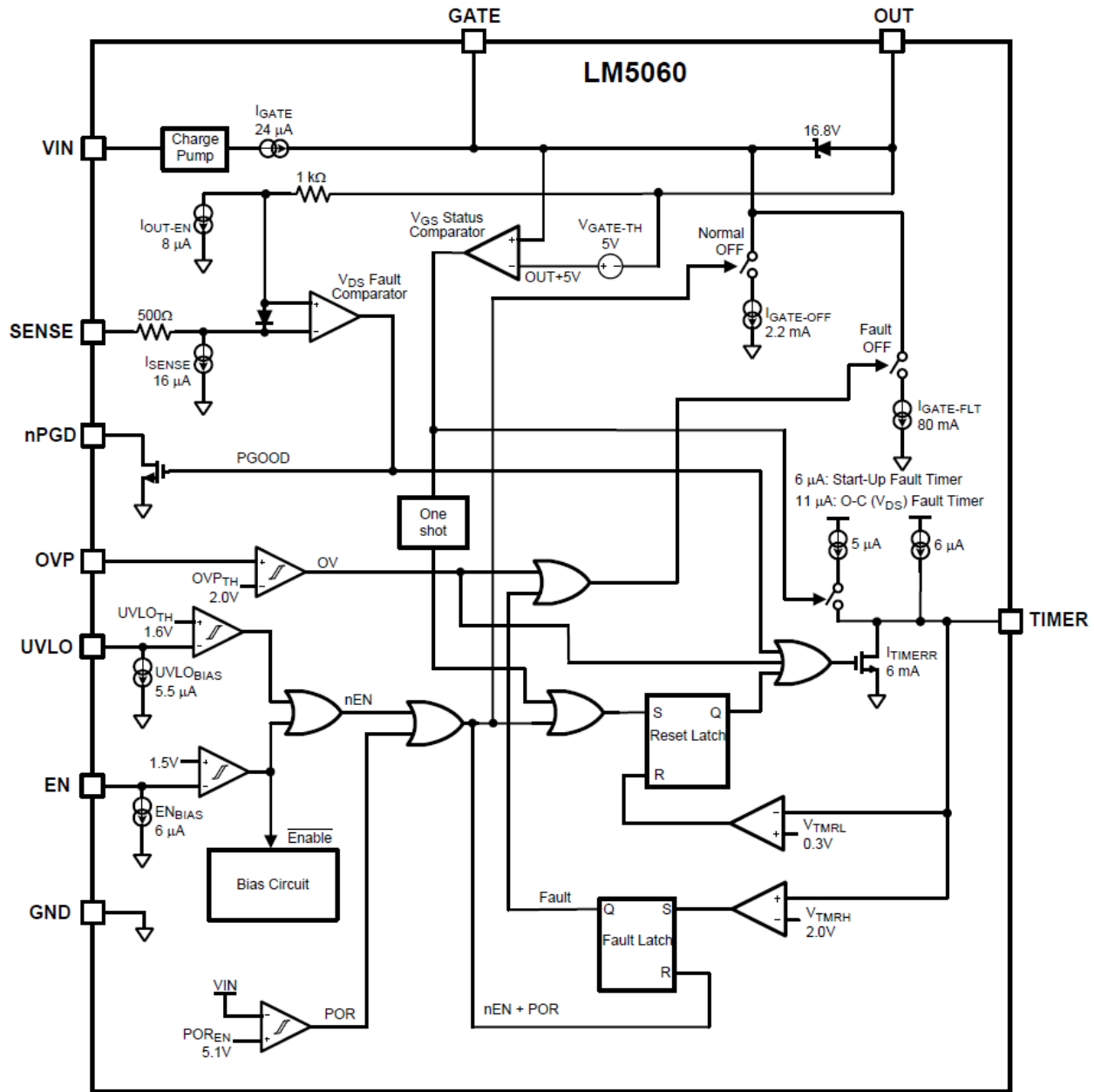


Figure 6: LM5060-Q1 High-Side Protection Controller with Low Quiescent Current

- The device has a wide operating range (5.5 V to 65 V) and high absolute maximum rating (75 V) is suitable for 48-V supply with tolerance variation.
- The device has an adjustable undervoltage lockout (UVLO) which inhibits operation when 48-V supply is too low.
- The device is qualified to AEC-Q100 temperature grade 1, which allows for operation in automotive applications with a temperature range from -40°C to $+125^{\circ}\text{C}$.

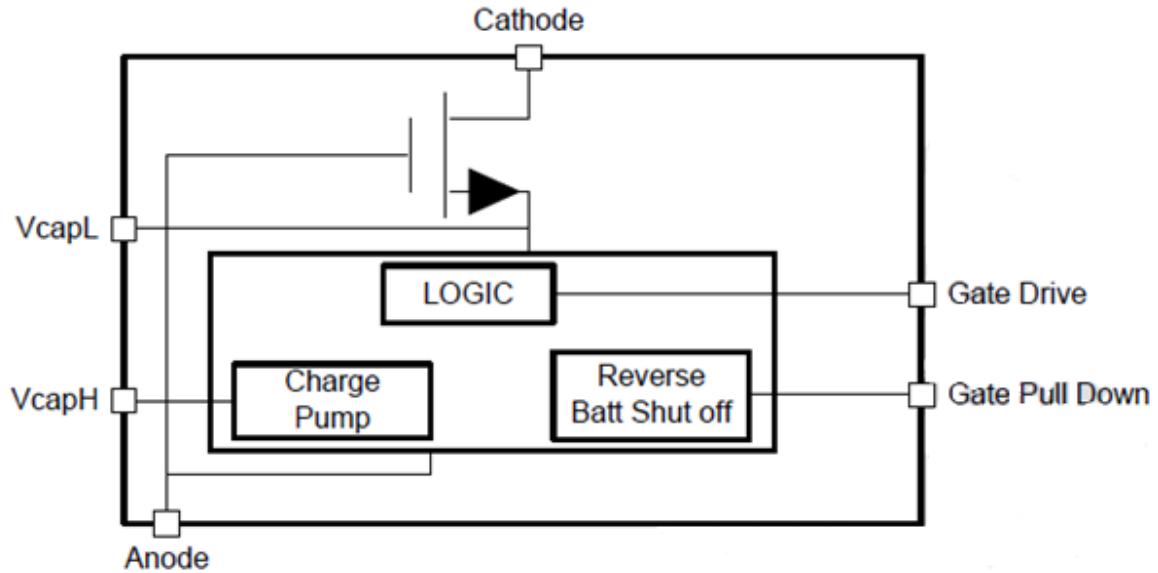


Figure 7: LM74610 Smart Diode for Reverse Battery Protection

- Satisfies the requirement for reverse-battery protection for automotive (12-V) electrical subsystems
- Controls an external NFET in series with the battery supply input to act as an ideal diode, reducing voltage drop and power loss as opposed to a discrete diode solution
- Quickly turns off the external FET when a reverse-battery condition is detected, isolating and protecting downstream circuitry
- Has no ground reference, leading to virtually zero I_Q operation. This helps the subsystem draw less standby current from the battery. Many OEMs have very small I_Q budgets.
- Because the voltage drop across the FET is negligible; this provides more input voltage headroom, and thus operation at low battery input voltages.
- The device is qualified to AEC-Q100 temperature grade 1, which allows for operation in automotive applications with a temperature range from -40°C to $+125^{\circ}\text{C}$.

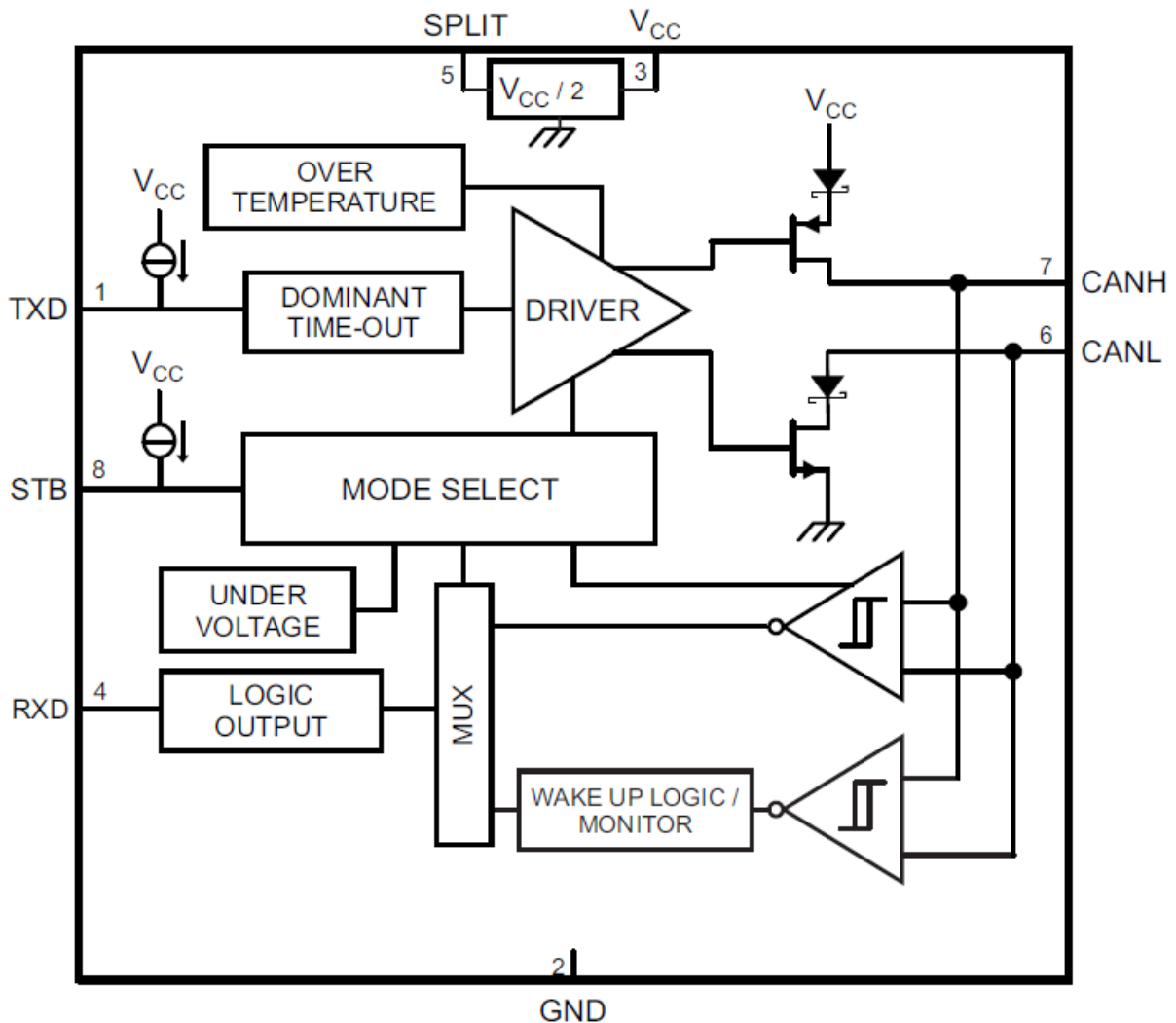


Figure 8: HVDA553-Q1 5-V CAN Transceiver

- This device meets the requirements of ISO 11898-2 and ISO 11898-5 for full compatibility with high-speed CAN networks.
- The device includes a SPLIT pin which provides a stable half-supply output voltage to stabilize the common-mode voltage of the bus for improved electromagnetic emissions.
- The device can be put into a low-power standby mode with very low standby current. Any valid CAN bus activity can be detected by the RXD wake-up request, allowing activation of remote nodes by the master node through CAN commands.
- The device is qualified to AEC-Q100 temperature grade 1, which allows for operation in automotive applications with a temperature range from -40°C to $+125^{\circ}\text{C}$.

3.1.7 OPA365-Q1 and OPA2365-Q1

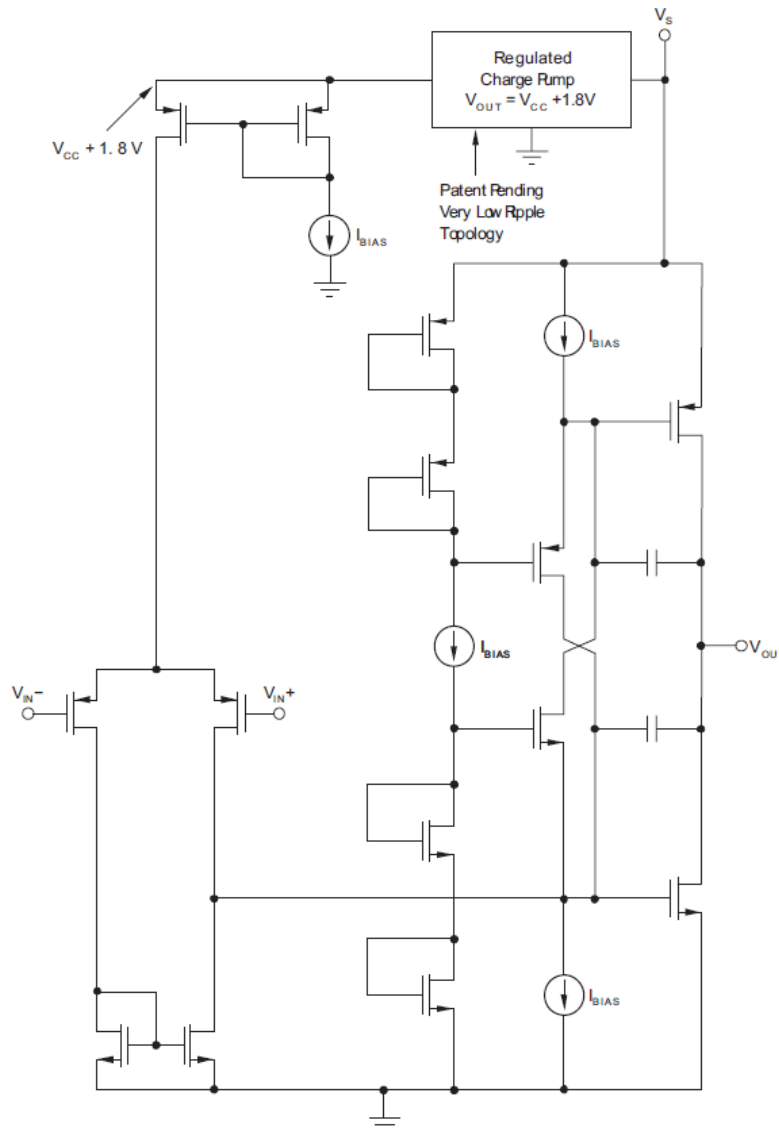


Figure 9: Simplified Schematic of OPA365-Q1

- The OPA365-Q1 and OPA2365-Q1 are similar; however, the OPA365-Q1 is a single op amp, and the OPA2365-Q1 consists of two separate op amps in the same package.
- These devices have gain-bandwidth (GBW) product of 50 MHz, which is suitable for amplification of the current sense signals.
- The devices have rail-to-rail operation, which allows more usable range for the analog-to-digital converters (ADCs), giving better resolution of motor current measurements.
- The devices have low input offset voltage (100 μ V), which gives the current sense measurement low error.
- The device is qualified to AEC-Q100 temperature grade 1, which allows for operation in automotive applications with a temperature range from -40°C to $+125^{\circ}\text{C}$.

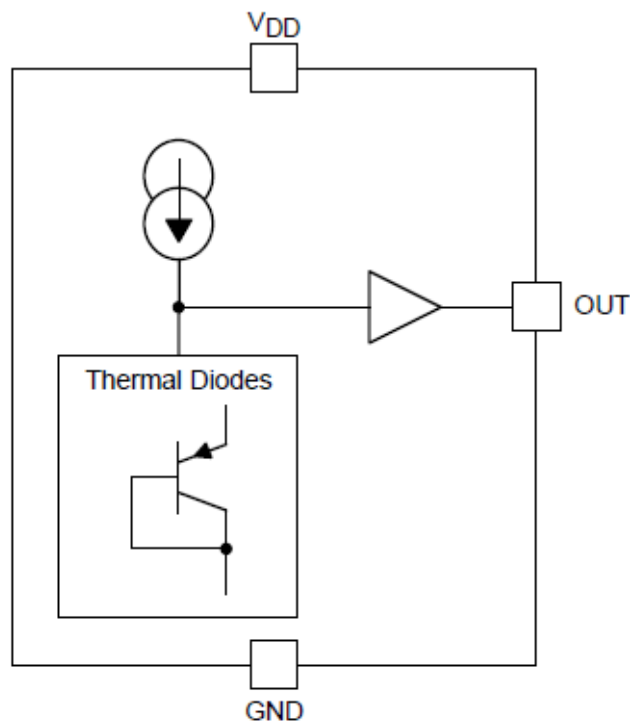


Figure 10: LMT86-Q1 Analog Temperature Sensors with Class-AB Output

- This device has a very accurate ($\pm 0.25^\circ\text{C}$) scale factor, which allows precise measurements of the board temperature.
- The devices are available in small SC70 package (2-mm x 2-mm) which facilitates placement close to the motor phase driver stages, thus reducing thermal time delay.
- A class-AB output structure gives the device strong output source and sink current capability that is well suited to an ADC sample-and-hold input.
- The device is qualified to AEC-Q100 temperature grade 0, which allows for operation in automotive applications with a temperature range from -50°C to $+150^\circ\text{C}$.

4 System Design and Component Selection

The following sections describe the considerations behind the design of each part of the system.

4.1 PCB / Form Factor

The goals for the board geometry were:

- Compatible with LaunchPad microcontroller development platform
- Mechanically stable for bench test
- Easy access to electrical test points throughout the design
- Sufficient size for high current and thermal dissipation

The layout concept locates the circuitry actively driving the motor within a circular area in the center of the board. Connectors are outside the reference circle, and were selected for ease of use rather than suitability for a production

design. The LaunchPad microcontroller board is mounted on connectors outside the circle, and lets designers use a variety of specific microcontrollers, depending on the requirements of the application.

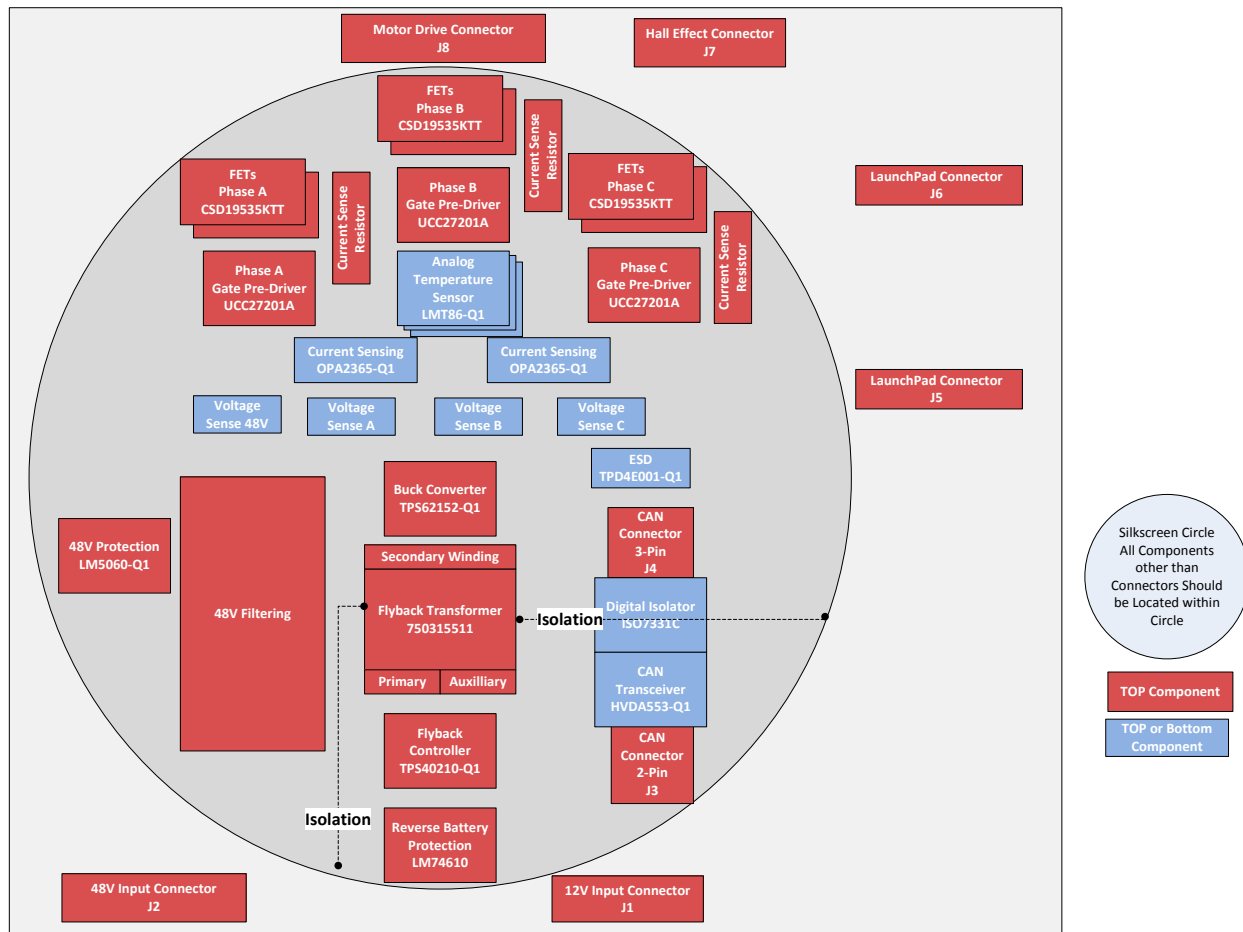


Figure 11: TIDA-00281 Board Simplified Floor Plan

4.2 Overall Considerations for Component Selection

In general, components were selected based on the performance requirements of the expected applications. Where practical, components with automotive ratings were selected. For active components, the components selected are AEC-Q100 qualified to either temperature grade 0 or temperature grade 1.

Capacitors are generally X7R grade (–55°C to +125°C) or higher, with size and value selected for the expected extremes of operation conditions. The voltage rating of the capacitors should be greater than the maximum voltage they could experience, and 2x the typical operating voltage to avoid DC bias effects. The amount of output capacitance used depends on output ripple and transient response requirements, and many equations and tools are available online to help estimate these values.

Consider the possible maximum voltage that could be experienced by the components. Capacitors should be derated by a minimum of 25% due to the drop in capacitance at 100% rated DC voltage of X7R and COG/NP0 ceramic capacitors (that is, Max voltage – 40 V; Capacitor voltage rating = 40V * 1.25 = 50V). The derating also helps protect components from unexpected voltage spikes in the system. During the design process the amount of BOM line items was considered. Therefore, capacitor voltage ratings may have been increased above the minimum desired rating. As an example, if

there was one 1- μ F, 25-V capacitor but nine 1- μ F, 50-V capacitors, then the lone 25-V capacitor was modified to become a 50-V capacitor and the schematic contains a note indicating that the voltage rating was increased for BOM simplicity.

Supplies in this solution were designed for a $\pm 2.5\%$ (5%) total transient response. Low-ESR ceramic capacitors were used exclusively to reduce ripple. For internally compensated supplies, see device-specific data sheets, because they may have limitations on acceptable LC output filter values.

For improved accuracy, all feedback resistor dividers should use components with 1% or better tolerance. Resistance tolerance in this design was selected to reduce the total amount of BOM line items. In the design considerations, it is noted where 5% or 10% precision resistors can be used to reduce the cost of a specific individual resistor. Using less precise resistors for cost reasons should be weighed against reducing the amount of BOM line items and ordering in higher volumes to reduce total BOM cost.

Zero-Ohm (0- Ω) resistors are used at the input and output of several of the circuit sections for testing purposes only, and could be removed, if needed, in a production board design.

4.3 12-V Input Protection

The 12-V supply can experience several excursions from the nominal 12-V value. This design includes protection against such typical hazards as transient overvoltage spikes, reverse battery conditions, and high-frequency electrical noise.

4.3.1 TVS Diodes

Transient voltage suppression (TVS) diodes are required on the supply input of the system to protect against positive and negative going transients. The transients are detailed in ISO 7637-2:2004, pulses 1 and 2a. Many systems in a vehicle can be disabled during these transients until the condition passes, but other applications have the requirement to continue operation. For this reason, this design uses TVS diodes to shunt the transients instead of using an overvoltage shutdown scheme for the 12-V supply.

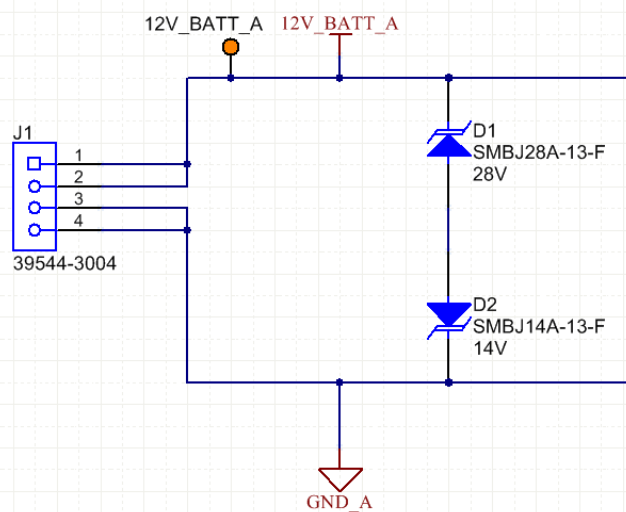


Figure 12: Input Transient Protection

The diode breakdown voltages should be chosen such that transients are clamped at voltages which will protect the rest of the system, but not conduct during normal operational input voltages. The positive clamping device should clamp above double-battery (jump-start) and clamped load dump voltages, but lower than the maximum operating voltage of

the downstream devices. This means starting to clamp around 32 V and having a maximum clamping voltage of approximately 45 V.

The reverse clamping device should clamp all negative voltages greater than the battery voltage so that the device does not short out during a reverse-battery condition.

Due to the energy of the pulses, SMB size TVS diodes with 600-W instantaneous peak power ratings are the minimum required.

The SMBJ28A-13F is specified for peak current of 13 A, with breakdown from 31.1 V to 45.4 V. The SMBJ14A-13F is specified for peak current of 25 A, with breakdown from 15.6 V to 23.2 V. Both diodes have an operating temperature range of -55 to $+150^{\circ}\text{C}$, with peak power of 600 W.

4.3.2 Reverse Battery Protection

Reverse battery protection is required in nearly every electronic subsystem of a vehicle, both by OEM standards, as well as ISO 16750-2, an international standard pertaining to supply quality.

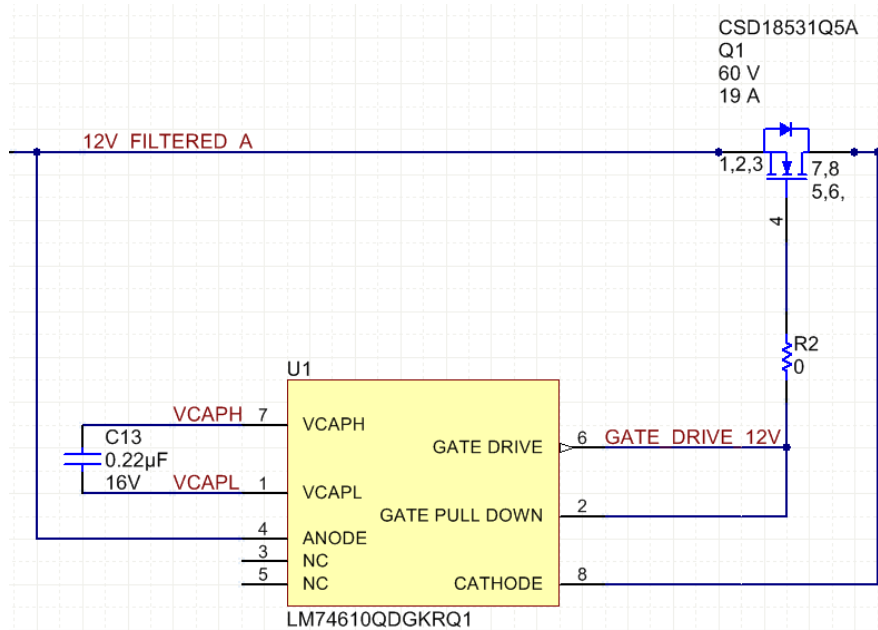


Figure 13: Reverse Battery Input Protection

Rather than use the traditional diode rectifier solution for reverse battery protection, this implementation uses an N-channel MOSFET driven by the LM74610-Q1 Smart Diode Controller. The power dissipation of the traditional diode can be significant due to the typically 600-mV to 700-mV forward drop ($P = I \cdot V$), whereas using the LM74610 solution results only in the loss due to the $R_{DS(ON)}$ of the FET; this loss can be significantly lower, resulting in greater efficiency and less thermal dissipation required.

The LM74610 team provides recommendations, as well as a tool, which can be used to help select a FET for any specific application. Here are the important considerations:

- Ensure that the continuous current rating is sufficient for the application.
- The V_{GS} threshold should be not more than 2.5 V.
- V_{SD} should be at least 0.48 V @ 2 A and 125°C .

For this design, the FET must be rated at least as high as the expected input voltage; a 45-V FET would be acceptable, but a 60-V FET such as the CSD18531 provides additional voltage headroom.

4.3.3 12-V Input filtering

Another consideration for the front-end protection is the input filtering. This design uses a set of capacitors and inductor to form a “pi” filter to remove unwanted AC components on the 12-V supply line. Due to the bidirectional format of the pi filter, incoming transients are blocked from entering the board, and any switching noise or clock noise generated on the board is blocked from propagating into the rest of the vehicle.

Due to flexion of the printed-circuit board (PCB), a ceramic capacitor can mechanically fail in an electrically shorted condition. If this happens to an input capacitor connected directly to the battery, this could cause a hard short at the battery terminals. To avoid this, typically two ceramic capacitors are used in series; if one fails, there is still another to avoid a short. The capacitors should also be aligned at 90 degrees with respect to each other on the layout; this gives a good chance that a flexion in one direction may only affect the capacitor aligned in that direction, but not the capacitor in the other direction.

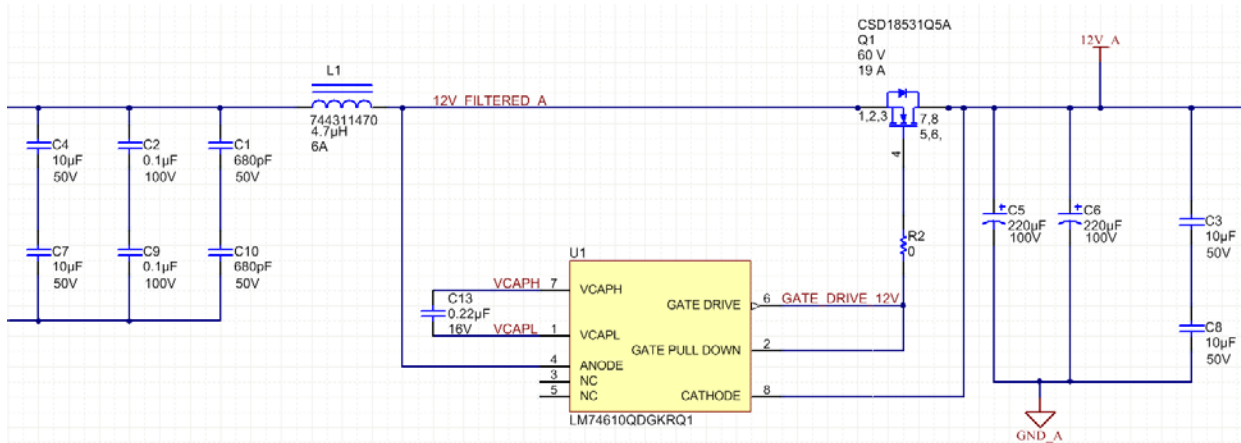


Figure 14 Filtering on the 12-V Supply

In general, the optimal amount of capacitance on the output side of the 12-V filtering may depend on the specifics of the application, including the current and electromagnetic compatibility (EMC) considerations. In this design, two large electrolytic capacitors (C5 and C6) are available for installation; the selection of one or both capacitors gives designers flexibility. In the testing which follows, C5 was installed and C6 was not installed.

4.4 Power Supplies

The motor drive stage switches power from the 48-V supply. All other bias supplies are derived from the 12-V automotive battery system. This scheme allows activation of the microcontroller and control circuits even when the 48-V supply is not available, and allows the microcontroller to actively control whether the 48-V supply is applied to the drive stage.

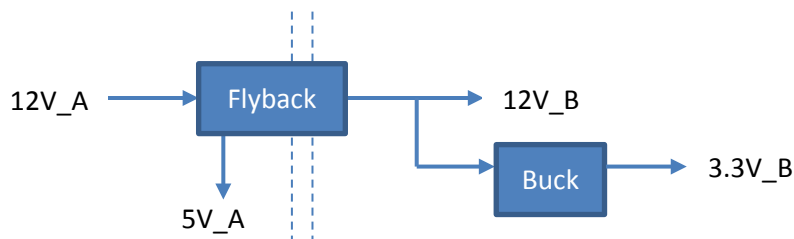


Figure 15 Power Supply Scheme

4.4.1 Flyback Supply

This design uses the TPS40210-Q1 to control the flyback regulator. The 12-V supply from the conventional automotive 12-V battery supplies the power, which is considered the primary-side supply. A 5-V winding on the primary side supplies the CAN transceiver and the primary side of the digital isolators, and this 5-V winding is regulated directly by the TPS40210-Q1. The secondary winding creates a 12-V nominal supply, which is discussed in the following paragraphs.

The switching frequency is set by C63, C64, and R40 to a nominal 450-kHz rate, which is below the lowest frequency in the AM radio band.

- Supply voltage nominal: 12 V
- Supply voltage range: 5 V to 30 V
- Operating current: 2.5 mA
- Device power consumption: 30 mW

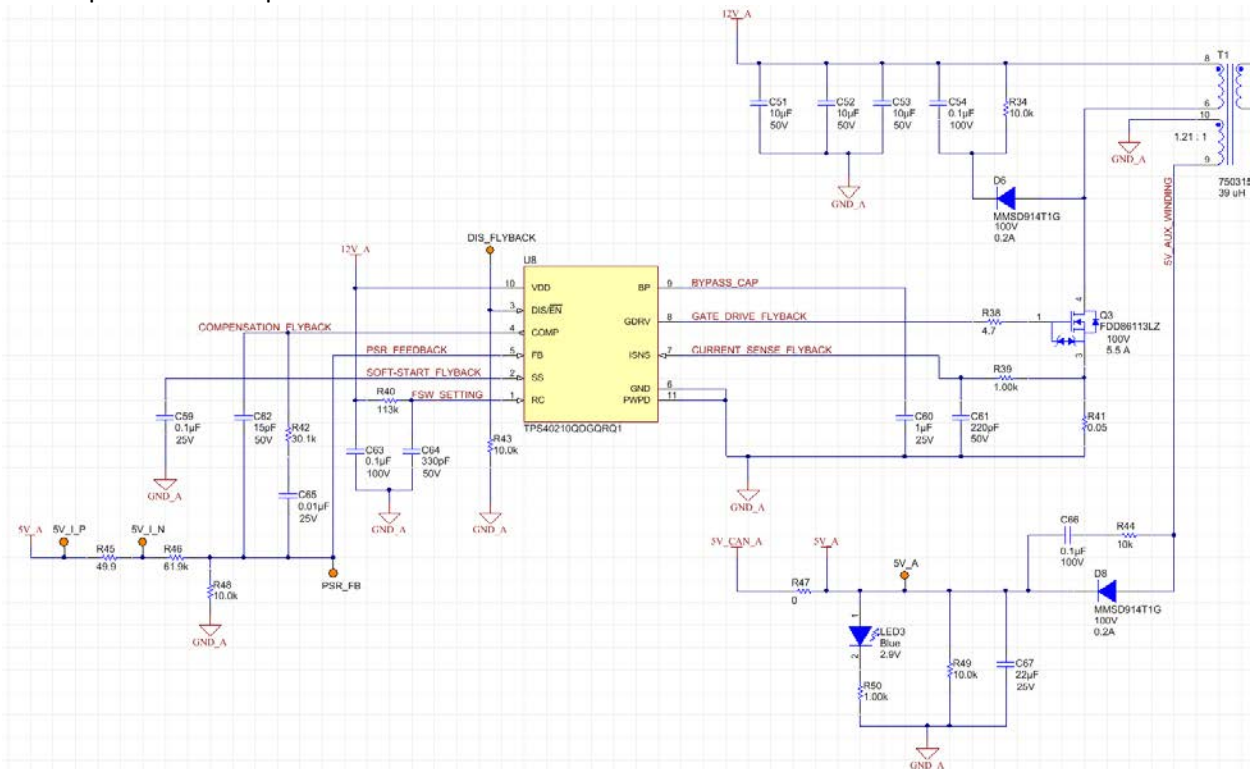


Figure 16: Primary Side of the Flyback Regulator

DIS/EN signal on pin 3 has an internal 1-M Ω pull-down resistor to GND. Leaving the pin open, or connected to ground, will enable the device. In this design a 10-k Ω resistor (R43) is used with a test point (DIS_FLYBACK) so that the device can be set to shutdown mode by overriding the 1-M Ω pull-down with an external signal.

R34 dissipates power linked to leakage energy and C54 ensures low-voltage ripple. C54 could be a 50-V capacitor but a 100-V capacitor was chosen to reduce the amount of BOM line items. Similarly, C63 can be a 50-V capacitor but a 100-V capacitor was chosen to reduce the amount of BOM line items.

The 0- Ω resistor R47 is available to provide a disconnect between the 5 V generated by the flyback and the rest of the system that is powered by the 5-V flyback auxiliary winding. This will not disconnect the 5 V from the feedback for the flyback controller. This allows unloaded testing if required. Specific load simulations can be accomplished by not populating R47 and by populating R49 with the appropriate load resistance.

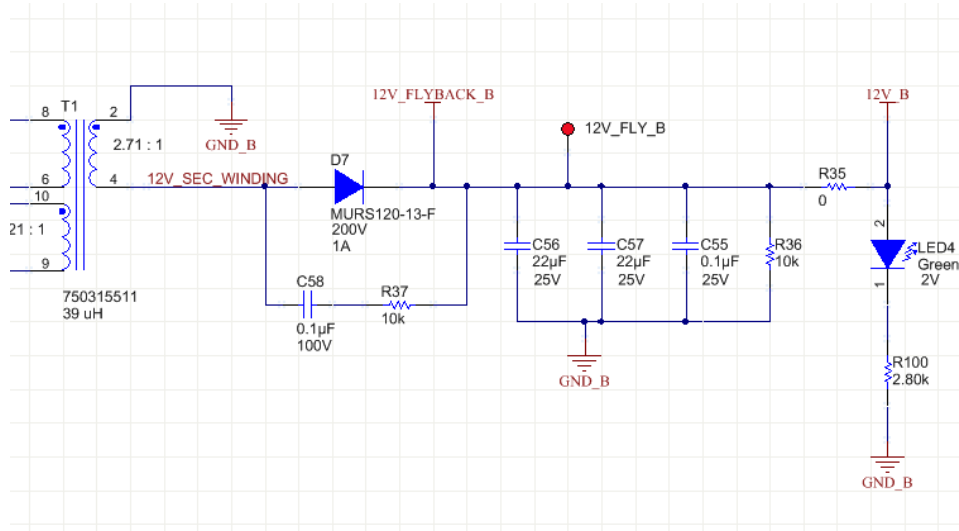


Figure 17 Secondary Side of the Flyback Regulator

The secondary 12-V supply (12V_B) is not directly regulated by the TPS40210-Q1, but is indirectly regulated through the coupling to the 5-V primary winding (5V_A). Precise regulation is not needed for the 12V_B supply, because the UCC27201A gate drivers tolerate a wide input voltage for their bias supply, and because the signal conditioning components in the feedback paths (which do require tight regulation) are supplied by a 3.3-V supply from the buck regulator discussed in the next section.

The RC (C58, R37) snubber across D7 can be used to dampen parasitic oscillations. High-frequency ringing can be due to parasitic inductance of the transformer and parasitic capacitance of the diode.

4.4.2 3.3-V Step-down (Buck) Regulator

A bias supply is needed for the signal conditioning circuits which create the feedback signals for the motor voltage, current, and temperature. These signals go to the microcontroller, which has a 3.3-V supply, and thus ADC input range from 0 V to 3.3 V. Thus, a 3.3-V supply is created from the 12 Vdc supplied by the secondary supply of the flyback converter.

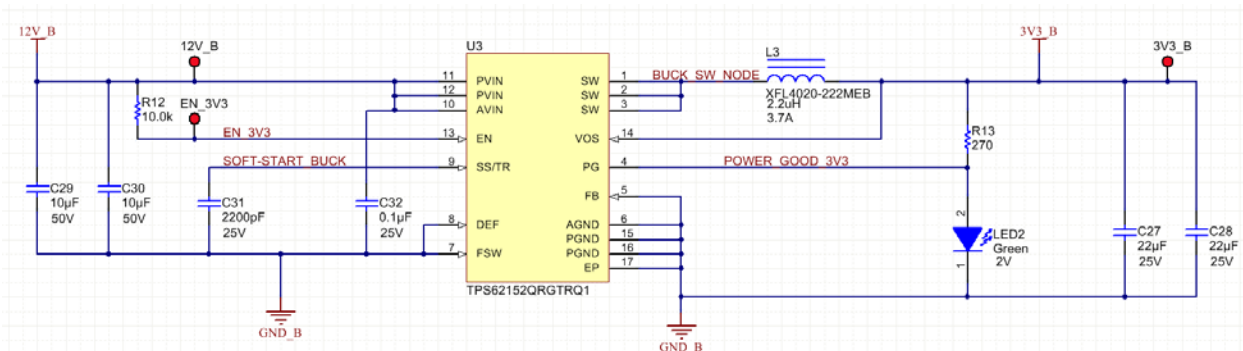


Figure 18: 12-V to 3.3-V Buck Regulator

The TPS62152-Q1 provides a small and efficient solution, with a minimum of external components. The TPS62152-Q1 operates at a switching frequency of 2.5 MHz, well above the AM band, when the FSW pin is tied to ground. The maximum input voltage of 17 V provides sufficient headroom above the 12-V nominal value to allow significant variation from the flyback converter. The 1 A maximum output current is sufficient for the expected load of LaunchPad plus op amps and temperature sensors.

- Input voltage: 12 V nominal (maximum is 17 V)
- Quiescent current, Max: 25 μ A
- Quiescent current, Typ: 17 μ A
- Device power, Max: 0.3 mW
- Device power, Typ: 0.204 mW

One 10 μ F input capacitor is recommended. However, additional capacitance can be added to reduce input current ripple further. Thus, C29 and C30 are installed in the design, but can be altered if a reduced size or cost solution is to be investigated.

Similarly, TI recommends using one output capacitor, but an additional can be added to help with load transients. Thus, C27 and C28 are installed in the design, and provide flexibility for designers to evaluate possible reduced solutions.

Only 25-V capacitors are needed but 50-V capacitors were chosen to reduce the amount of BOM line items. R12 does not need to be a 1% resistor, but it was chosen to reduce BOM line items.

The output voltage is fixed at 3.3 V, therefore FB pin is tied to GND plane to improve thermal performance.

To disable the buck converter, remove R12 and deliver an external signal through EN_3V3. To re-enable the buck, connect from test point 12V_B to test point EN_3V3.

A macro model of the TPS62152 is available for circuit performance simulation using Texas Instruments' TINA or other SPICE-based circuit analysis tools. Figure 19 shows a transient analysis of the initial turn-on of the 12-V to 3.3-V buck circuit, with a 33- Ω load, giving a final load current of 100 mA. The start-up transients have stabilized after less than 2 milliseconds.

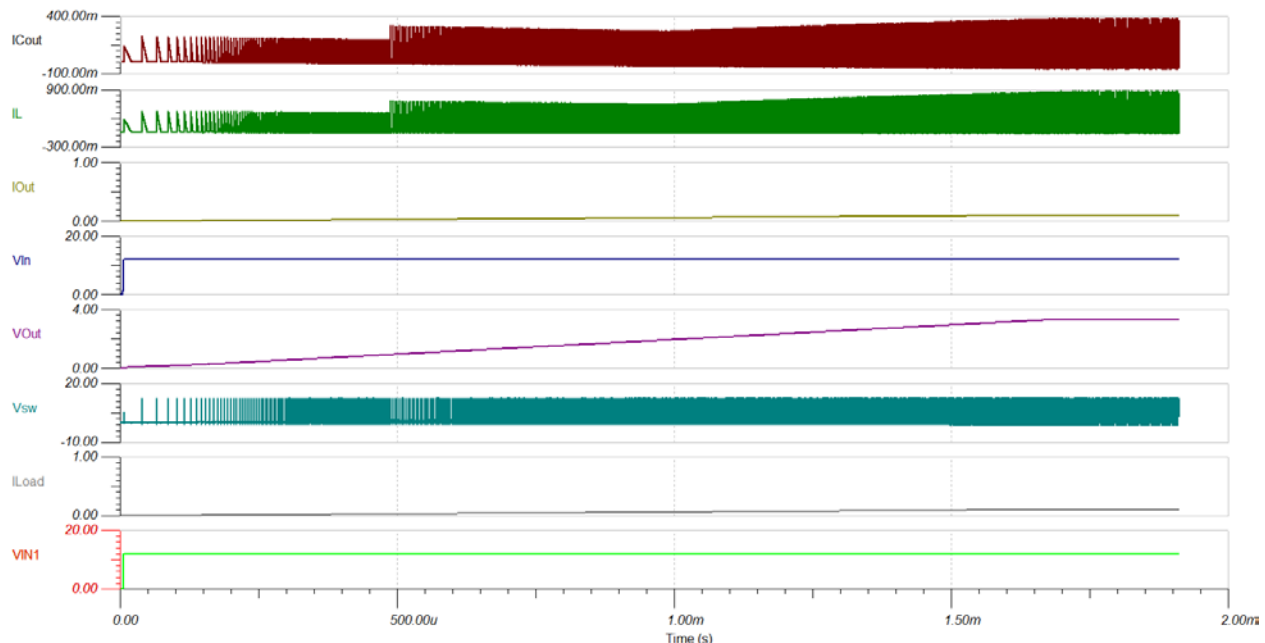


Figure 19 TINA Simulation Results for 3.3-V Buck Circuit

4.5 48-V Protection

The 48-V supply will typically originate from a 48-V battery with an associated charging system, such as a belt-driven or integrated starter/generator. Because it is not expected to have road-side connections to another 48-V vehicle (similar to jumper cables for 12-V systems), reverse battery protection is not anticipated as a critical requirement for the 48-V

electrical system. However, there is still a need for filtering out high-frequency noise, and for maintaining intelligent control of the 48-V supply, especially in the event of overvoltage, undervoltage, or overcurrent conditions.

4.5.1 48-V Filtering

Filtering on the 48-V supply functions to reduce externally generated electrical noise from entering the motor drive circuit, and it also prevents internally generated transients, such as switching noise, from propagating to the rest of the vehicle.

The pi filter arrangement shown in Figure 20 blocks the unwanted high frequencies while passing the desired steady-state current. Due to the high current levels anticipated, these components (especially L2, C16, and C17) are physically large, as discussed in the section on board layout.

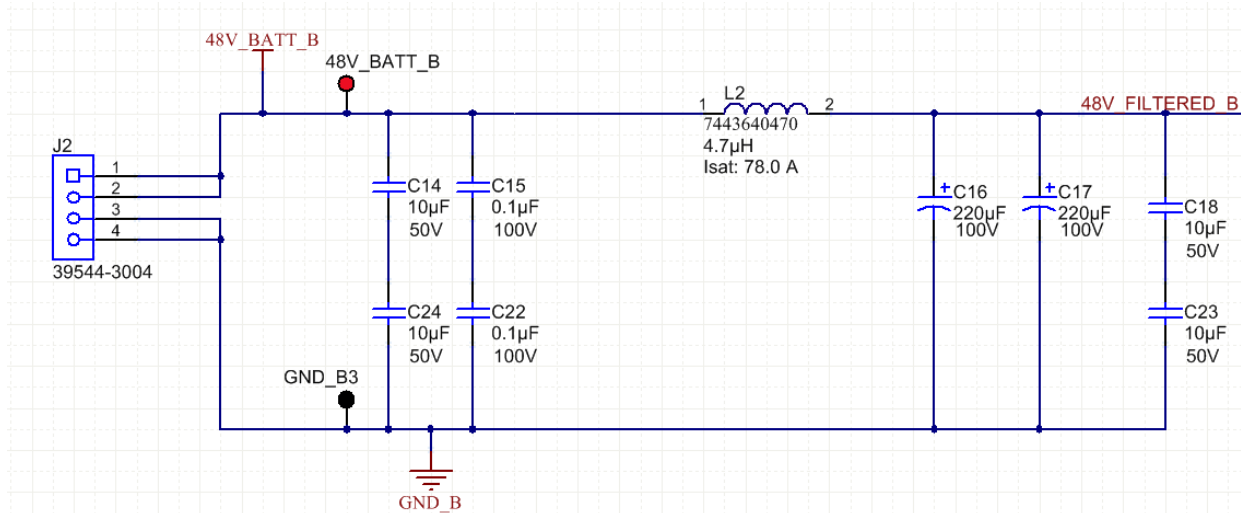


Figure 20 48-V Supply Filtering

Both the 48V_BATT_B and 48V_FILTERED_B rails must withstand a maximum voltage of 70 V (per LV148). Therefore, the summation of capacitors in series could equal 87.5 V by applying a 25% margin on 70-V max voltage.

The voltage ratings of the series output capacitors C18 and C19 are higher than necessary, but were selected to reduce the number of BOM line items.

4.5.2 48-V Switching

The LM5060-Q1 provides active control over the application of the 48-V supply to the motor drive circuit. This circuit is shown in Figure 21.

Due to the maximum current of 30A and worst-case $R_{DS(ON)}$ of a single FET, the power dissipation would cause the temperature rise to be too significant. By using two FETs in parallel (Q2 and Q10), the total $R_{DS(ON)}$ is reduced by half which reduces the power dissipation and, in turn, reduces the temperature rise.

The resistor divider formed by R4, R8, and R11 sets the levels at which the UVLO and overvoltage lockout (OVLO) activate. This prevents possible damage or poor performance when the 48-V supply is outside the desired range.

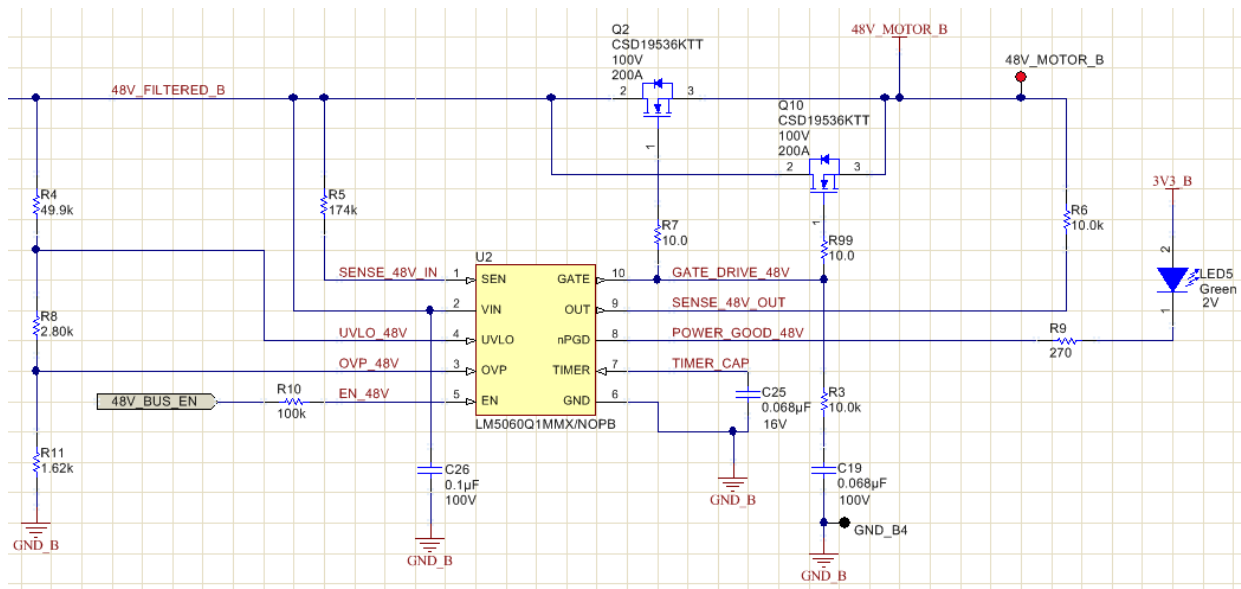


Figure 21 48-V Switching Circuit

The values of R4, R8, and R11 set the undervoltage and overvoltage thresholds such that:

- Q2 and Q10 are off for values of 48V_FILTERED_B less than 19 V (UVLO)
- Q2 and Q10 are disabled when 48V_FILTERED_B increases above 67 V (OVLO set)
- Q2 and Q10 are re-enabled when 48V_FILTERED_B decreases below 59 V (OVLO reset)

A timer capacitor (C25) allows a finite amount of time for the gate to charge and the output voltage to rise during start-up before indicating a fault condition.

The indicator LED5 is illuminated when the 48 V is correctly switched to provide supply to the motor drive circuit. When the external MOSFET VDS decreases such that the OUT pin voltage exceeds the SENSE pin voltage, the nPGD indicator is active (low = no fault) and LED5 is illuminated. There is a 16- μ A current sink on the SENSE pin, and an 8- μ A current sink on the OUT pin, so resistors R5 and R10 affect the relative measurements of the voltages across the MOSFET drain-to-source.

4.6 Motor Drive

The motor drive stage delivers 48-V power to the 3 phases of the BLDC motor as a pulse-width modulated (PWM) voltage. One of the three identical motor drive stages is shown in Figure 22.

The high-side and low-side gate driver (U10) receives PWM signals from the microcontroller and generates the corresponding level-shifted (higher amplitude) signals to drive the gates of the high-side MOSFET (Q4) and low-side MOSFET (Q5). U10 is biased by the 12V_B supply, with allowable supply tolerance from 8 V to 17 V.

The PWM switching frequency can range from 15 kHz to 50 kHz. This frequency is set by the parameters of the MotorWare software running on the LaunchPad microcontroller board.

Resistors R55 and R58 reduce the turnon slew rate for the transistors, and can be adjusted if faster switching or lower emissions are required. Diodes D9 and D12 bypass those resistors to speed up the transistor turnoff transitions, thus reducing the possibility of shoot-through current.

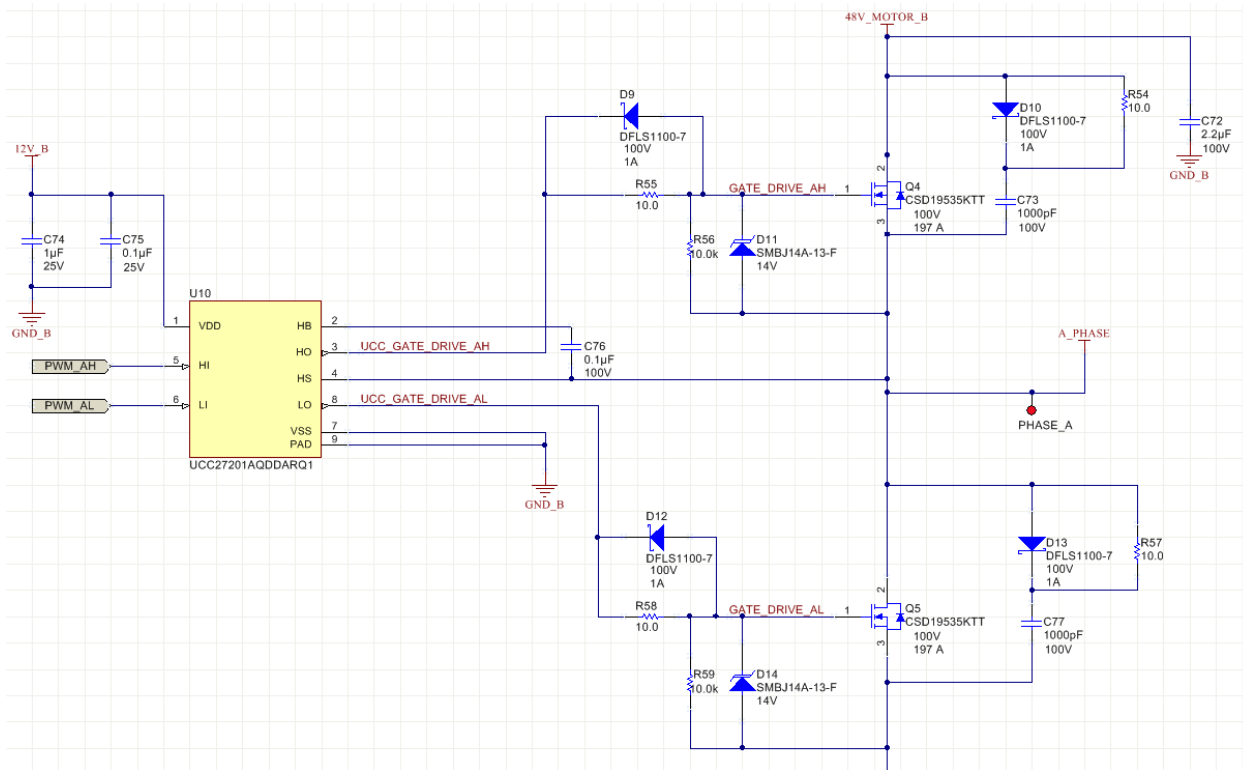


Figure 22: Motor Drive Circuit

Several components (R56, D11, R54, C73, D10, R59, D14, C77, D13, and R57) around the high-side and low-side drive transistors can be used to tune the circuit for best performance in terms of switching transition time, overshoot and ringing during switching, and conducted and/or radiated emissions. In general, the specific values will depend on the motor being driven and the application parameters such as speed, torque, and so forth.

TVS diodes (D11, D14) across the gate to source nodes protect the MOSFETs gate in the event of overvoltage transients.

The RCD clamps across each FET (R54, C73, D10 and R57, C77, D13) clamp the positive ringing drain to source and avoid the FET being pushed in avalanche condition. The RC circuit values may require tuning.

4.7 Motor Control Feedback

The algorithm for controlling the motor makes use of sampled measurements of the motor conditions, including 48-V supply voltage, the voltage on each motor phase, the current of each motor phase, and in the case of sensored commutation, the position feedback from motor-mounted sensors such as Hall effect sensors. For reliability, the temperature of each motor drive stage is also monitored.

4.7.1 Motor Current Feedback

During each PWM cycle, the current through the motor is sampled by the microcontroller as part of the motor control algorithm. The circuit shown in Figure 23 shows how the motor current is represented as a voltage signal, with filtering, amplification, and offset to the center of the ADC input range. This circuit is used for each of the three motor phases.

The low-side current through phase A flows through R61, giving a scale factor of 1 mV per amp. Optional low-pass filtering is provided by R60, R62, C78, C79, and C80 with differential symmetry maintained with equal values of R60 and R62, and C78 equal to C80.

The differential gain amplifier circuit (U6A and surrounding components) has a differential gain of 20, with an offset of approximately 1.65 V provided by the ADC_HALF_VREF_B voltage. After the gain provided by the op amp circuit, the motor current scale factor at the input to the ADC is 20 mV/A, with a voltage of 1.65 V representing zero motor current. Thus, with a range of 0 V to 3.3 V at the input of the ADC, motor currents of ± 82.5 A can be measured.

Low-pass filtering can be accomplished by selecting C43 to reduce the amplifier gain at high frequencies. However, if the filter time constant is longer than the shortest PWM pulse, the current measurement will be affected.

Note: For the following test results, C43, C78, and C80 are not installed, and the value of C79 is 1 nF.

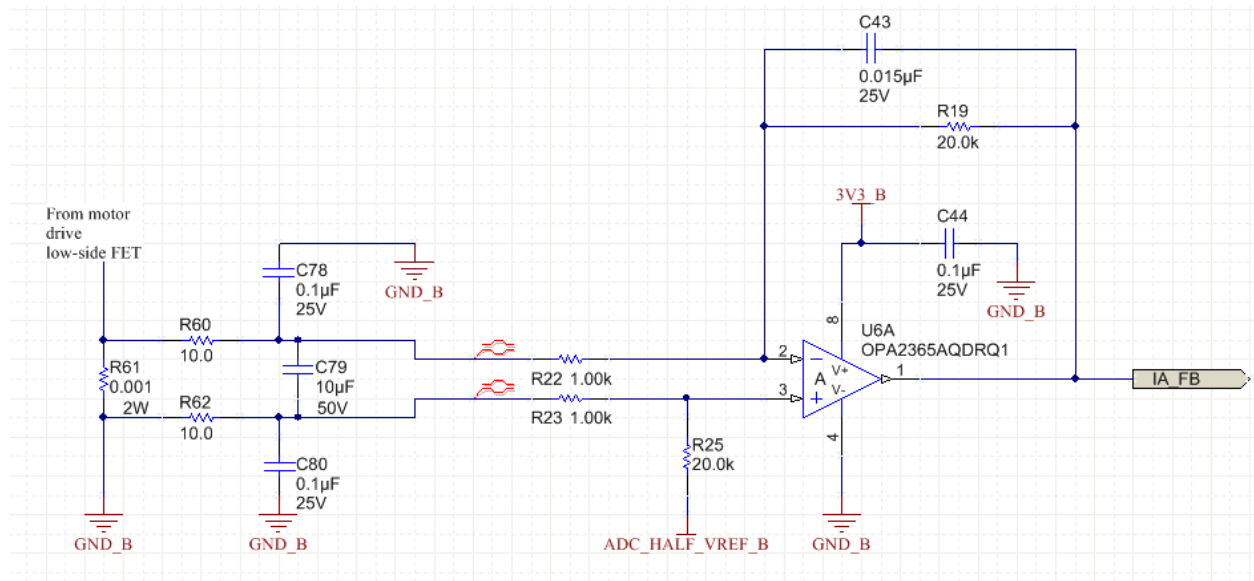


Figure 23 Motor Current Feedback Circuit

4.7.2 Motor Voltage Feedback

The voltage of each of the three motor phases is sampled by the microcontroller as part of the motor control algorithm. The circuit shown in Figure 24 shows how the motor voltage is filtered and scaled for the ADC input range. A fourth identical circuit is used to measure the 48-V supply applied to all three of the motor phase drive circuits.

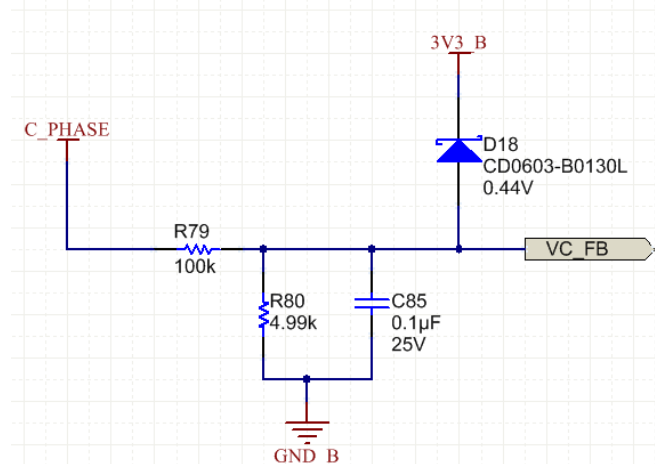


Figure 24 Motor Voltage Feedback Circuit

The resistor divider formed by R79 and R80 attenuates the motor phase voltage by a factor of 21:1, allowing voltages up to 69 V to be within the 0 V to 3.3 V range of the LaunchPad ADC. In case of motor voltages higher than 69 V (for example, caused by back EMF from the motor), D18 clamps the signal to slightly above the 3.3-V supply.

The RC time constant formed by C85 and R80 give a low-pass filter with corner frequency 318 Hz. This frequency allows all expected motor drive voltage waveforms to pass (318 Hz is 19 kRPM) while averaging the PWM switching pulses and filtering out higher frequency noise.

A macro model of the OPA2365A is available for circuit performance simulation using Texas Instruments' TINA or other SPICE-based circuit analysis tools. Figure 25 shows a frequency transfer function analysis of the motor voltage feedback circuit. As expected, the low-frequency gain is -26.4 dB (corresponding to an attenuation of 21:1), and the first low-frequency corner frequency is approximately 300 Hz.

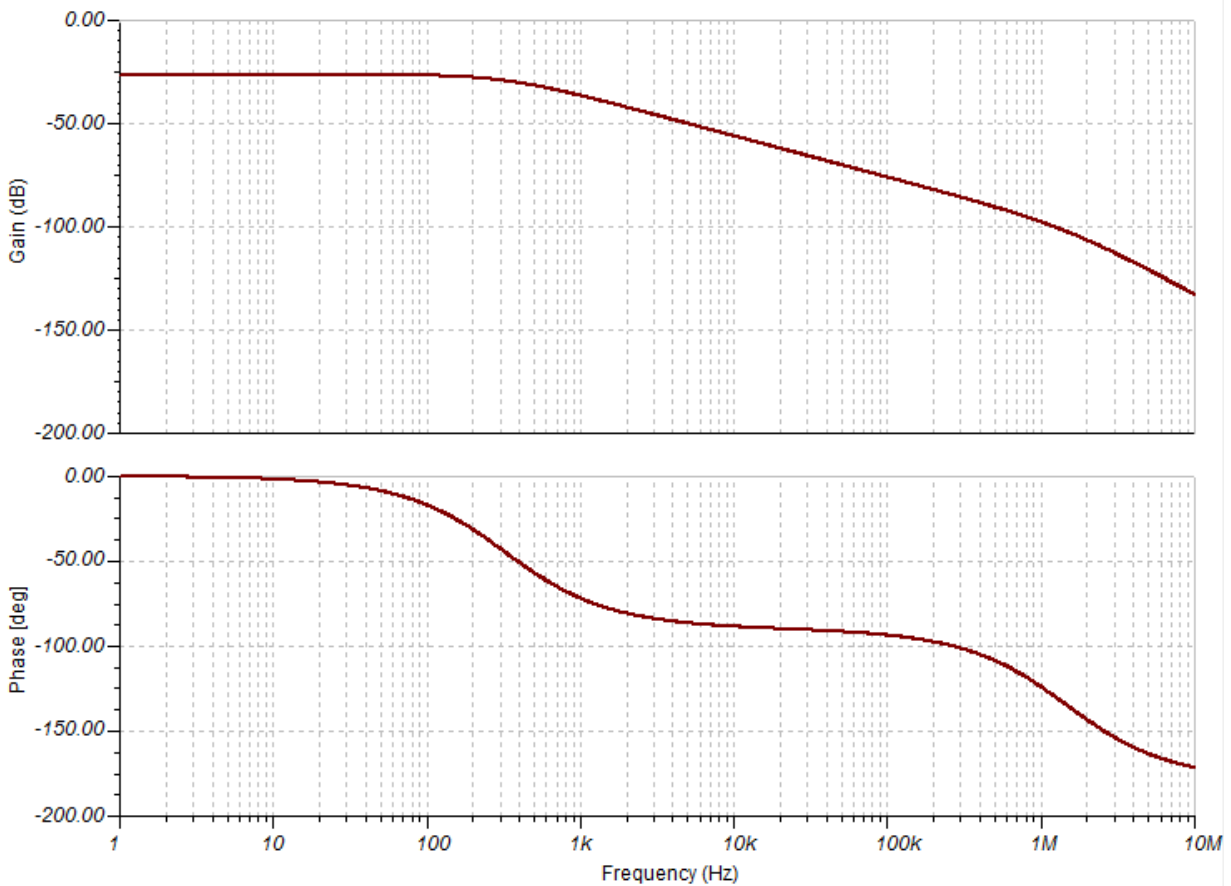


Figure 25 Simulation Results for Voltage Feedback Circuit

4.7.3 Motor Drive Temperature Feedback

The temperature of each pair of motor drive MOSFETs is sampled by the microcontroller as part of the motor diagnostic scheme.

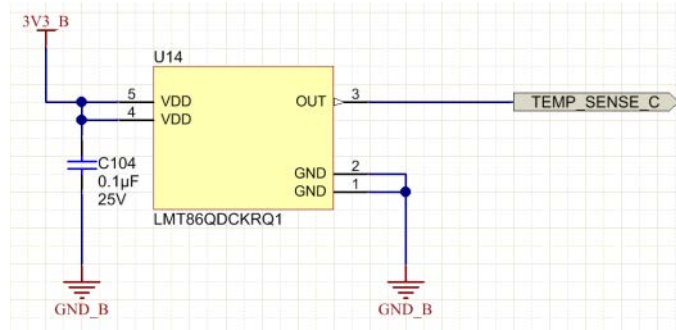


Figure 26 Motor Drive Temperature Sense

The scale factor from the LMT86 is $-10.9 \text{ mV}/^\circ\text{C}$ with a range of -50°C to $+150^\circ\text{C}$, covering an output range of 0.4 V to 2.6 V, which is within the input voltage range of the ADC. Due to the integrated features of the LMT86-Q1, very few external components are needed.

4.7.4 Motor Position Feedback (Hall effect sensors)

Some applications may make use of Hall effect or similar sensors to provide motor position feedback to the motor controller, facilitating simplified commutation of the 3-phase brushless motor. This design includes components to bias and buffer those signals, as shown in Figure 27.

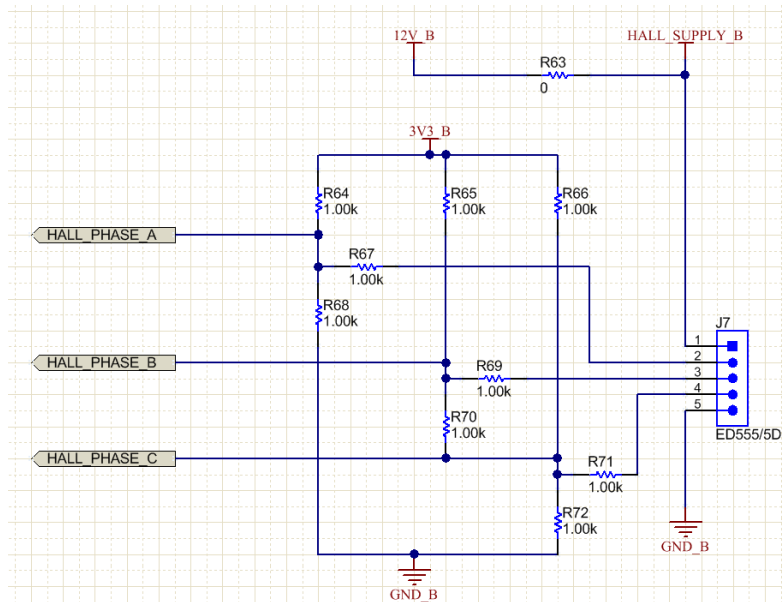


Figure 27 Connections to Optional External Hall Effect Sensors

The 1-k Ω resistors (R64-R72) allow connection to sensors with push-pull, or open-collector outputs with either pullup or pulldown biasing. In all cases, the resistor values can be changed to provide any signal attenuation needed to adjust signals with higher voltage levels to match the 3.3-V signal levels expected at the interface to the LaunchPad microcontroller board.

4.8 LaunchPad

LaunchPads are microcontroller development kits from Texas Instruments. They come in a variety of types to address various needs. All LaunchPad kits include everything needed to begin developing applications in minutes.

The C2000 Piccolo™ LaunchPad evaluation kit, based on the F28027 microcontroller (MCU), is a modular, quick-launch evaluation kit that contains everything needed – device, emulation and software – to explore the latest digital control techniques in areas such as power, lighting, and motor control.

The 40 pins on the LaunchPad headers allow for easy access to all the peripherals on the F28027x device. These pins enable modularity by supporting 20-pin and 40-pin BoosterPack™ modules such as motor drive inverters, LED lighting, and much more. The TIDA-00281 board is designed with two corresponding 20-pin headers (J5 and J6) to interface with the LaunchPad pins.

The TIDA-00281 supplies 3.3-V power (and ground) to the LaunchPad through the standard header pins. The programming emulator and USB connection on the LaunchPad is isolated from the 3.3-V power supplied by the TIDA-00281 board (with LaunchPad jumpers JP1, JP2, and JP3 removed).

For more information on the LaunchPad microcontroller development kits, go to www.ti.com/launchpad.

Figure 28 shows the connections on J5 (20-pin connector) and J9 (3-pin connector). The pin assignments are in accordance with the BoosterPack standard, allowing connection to various LaunchPad boards. All signals are referenced to the 3.3-V supply derived from the secondary of the flyback converter.

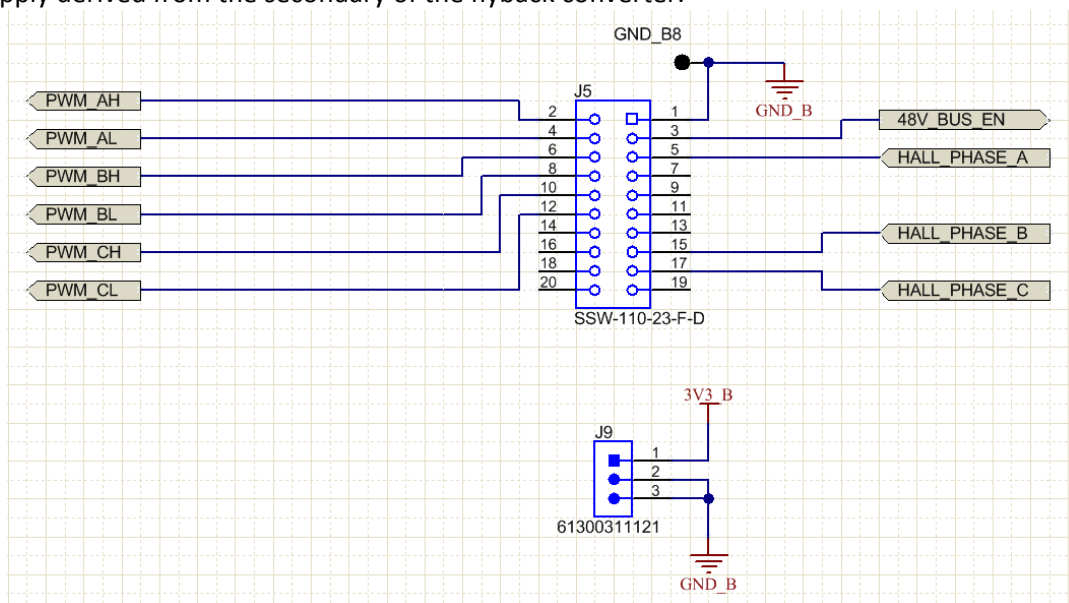


Figure 28 J5 and J9 Connections to LaunchPad

The PWM signals are generated by the microcontroller, and connect with the UCC27201A-Q1 gate drivers. The HALL signals come from the motor position sensors, and connect to the microcontroller for sensed commutation. The 48V_BUS_EN signal comes from the microcontroller, and enables the 48-V supply to the motor drive circuits.

Figure 29 shows the connections on the J6 (20-pin connector) to the LaunchPad board. The feedback signals (voltage, current, and temperature) are filtered by the RC components, with a low-pass corner frequency of 1.4 MHz to reduce high-frequency noise. These filter components can be modified if designers find specific noise frequencies which must be attenuated.

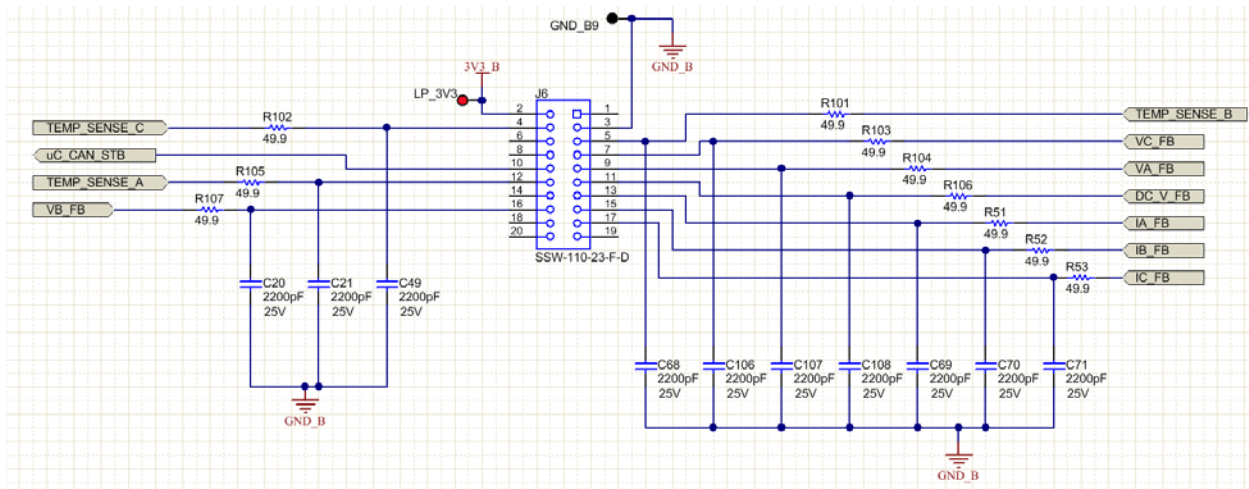


Figure 29 J6 Connections to LaunchPad

4.9 Isolated CAN

A high-speed CAN interface is part of the design of the TIDA-00281 board. The CAN transceiver is powered by the 5-V supply derived from the 12-V automotive battery power, and shares a common ground with the 12-V supply on the primary side of the flyback voltage converter. The CAN interface is isolated from the 48-V battery supply by a 3-channel digital isolator (U5). The CAN circuit is shown in Figure 30.

The logic signals CAN_TX and CAN_RX and CAN_STB are connected to 3-pin header J4, allowing connection to signals from a CAN-enabled microcontroller. These signals are referenced to the 3.3V_B ground, which is derived from the 12-V supply from the flyback converter secondary.

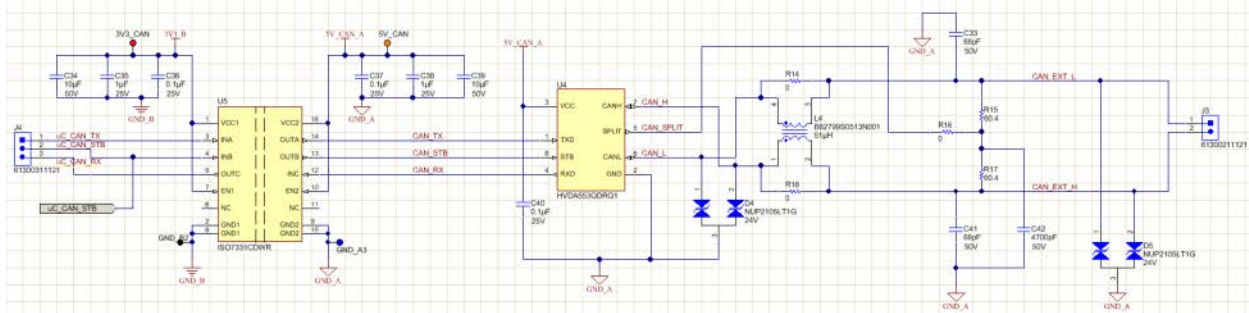


Figure 30 Isolated CAN Circuit with Transient Voltage Protection

Various schemes are implemented by different automotive manufacturers to provide transient voltage protection and EMC performance on CAN networks. The common-mode choke (L4) and protection diodes (D4 and D5) give designers flexibility in how to implement the protection for this CAN circuit.

Use termination resistors (R15 and R17) if this board is used as one of the two terminating nodes in a CAN network, otherwise remove these resistors.

System requirements determine the bias capacitors needed on digital isolator (U6). The device will work in many applications with only a single 0.1- μ F capacitor (C36, C37) on both VCC1 and VCC2. Additional capacitors C34, C35, C38, C39 are provided for flexibility in design.

Either the 0- Ω bypass resistors R14 and R18 or choke inductor L4 should be populated (but not both). Because either the resistors or the common-mode choke should be populated, in the board layout the resistors are placed on the pads of the choke filter.

D4 should not be installed between the transceiver and the choke unless inductive flyback transients occur from common-mode choke. TVS diodes should, in a typical scenario, be installed closest to the connector as shown by the location of D5. See Figure 30.

5 Getting Started Hardware

In order to fully demonstrate the TIDA-00281 design, several hardware components are needed. These include:

- The TIDA-00281 motor drive board
- A LaunchPad with InstaSPIN-FOC-enabled microcontroller, such as the LAUNCHXL-F28027F
- A brushless DC motor, with or without commutation sensors (e.g. Hall effect sensors)
- A 12V power supply, capable of providing at least 150 mA of current
- A 48V power supply, capable of providing the current expected to drive the BLDC motor
- A computer with the software installed to control the system

5.1 Install LaunchPad

The TIDA-00281 board is designed to accommodate an F28027F LaunchPad board. The board-to-board connections are made through two 20-pin headers, in accordance with the LaunchPad/BoosterPack development environment. A third header with 3-pins includes additional connections for 3.3V power and ground, and helps to assure correct orientation of the LaunchPad board.

Use caution when mounting the LaunchPad to the TIDA-00281 board, as misalignment of the header pins during installation may cause damage.

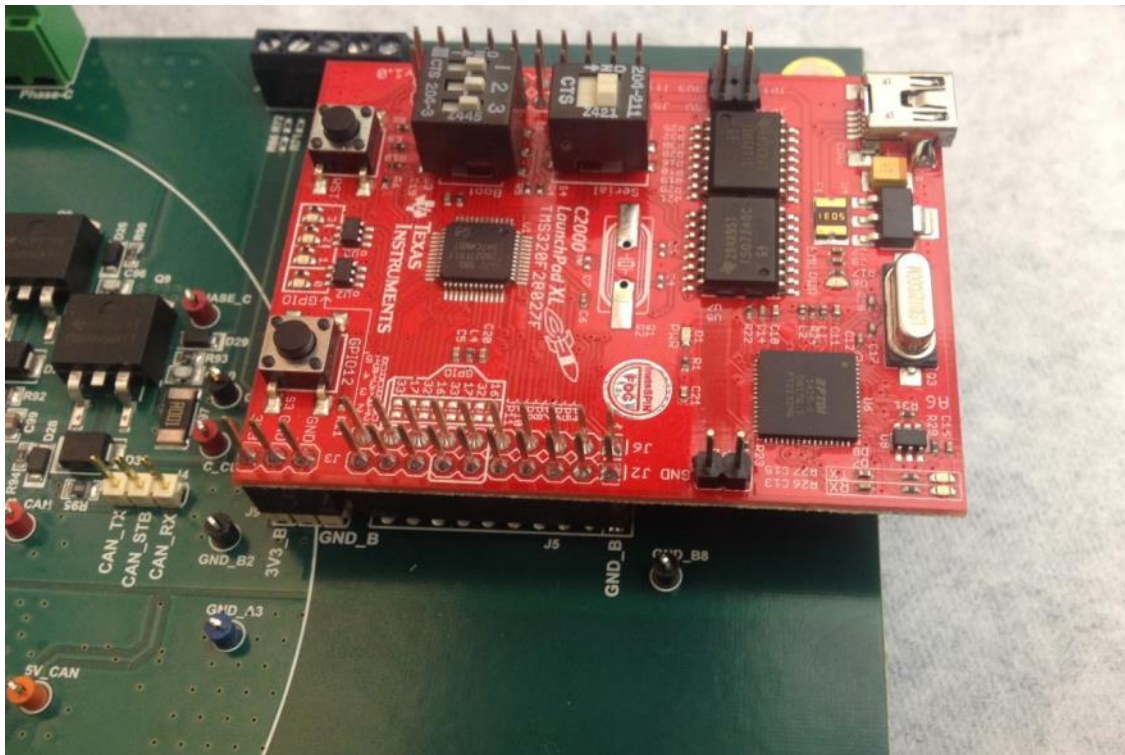


Figure 31 F28027F LaunchPad installed on TIDA-00281 board

Note that the TIDA-00281 board is designed to allow mounting the LaunchPad board either on the top side (preferred) or the bottom side (optional). If mounted on the top side, the LaunchPad indicator LEDs will be easily visible, and the push-button switches will be easily accessible.

During operation with the TIDA-00281 board, the LaunchPad will be powered from the 3.3V supply generated by the TIDA-00281 flyback and buck regulator. **Therefore, the shunts on jumpers JP1, JP2, and JP3 on the LaunchPad board should be removed.**

There are additional switches on the Launchpad which must be set correctly; S1 (boot mode selection) and S4 (serial connectivity select).

The LaunchPad's microcontroller includes a boot ROM that performs some basic start-up checks and allows for the device to boot in many different ways. S1 has been provided to allow users to easily configure the pins that the bootROM checks to make this decision whether to perform an emulation boot or a boot to flash. In general all 3 switches on S1 should be in the ON position. More information about boot mode selection can be found in the TMS320x2802x Piccolo Boot ROM Reference Guide (SPRUFN6).

When S4 is in the up (ON) position, the Piccolo device's SCI is connected to the XDS100 and users are able to receive and send serial information from or to the board via the USB connection. When S4 is in the down position, the Piccolo device's SCI is disconnected from the XDS100 and BoosterPacks.

5.2 Power Connection

For full operation, this design requires connection to a 12V supply with at least 150 mA current capability, and a 48V supply, with current capability as dictated by the motor to be driven, typically in the range of several Amps.

5.2.1 12V Supply Connection

Connect leads to the 4-contact screw terminal block on the side of the board. The screw terminals are labeled to indicate the proper polarity of the supply. Note that there are two terminals for +12V and two terminals for ground (12V return). Each pair is electrically connected to the same node on the board, so it is sufficient to connect to only one of each of the terminals, as shown in Figure 32.

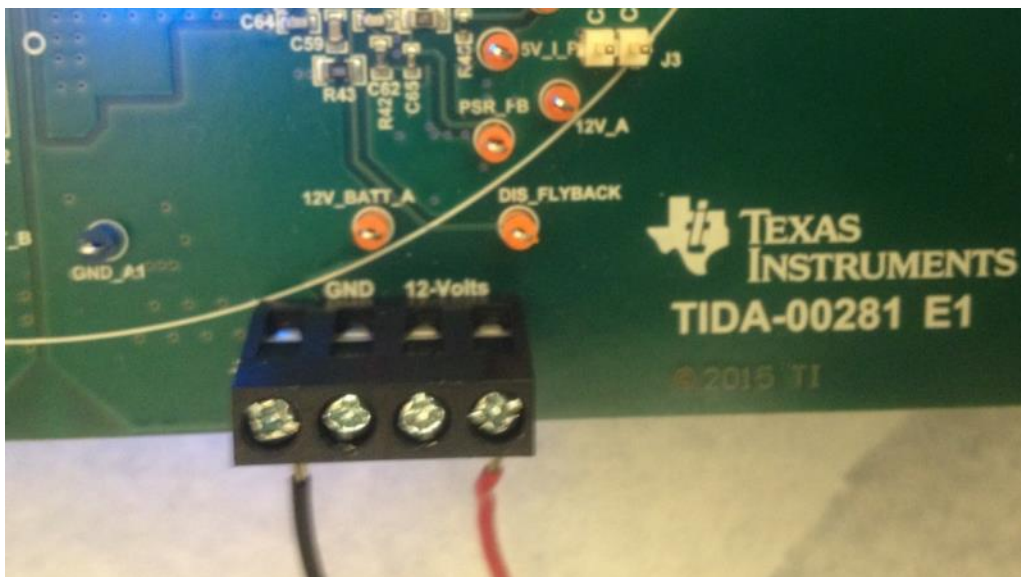


Figure 32 12V supply connections

5.2.2 48V Supply Connection

Connect leads (recommend using at least 18 AWG) to the 4-contact screw terminal block on the side of the board. The screw terminals are labeled to indicate the proper polarity of the supply. Note that there are two terminals for +48V and two terminals for ground (48V return). Each pair is electrically connected to the same node on the board, so it may be sufficient to connect to only one of each of the terminals, as shown in Figure 33. However, the current required by the motor can be several Amps, so consider the size and number of wires necessary for the expected motor current.

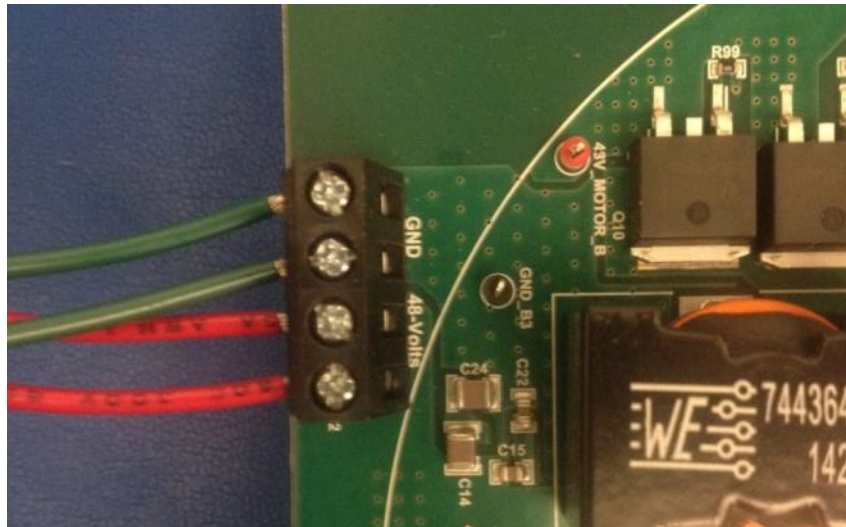


Figure 33: 48V supply input terminals

5.3 Motor Connection

5.3.1 Motor Phase Connection

The board is designed for a 3-phase brushless DC motor. The motor connections are suitable for a motor configured in either a Y or Δ configuration. The phase voltages (A,B,C) are marked next to the corresponding terminals. Note that the order of the phases is not critical, but that reversing any two phases will cause a reversal in the motor direction. Connection to the GND terminal is not required.

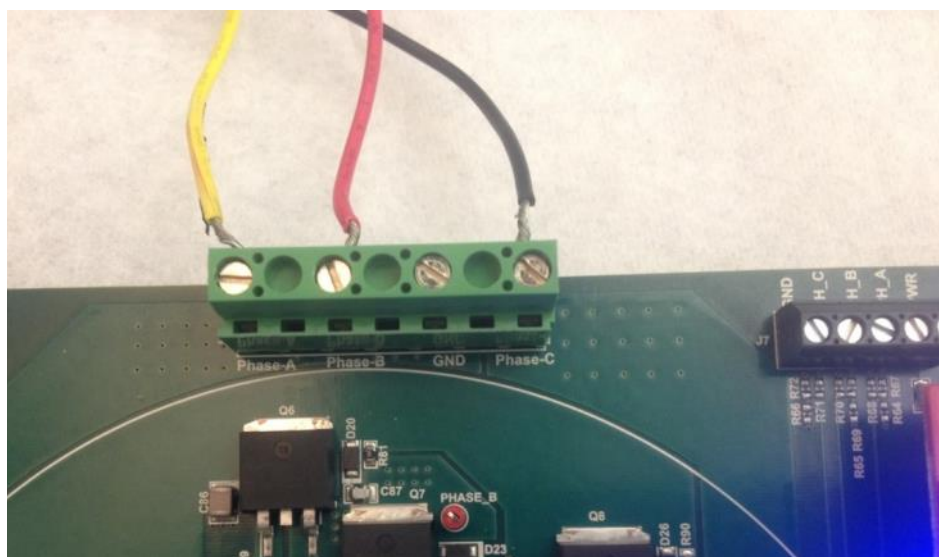


Figure 34 Motor phase connections

5.3.2 Motor Commutation Feedback Connection

The board is designed to accept commutation feedback signals, such as Hall-effect sensors, from the motor. If these sensors are used, connect to the 5-position terminal block J7. The signals are labeled near the corresponding terminals. A connection to the 12V_B supply is included on J7, which can be used to bias the Hall effect sensors, if needed.

6 Getting Started Software

6.1 Download and Install Code Composer Studio™

Code Composer Studio™ (CCStudio) is an integrated development environment (IDE) for Texas Instruments (TI) embedded processor families. CCStudio comprises a suite of tools used to develop and debug embedded applications. It includes compilers for each of TI's device families, source code editor, project build environment, debugger, profiler, simulators, real-time operating system and many other features. The intuitive IDE provides a single user interface taking you through each step of the application development flow. Familiar tools and interfaces allow users to get started faster than ever before and add functionality to their application thanks to sophisticated productivity tools. See the Code Composer Studio web page at <http://www.ti.com/tool/ccstudio> for information on downloading the integrated development environment for the C2000 code.

6.2 Download and Install Motorware™

The TIDA-00281 board can be operated using a LaunchPad microcontroller development board. In the following discussion, set-up using the the C2000 LaunchPad LAUNCHXL-F28027F will be described. A link can be found in section 10.

The TIDA-00281 board and connected LaunchPad board was tested using Texas Instruments' MotorWare software, with some additional files necessary to adapt to the specific hardware configuration of the TIDA-00281 board.

MotorWare is the software infrastructure and distribution mechanism for the InstaSPIN-FOC and InstaSPIN-MOTION motor control solutions. It includes source code object oriented APIs for peripheral drivers and modules (including a freshly updated set of motor control functions). These APIs are used to build multiple InstaSPIN-FOC projects that demonstrate the different modes and capability, documented through the Projects and Lab User's Guide.

The MotorWare software can be downloaded from the Texas Instruments web site at <http://www.ti.com/tool/MOTORWARE> . Follow the installation instructions to install on your local computer.

After installation of the MotorWare software, follow the steps below to add the files necessary to use MotorWare with the TIDA-00281 board. Note that version 14 of MotorWare was used during testing; if a newer version of MotorWare is used, replace the "14" in the steps below with the appropriate corresponding version number.

1. Navigate to C:/TI/motorware/motorware_1_01_00_14/sw. All changes made for this TI Design are completed in "sw" subfolders.
2. The first subfolder to add will be under sw/modules/hal/boards. Take the zip folder labeled "TIDA-00281_sw_modules_hal_boards.zip" and copy into this directory.
3. Right click on the zip folder and select "Extract All..."
4. Before clicking extract, modify the "Files will be extracted to this folder:" destination so that the folder name is C:/TI/motorware/motorware_1_01_00_14/sw/modules/hal/boards. This is very important because some .c and .h files in the InstaSPIN routines call upon this specific folder.
5. Now click extract
6. Return to the folder in step 1; C:/TI/motorware/motorware_1_01_00_14/sw

7. Proceed to sw/solutions/InstaSPIN_foc/boards. Take the zip folder labeled “TIDA-00281_sw_solutions_InstaSPIN_foc_boards.zip” and copy into this directory.
8. Right click on the zip folder and select “Extract All...”
9. Before clicking extract, modify the “Files will be extracted to this folder:” destination so that the folder name is C:\TI\motorware\motorware_1_01_00_14\sw\solutions\InstaSPIN_foc\boards. This is very important because some .c and .h files in InstaSPIN call upon this specific folder.
10. Now click extract

6.3 Run the Example Software

Step 1: Import the existing project, for example proj_lab02b, from the motorware directory. In this instance, there are two projects in the directory.

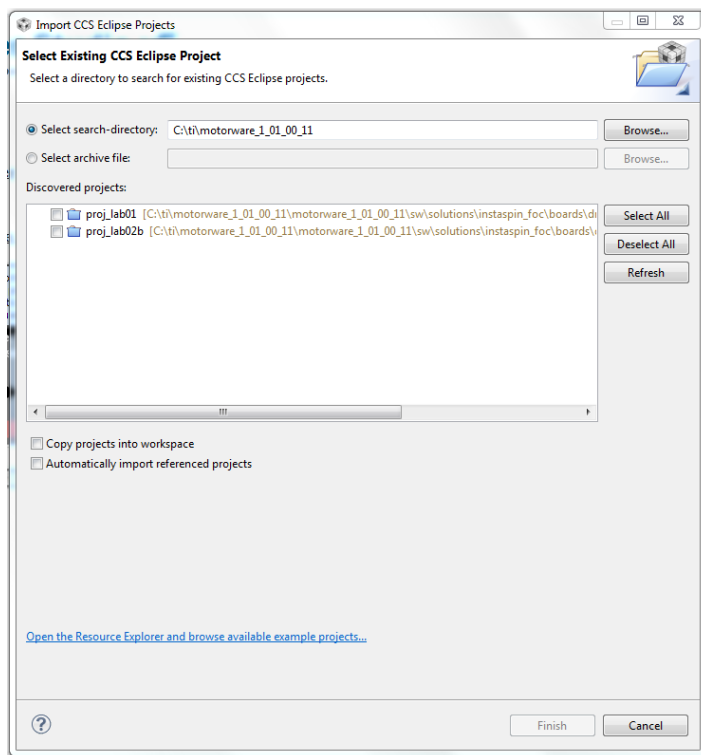


Figure 35 Import Existing CCS Eclipse Project screen

Step 2: Import the project lab2b

Note that this design will work with other projects in the MotorWare libraries, but lab02b has all the features needed to exercise the design as documented in this report.

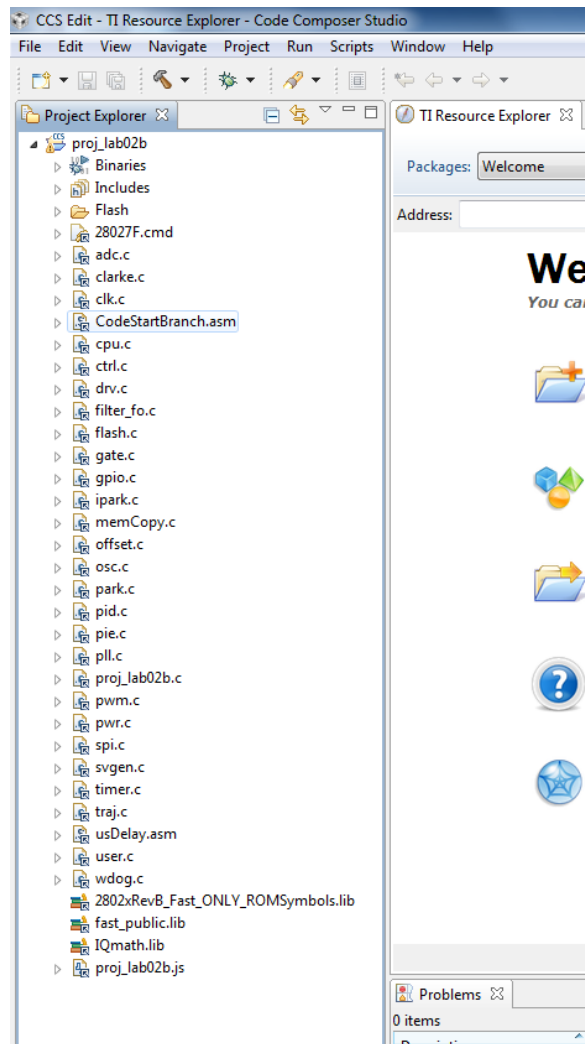


Figure 36 Imported project file and sub-files

Step 3: Set the target configuration:

The connection will depend on the JTAG emulator you use. For the LAUNCHXL-F28027F LaunchPad, the XDS 100 v2 emulator should be selected from the “Connection” pull-down menu. The target device on this board is the TMS320F28027 piccolo microcontroller. After selecting the connection and target device, save the configuration set-up by clicking the “Save” button.

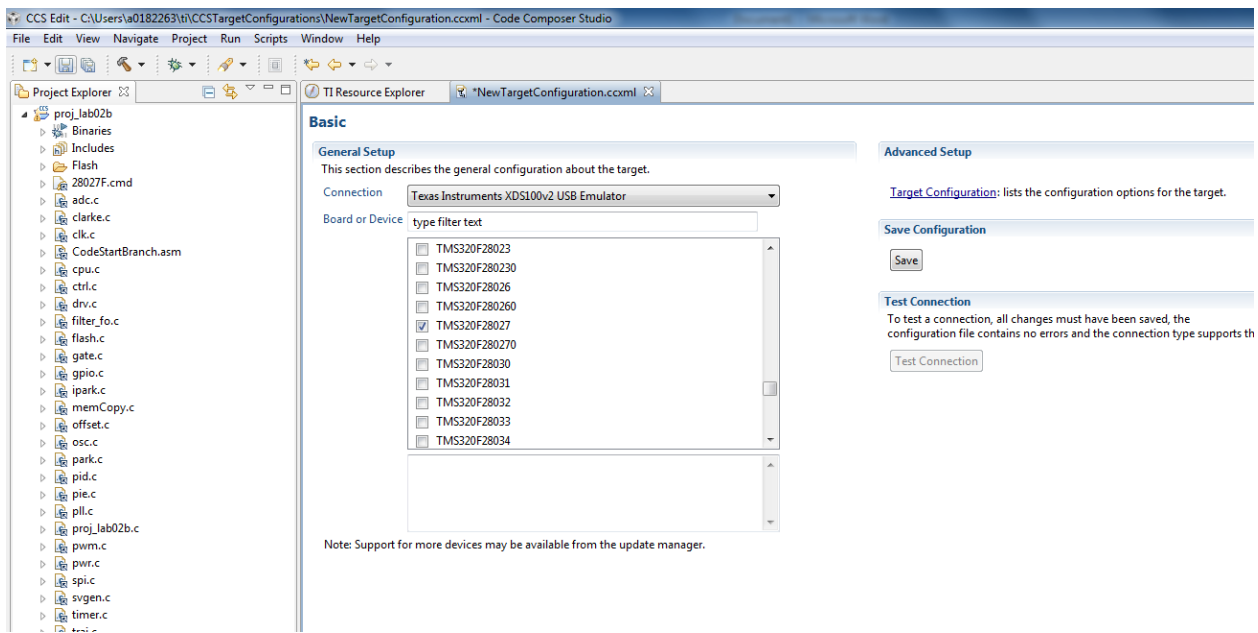


Figure 37 New target configuration screen

Step 4: Test the connection to the target.

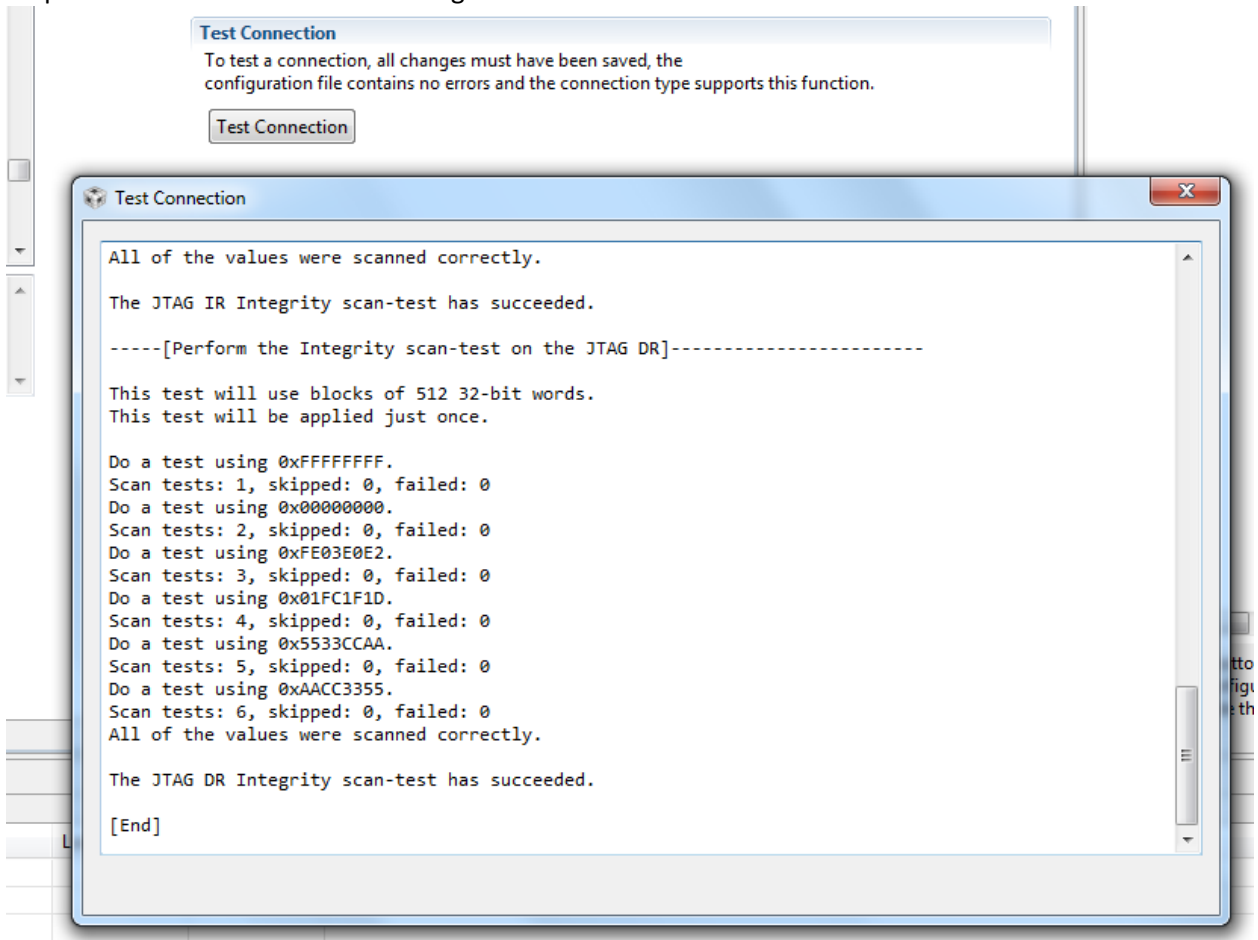

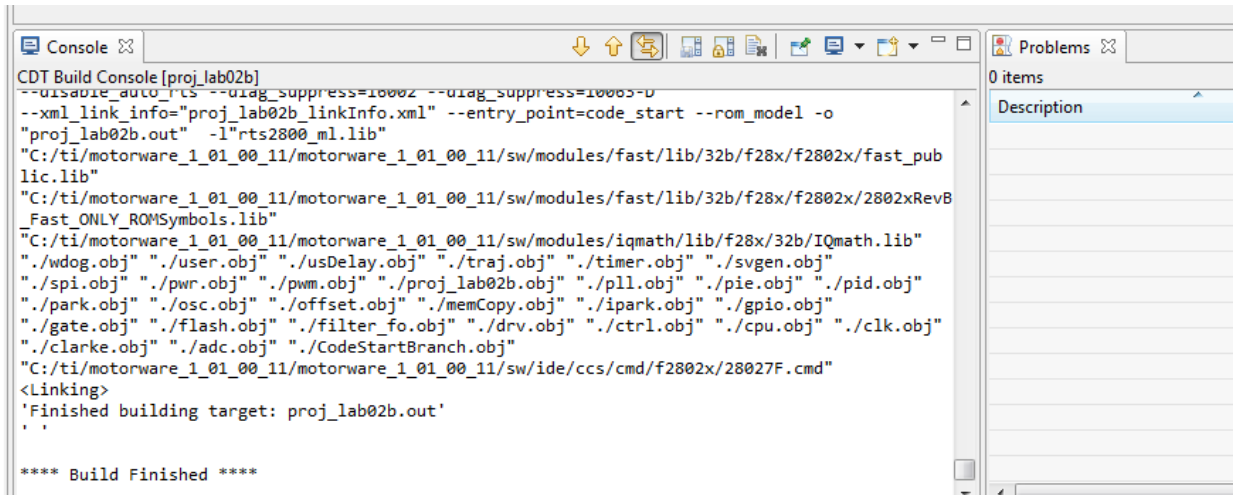


Figure 38 Test connection window after completion of connection test

Step 5: Build the project.

Make sure the project is active by clicking on the project name (for example proj_lab02b) in the Project Explorer window. Build the project by clicking the hammer icon  on the CCS Edit toolbar. If the project builds correctly, the message “Build Finished” will display at the end of the text in the Console window. See Figure 39.


Note, in case of errors during build or execution, there may be states where the project build encounters problems due to previous build and/or execution. Performing a “Clean” build (select Clean under the Project menu) will rebuild the project from a completely reset state.



```
CDT Build Console [proj_lab02b]
--uisabie_auto_rts --diag_suppress=10002 --diag_suppress=10005-D
--xml_link_info="proj_lab02b_linkInfo.xml" --entry_point=code_start --rom_model -o
"proj_lab02b.out" -l"rts2800_ml.lib"
"C:/ti/motorware_1_01_00_11/motorware_1_01_00_11/sw/modules/fast/lib/32b/f28x/f2802x/fast_public.lib"
"C:/ti/motorware_1_01_00_11/motorware_1_01_00_11/sw/modules/fast/lib/32b/f28x/f2802x/2802xRevB_Fast_ONLY_ROMSymbols.lib"
"C:/ti/motorware_1_01_00_11/motorware_1_01_00_11/sw/modules/iqmath/lib/f28x/32b/IQmath.lib"
"./wdog.obj" "./user.obj" "./usDelay.obj" "./traj.obj" "./timer.obj" "./svgen.obj"
"./spi.obj" "./pwr.obj" "./pwm.obj" "./proj_lab02b.obj" "./pll.obj" "./pie.obj" "./pid.obj"
"./park.obj" "./osc.obj" "./offset.obj" "./memCopy.obj" "./ipark.obj" "./gpio.obj"
"./gate.obj" "./flash.obj" "./filter_fo.obj" "./drv.obj" "./ctrl.obj" "./cpu.obj" "./clk.obj"
"./clarke.obj" "./adc.obj" "./CodeStartBranch.obj"
"C:/ti/motorware_1_01_00_11/motorware_1_01_00_11/sw/ide/ccs/cmd/f2802x/28027F.cmd"
<Linking>
'Finished building target: proj_lab02b.out'
'
**** Build Finished ****
```

Figure 39 CCS console window after successful build of the project

Step 6: Start a Debug session with the project.

Start a debug session by clicking the bug icon  on the CCS Edit toolbar. The built project will be downloaded to the LaunchPad microcontroller through the USB port and JTAG emulator.

Step 7: Run the project

Begin program execution by clicking the green Run/Resume icon in the CCS Debug toolbar. Enable Silicon Real-time mode by clicking the “clock” icon in the CCS Debug toolbar. Open the Expressions tab, which should be populated with the motor variable expressions as shown in Figure 40.

Expression	Type	Value
gMotorVars	struct _MOTOR_Vars_t_	{...}
gMotorVars.UserErrorCode	enum unknown	USER_ErrorCode_NoError
gMotorVars.CtrlVersion	struct _CTRL_Version_	{...}
gMotorVars.Flag_enableSys	unsigned char	1 (Decimal)
gMotorVars.Flag_Run_Identify	unsigned char	1 (Decimal)
gMotorVars.Flag_enableForceAngle	unsigned char	1 (Decimal)
gMotorVars.Flag_enablePowerWarp	unsigned char	0 (Decimal)
gMotorVars.CtrlState	enum unknown	CTRL_State_OnLine
gMotorVars.EstState	enum unknown	EST_State_OnLine
gMotorVars.SpeedRef_krpm	long	0.2999999523 (Q-Value(24))
gMotorVars.MaxAccel_krpmps	long	0.1999999881 (Q-Value(24))
gMotorVars.Speed_krpm	long	0.2950395942 (Q-Value(24))
gMotorVars.MagnCurr_A	float	0.0
gMotorVars.Rr_Ohm	float	0.0
gMotorVars.Rs_Ohm	float	0.04401823
gMotorVars.Lsd_H	float	7.708059e-05
gMotorVars.Lsq_H	float	7.708059e-05
gMotorVars.Flux_VpHz	float	0.1185086
gMotorVars.I_bias	struct _MATH_vec3_	{...}
gMotorVars.V_bias	struct _MATH_vec3_	{...}
gMotorVars.VdcBus_kV	long	0.04879146814 (Q-Value(24))

Figure 40 Expressions window in the debug view of CCS, program running

Step 8a: Set the Flag_enableSys to 1 by clicking in the value field and entering a 1.

At this point the operation of the system can be verified by observing that the 48V supply voltage is correctly being monitored. Change the expression VdcBus_kV to Q-Value(24) by right-clicking in the Value field, then selecting Q-values and “24”. Verify that the value for VdcBus_kV corresponds to the DC supply voltage. In this case (Figure 40), the supply voltage is 48.8V.

Step 8b: Set the Flag_Run_Identify to 1 by clicking in the value field and entering a 1.

The motor will be driven with small and large motions, drawing up to several Amps. After about a minute, the Flag_MotorIdentified is set to 1 by the controller. This indicates the motor has been successfully identified for sensorless operation.

Step 9: When the motor has been successfully identified, the Flag_Run_Identify will be reset to 0. At this point, again set the Flag_Run_Identify to 1 by clicking in the value field and entering a 1. This will allow the system to operate with the motor parameters already determined. After a moment, the motor will begin to spin at the speed set by the SpeedRef_krpm parameter value.

Step 10: To change the commanded speed, click on the value field of SpeedRef_krpm and enter a new value (in kRPM). To change the acceleration, click on the value field of MaxAccel_krpmps and enter a new value (in kRPM per second). Note that the speed reference can be either positive or negative, affecting whether the motor rotation is clockwise or counterclockwise.

7 Testing

The following sections show the test data from characterizing the design.

7.1 Power Supplies

7.1.1 12V supply range of operation

The design is intended for operation with a range of voltage on the 12V automotive battery supply. Figure 41 shows the measured input current for a positive range of input voltage on J1-1 with no LaunchPad installed. The curve indicates operation beginning at about 5V, where the flyback circuit begins to operate. The input current decreases as the input voltage increases, until about 33V, where the input clamping Zener diodes begin to conduct.

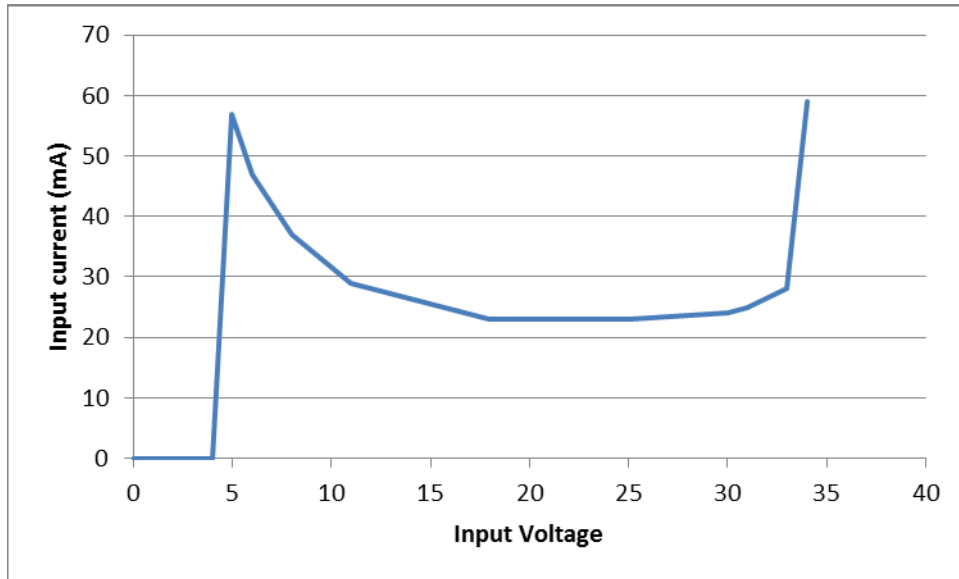


Figure 41 Input current versus positive input voltage on 12V_BATT_A

The reverse-battery performance is shown in Figure 42. Note that at about 17V, the Zener diode D2 begins to conduct, and the reverse current increases. Refer to Figure 12 and Figure 13 for the electrical schematics for this circuit.

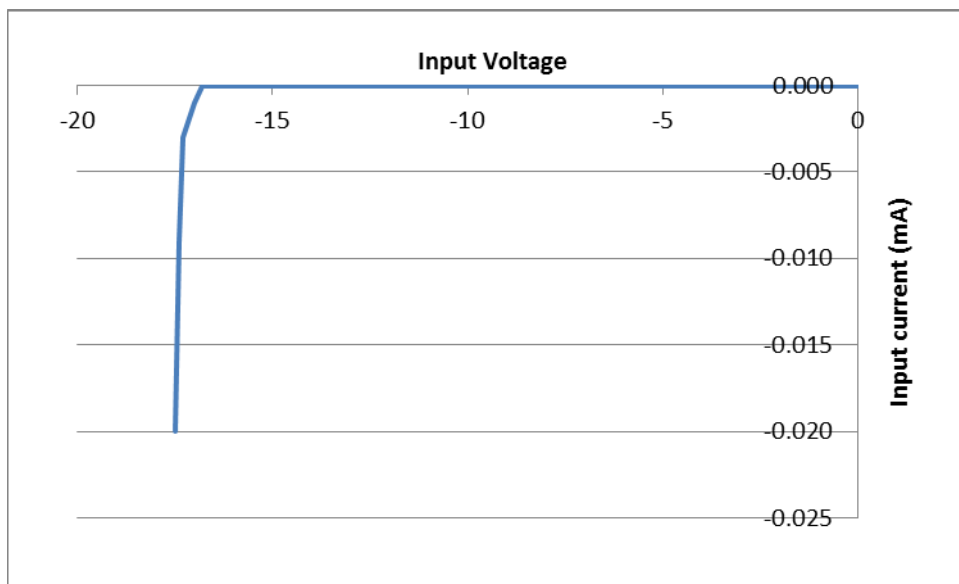


Figure 42 Input current versus negative input voltage on 12V_BATT_A

7.1.2 Flyback efficiency

The efficiency of the 12V-to-12V flyback converter was measured by placing current and voltage meters at the input 12V_A connector and the output 12V_B. This means it also bridges across the reverse polarity protection. These measurements were also taken by pre-loading the 5V rail with various loads from a decade box (certain amount of tolerance with setting the resistive loads) in order to get better regulation. The 12V load was set by removing R35 zero Ohm resistor which disconnected all the circuits that the 12V_B rail powers. Then an electronic load was used to provide a constant load current value. This current and voltage were used to determine power output on the 12V rail. Comparing the output power with input power yields efficiency from 12V input connector to the secondary flyback winding.

The curves in Figure 43 show that the 12V-to-12V efficiency is greater than 70% for output currents greater than 50 mA when the input voltage is at the nominal 12V level. Note that for these curves, the 5V supply on the primary side of the winding was loaded with a 4kOhm resistor. This would be a lightly loaded condition for the 5V supply, with only about 1.25 mA of current.

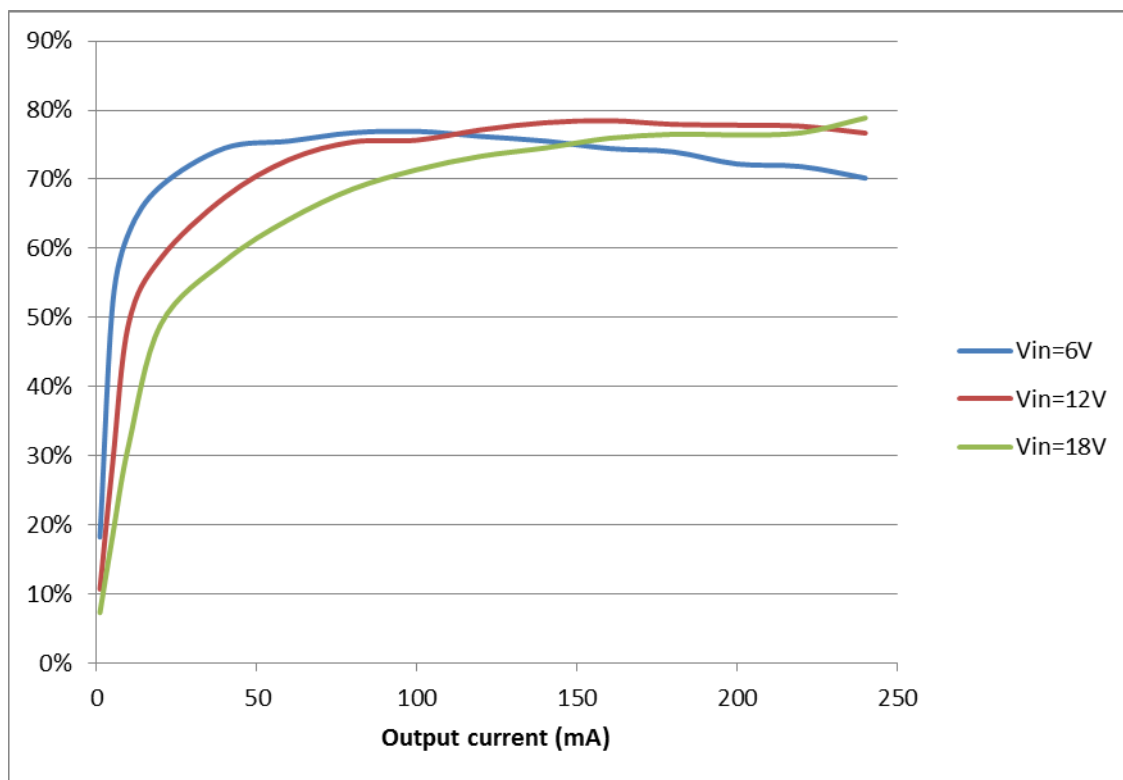


Figure 43 Flyback efficiency with 4000 Ohm load on 5V supply

The curves in Figure 44 show the efficiency when the 5V supply on the primary side of the winding is loaded with a 100 Ohm resistor. This would be a typical loaded condition for the 5V supply, with about 50 mA of current for the CAN transceiver and digital isolators. Note that for these curves, the 12V-to-12V efficiency is greater than 60% for output currents greater than 60 mA when the input voltage is at the nominal 12V level.

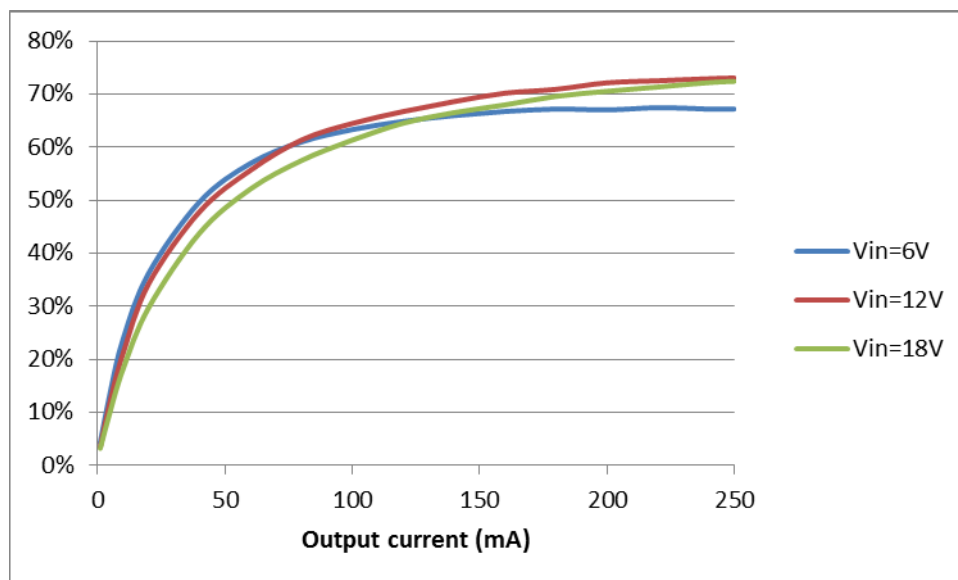


Figure 44 Flyback efficiency with 100 Ohm load on 5V supply

7.1.3 3.3V Buck Efficiency

The 3V3 efficiency measurements are taken based upon the entire system from the 12-V connector all the way to 3V3 delivered to the LaunchPad. The board layout didn't adapt well to separate out the buck converter from the 12V flyback rail and from all 3V3 devices. So to get an approximation of buck converter efficiency it is required to know the approximate efficiency of 12-V connector to 12V_FLY_B as discussed above and then measure 3V3 efficiency (total power efficiency minus 48-V rail) by pre-loading the 5V aux winding (for good 12V_FLY_B regulation) and then attaching an electronic load on a 3V3_B test point to pull at different constant current values. Efficiency of the buck converter is therefore represents efficiency of the buck + op-amps + temperature sensors + other discrete circuits. The measured 3V3 efficiency = 12V efficiency (as discussed above) * buck efficiency.

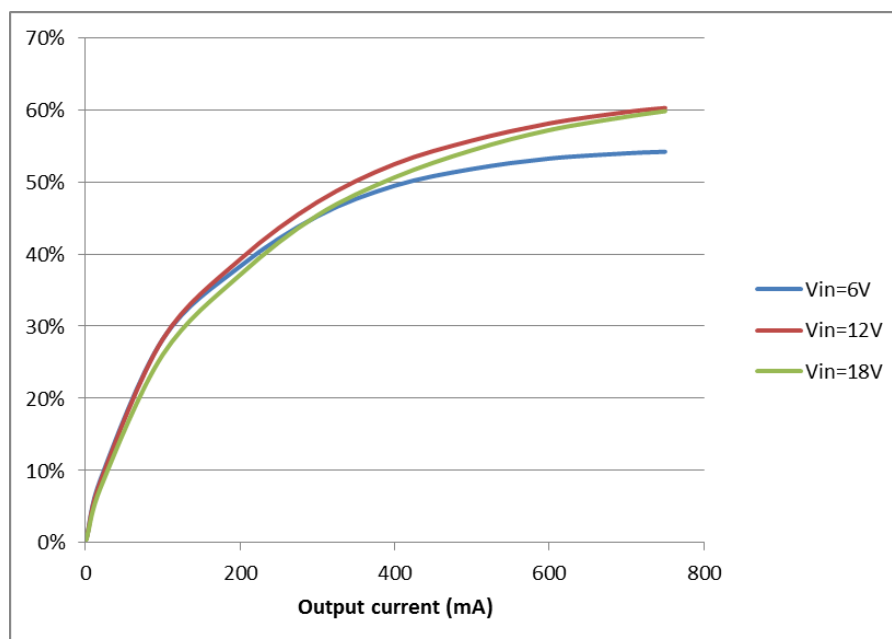


Figure 45 Combined efficiency, 12V flyback and 3.3V buck with 100 Ohm load on 5V supply

7.1.4 48V switching

The 48V switching circuit (refer to Figure 21) allows the local microcontroller to maintain active control over the application of power to the motor drive circuit. Timely application and removal of the 48V power at the drive stage ensures the motor can be used when needed, and quickly disabled when a fault is identified.

In the following oscilloscope plots, channel 1 (yellow) is connected to 48V_BUS_EN on U2-5, the enable pin for LM5060Q1 high-side controller. Channel 2 (purple) is connected to 48V_BATT_B the 48V input, and channel 3 (blue) is connected to 48V_MOTOR_B, which supplies the motor drive stages.

Figure 46 shows the voltages when the 48V supply to the motor drives is enabled by the microcontroller. There is about 4 milliseconds of delay between the 48V_BUS_EN signal going high and when the 48V_MOTOR_B supply is applied to the drive circuits. A slight dip in the 48V input voltage is also noticeable; this is due to the charging current for the capacitors connected to the 48V_MOTOR_B supply.

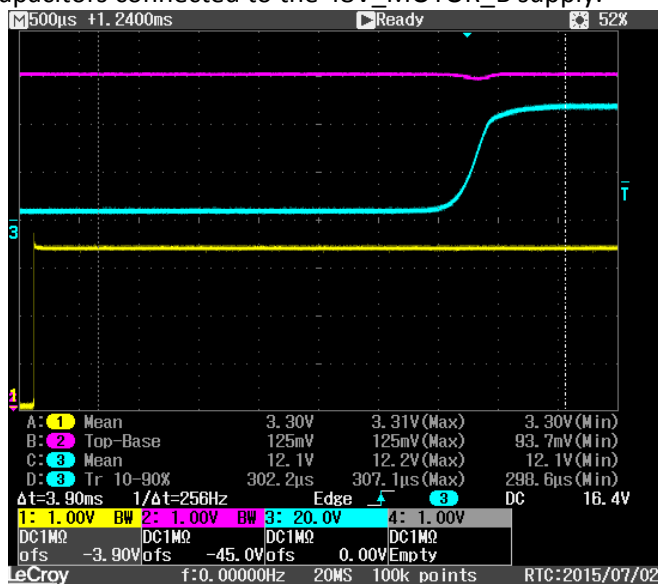


Figure 46 Switching sequence for enabling the 48V supply

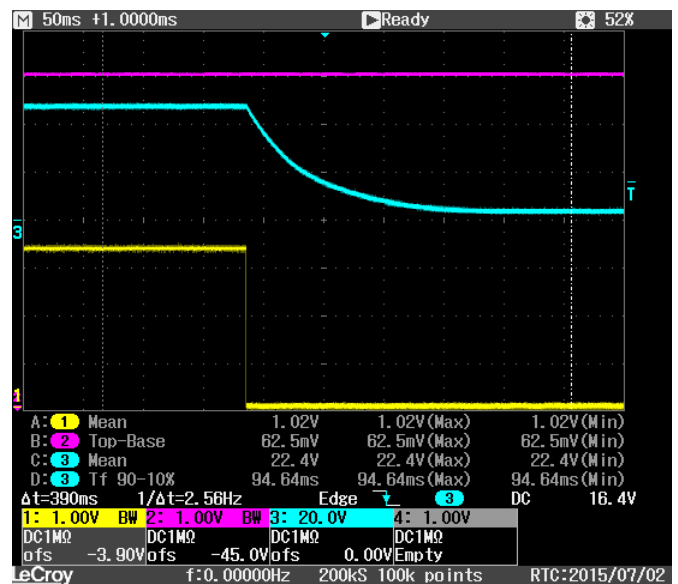


Figure 47 Switching sequence for disabling the 48V supply

Figure 47 shows the voltages when the 48V supply to the motor drives is disabled by the microcontroller. After a brief delay, the 48V_MOTOR_B supply begins to discharge. During this test, no motor load was applied, so the discharge takes about 150 milliseconds to reach relatively low voltage levels.

7.2 Motor Operation

7.2.1 Motor Operation Test Set-Up

This design was tested with various 3-phase BLDC motors. Brief specifications for these are listed in the appendix. To provide a known load for the motor, a dynamometer was coupled to the motor shaft. Figure 48 shows one such motor coupled to the dynamometer, with the boards being tested driving the motor.

Several items should be noted related to this test set-up:

1. The motor will be rotating at high speeds, and has sufficient torque to cause damage or injury. Care should be taken to keep clothing, tools, etc. away from the rotating shaft during testing.

2. Supply voltages above 50V may present a shock hazard. Use caution when setting the 48V supply to higher than nominal values.
3. Alignment of the motor shaft to the dynamometer shaft is important for safe operation and for accurate measurement of the motor performance. Misalignment may lead to damage of the coupling or incorrect torque readings.
4. Rapid changes of the motor speed may lead to overvoltage generated by the motor. Be aware that the generated voltage may exceed the voltage set-point of the 48V supply.

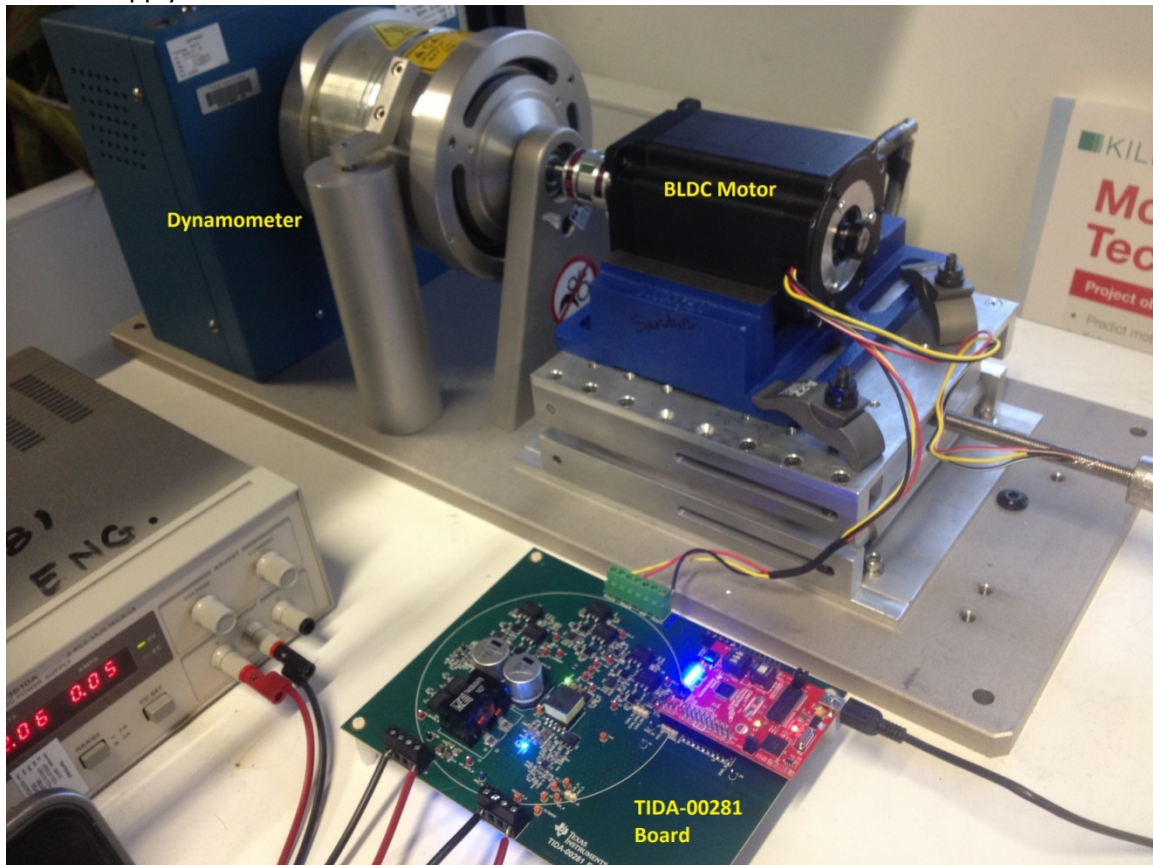


Figure 48 Test set-up with 600W BLDC motor and dynamometer

The dynamometer used during this testing was the Magtrol model HD-705-6N, which is rated for 300W continuous operation, with maximum power up to 1400W for short periods. It is capable of rotation up to 25000 RPM, and can apply up to 55 in-lb (6.2 N-m) of torque. The dynamometer controller was a Magtrol model DSP6001, which can be controlled manually or using the M-TEST software through a serial link to an external computer.

Figure 49 shows one of several user interface screens available in the M-TEST software to set the dynamometer. Later figures will show M-TEST screens which display various dynamometer measurements, including rotational speed, applied load torque (also called dynamometer braking) and power delivered to the load (dynamometer).



Figure 49 User interface for control of the dynamometer hardware configuration

7.2.2 Motor no-load speed and current versus 48V supply voltage

The 48V automotive battery supply can be expected to vary in real-world applications. This design should maintain control of the motor over a range of at least 36V to 60V, but the motor drive performance is affected by the supply voltage.

- At any given supply voltage, the current required to maintain a specific speed will vary more or less directly with the speed.
- Assuming constant load, the maximum attainable speed will increase as the applied supply voltage increases.
- At any given speed, the motor current will vary inversely with the applied voltage, assuming a constant load.

The plots in Figure 50 show these relationships for the BLY344S motor. Note that these measurements were with no dynamometer attached. The maximum no-load speed for each supply voltage is indicated by the endpoint of the corresponding line.

Unless otherwise specified in later sections, the motor supply for all remaining measurements was set to the nominal value of 48V.

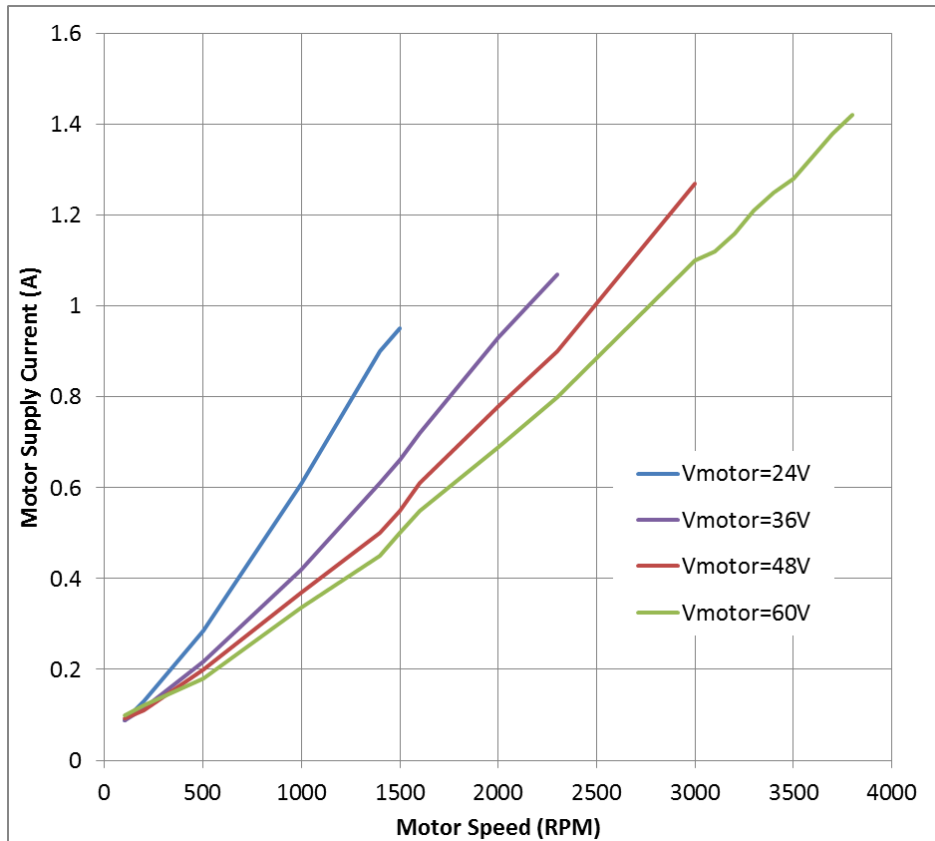


Figure 50 Motor no-load current versus speed for various supply voltages

7.2.3 Motor speed versus constant load

One basic measure of motor performance is operation at various speeds with a constant load. In Figure 51 the EC motor was connected to a dynamometer with a constant 0.5 N-m brake load. The plot shows the measured power applied to the dynamometer load in green, and the measured electrical power from the 48V supply in red. The conversion efficiency from electrical supply power to mechanical load power is shown as the efficiency percentage curve in purple. The factors which contribute to the efficiency losses include the electric power consumed by the components on the circuit board (fairly constant), electrical losses in the motor, and mechanical losses in the coupling and dynamometer.

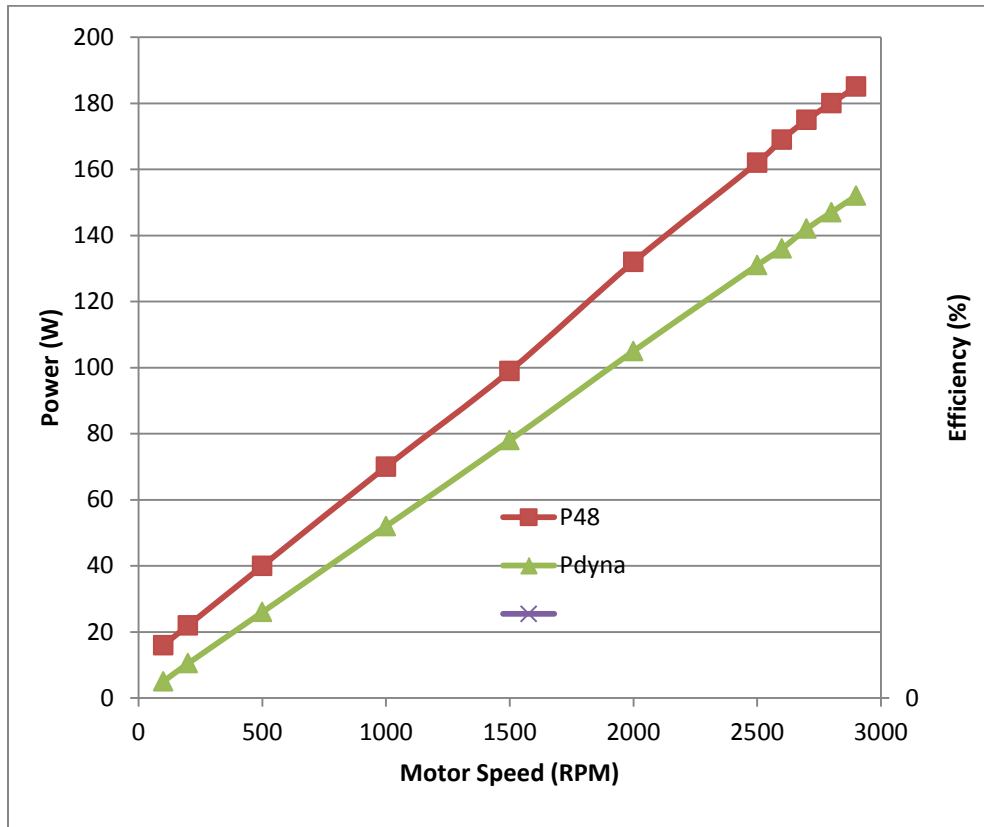


Figure 51 Power versus speed, ElectroCraft motor, 0.5 Nm brake load

Another view of the system performance is the operation with varying torque loads at constant speed. As discussed in later sections, there is a transient speed error when the torque load instantaneously changes. The actual speed then returns to the commanded speed, with motor current proportional to the total torque. Figure 52 shows the electrical power from the 48V supply and the mechanical power measured by the dynamometer as the brake load is varied. The commanded speed was constant at 3000 RPM. Note that even with zero commanded brake load, there is some (approximately 6.5W) of parasitic torque load measured by the dynamometer. Similarly, there is about 30W of electrical power provided by the 48V supply. As the controlled load torque is increased, both the measured dynamometer power and electrical power increase fairly linearly.

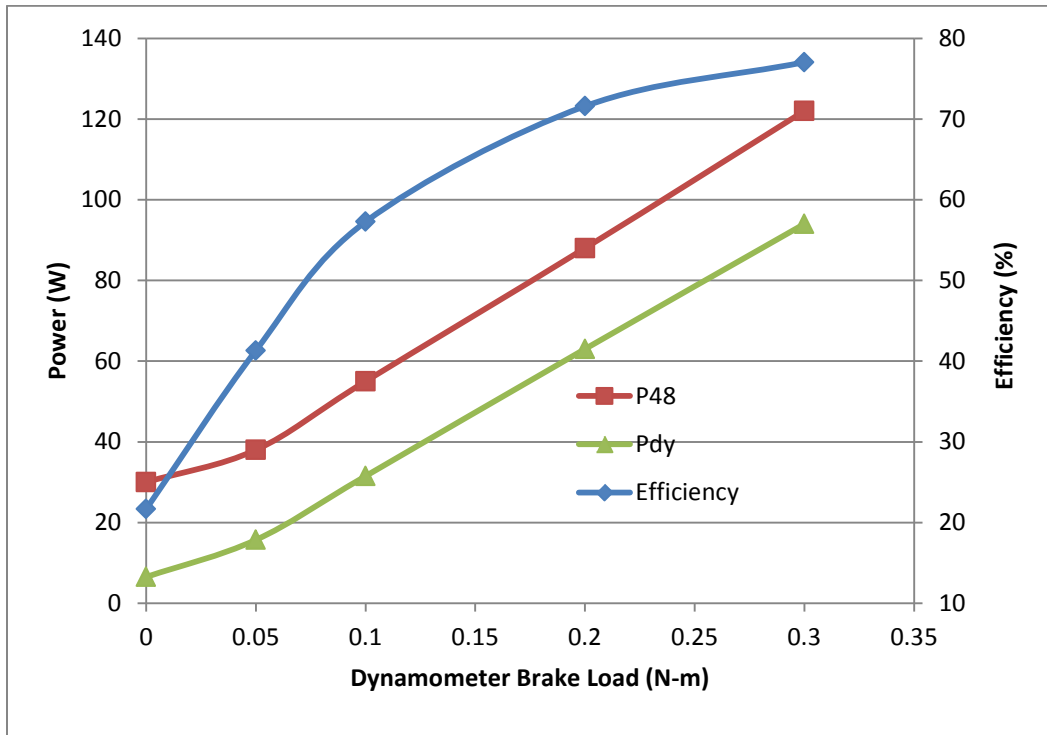


Figure 52 Power vs. Brake Load at Constant Speed

The effect of changing both motor speed and applied brake load is illustrated in Figure 53. Note that (as above) there is a small (e.g.125 mA) electrical current from the 48V supply, even at low speed and negligible load. The supply current (and thus electrical power) increases linearly as the speed increases, and also increases proportionally as the applied brake load is increased.

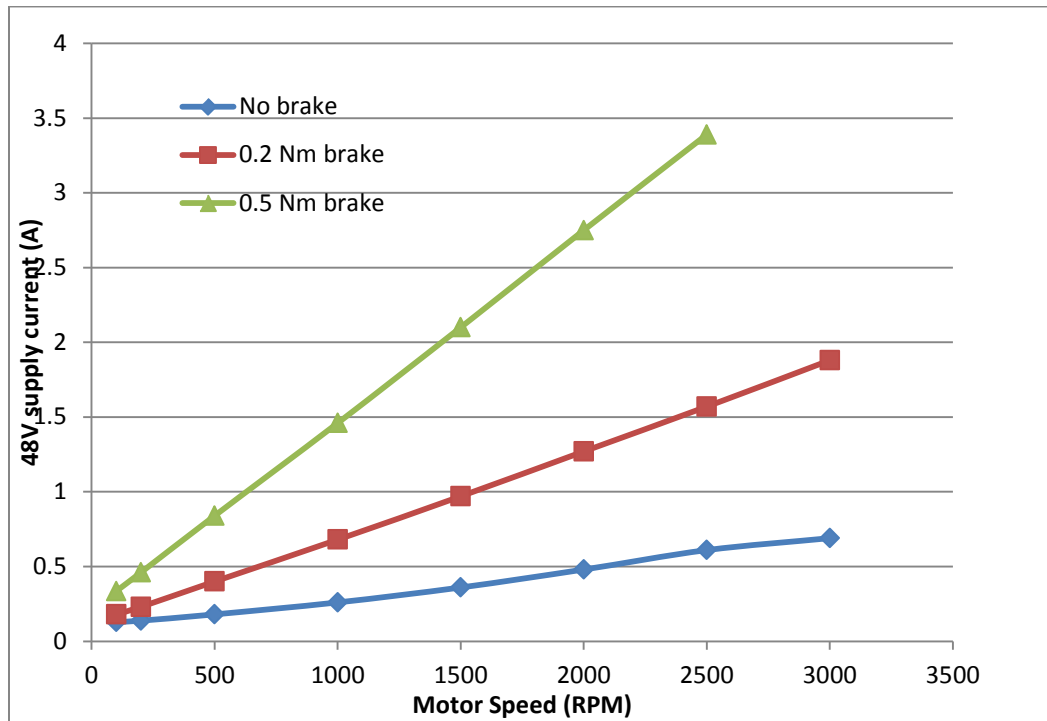


Figure 53 Power supply current vs. motor speed and dynamometer brake load

7.3 Motor Current Feedback

The current through the motor is sensed with an in-line (shunt) resistor between the low-side driver FET and ground. The resistor value is small (1 m Ω) and gain is needed before the signal is sampled by the microcontroller.

In the following oscilloscope plots, signal traces are captured at four points along a single phase of the motor drive circuit. Channel 1 (yellow) is the high-side PWM signal (PWM_AH) from the Launchpad microcontroller to the UCC27201A-Q1 gate drive chip. Channel 2 (pink) is the voltage at the gate of the high-side FET (GATE_DRIVE_AH). Channel 3 (blue) is the motor phase voltage (A_PHASE). Channel 4 (green) is the current feedback signal after amplification by a gain of 20 V/V, giving it a scale factor of 20mV/A (IA_FB).

In each of the following plots, note that the current feedback signal (Channel 4; green) is synchronously sampled by the microcontroller during the time that the low-side drive FET is turned-on. This is when the corresponding high-side drive FET is switched off; that is, when the signal on Channels 1 and 2 is low.

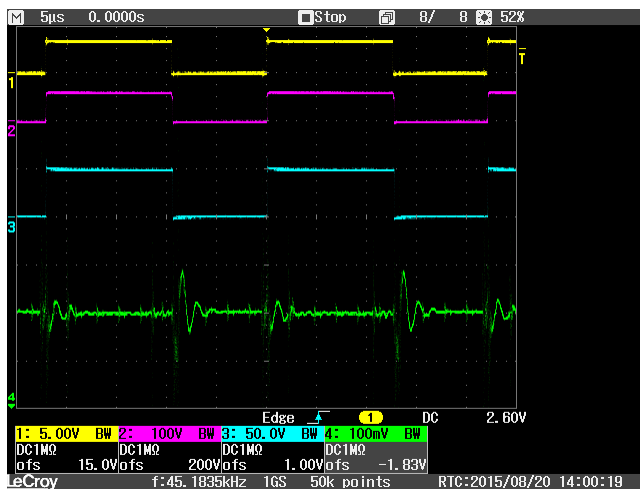


Figure 54 Motor speed 1000 RPM, no load, minimal 48V current (180 mA)

In Figure 54, the PWM signals (Channels 1, 2, and 3) are synchronized, and no significant delay is observable as the high-side signal propagates through the component chain. Channel 4 (green, IA_FB) shows the current has transients during the PWM switch points, but otherwise is relatively stable around the 1.65V offset (half of the 3.3V supply). This allows the effectively “zero” current to be centered in the middle of the usable range of the 3.3V analog-to-digital converters on the LaunchPad.

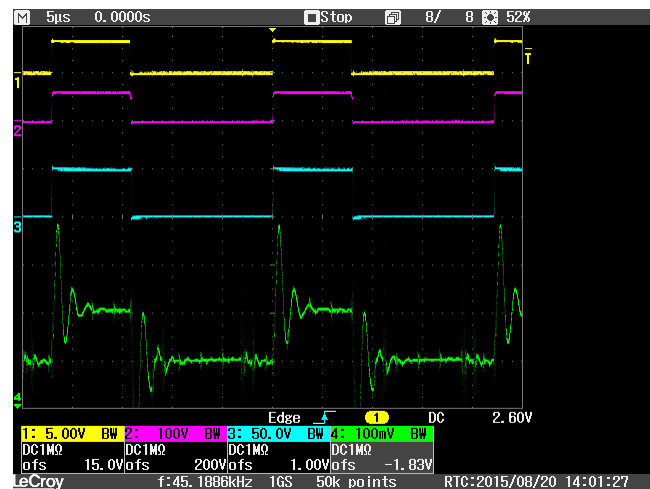


Figure 55 Motor speed 1000 RPM, 20% brake load (0.283 N·m), negative current, 48V current is 0.87A

As the motor current increases, the green signal on Channel 4 shows a departure from the 1.65V “quiescent” point. Note that when the high-side PWM signal is high, the high-side FET is turned on, and there is no current through the low-side FET. Thus the current feedback signal is at the 1.65V quiescent point when the high-side is active. When the high-side signals are low, the low-side FET is on, and the current through the sense resistor is negative (in this case), thus the current feedback signal is less than 1.65V.

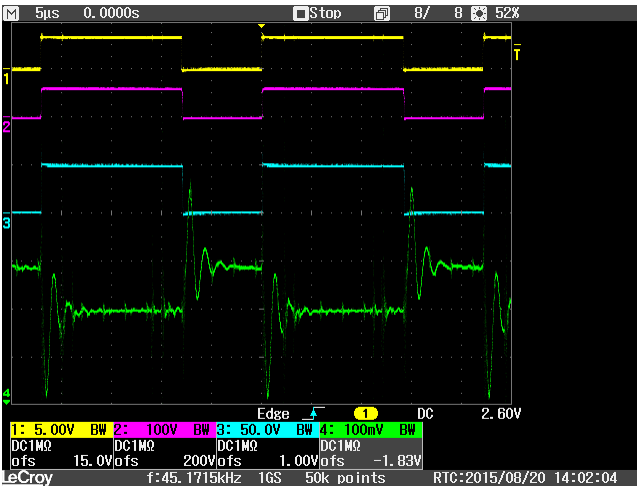


Figure 56 Motor speed 1000 RPM, 20% brake load (0.283 N-m), positive current, 48V current is 0.87A

in Figure 56, the motor speed and overall current are the same as the previous figure, but in this case the signal on Channel 4 indicates positive current going through the sense resistor. The IA_FB signal is still at the 1.65V quiescent point when the PWM signals are high, but is higher than 1.65V when the PWM signals are low. Thus a positive phase A motor current is fed back and sampled by the real-time microcontroller on the LaunchPad.

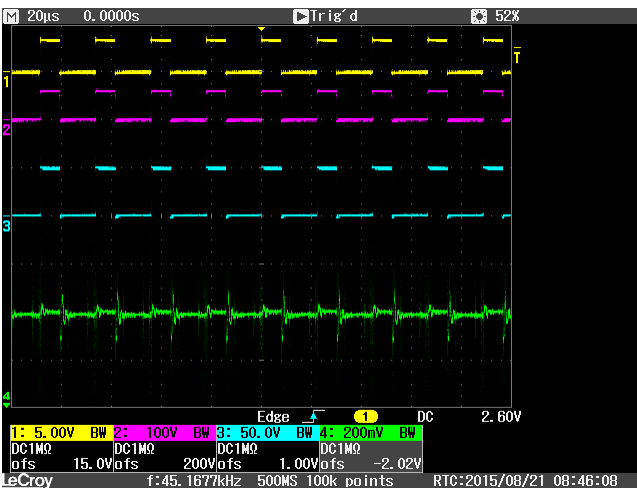


Figure 57 Motor speed 1200 RPM, no brake load, 48V current is 0.22A

The horizontal scale in Figure 57 and Figure 58 is changed to 20 microseconds per division, and the motor speed is increased to 1200 RPM. At this motor speed, one mechanical rotation of the motor takes 50 milliseconds; since the motor has 4 pole pairs, each electrical cycle has a period of 12.5 milliseconds. This electrical period will be more observable in later figures.

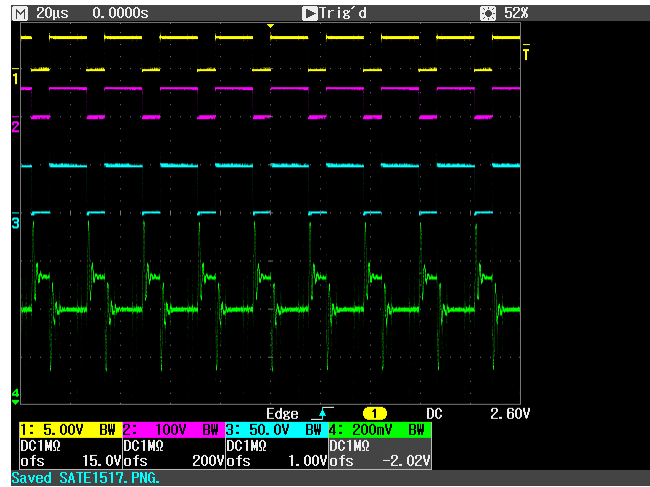


Figure 58 Motor speed 1200 RPM, 0.4 N-m dyno load, 48V current is 1.45A

The horizontal time scale has been lengthened to 200 microseconds per division in Figure 59. Although the PWM signals are less distinct, the current feedback signal on the green channel shows the time-varying characteristics as the current through this phase changes with the motor angular position. Again note that during the time when the high-side FET for phase A is active, there is no current through the corresponding low-side FET, thus the feedback signal is at the 1.65V quiescent position during part of each PWM period.

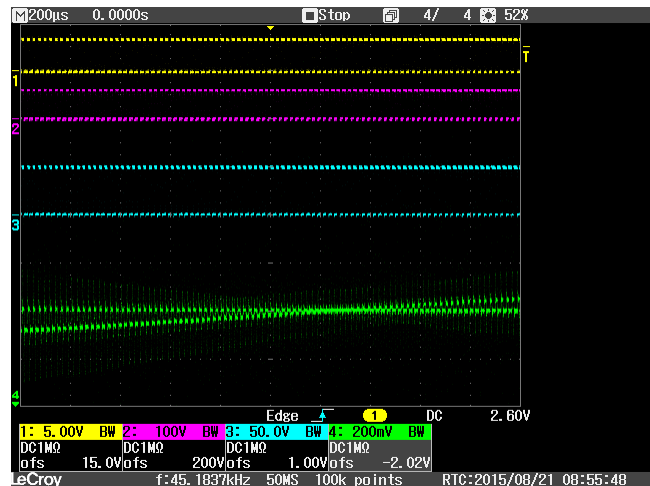


Figure 59 Envelope of motor phase current feedback signal, 1200 RPM, showing variation as motor angle changes

In Figure 60 through Figure 65, the increasing amplitude of the current feedback signal is illustrated, as the load applied by the dynamometer is increased. The motor speed is held constant at 1200 RPM in these figures.

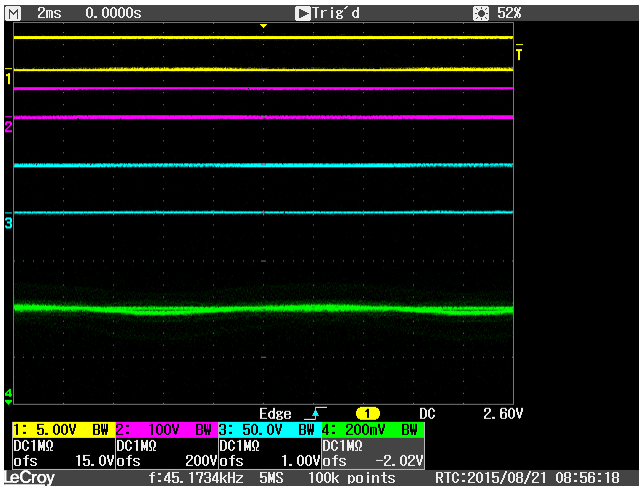


Figure 60 Envelope of motor phase current feedback signal, 1200 RPM, no brake load

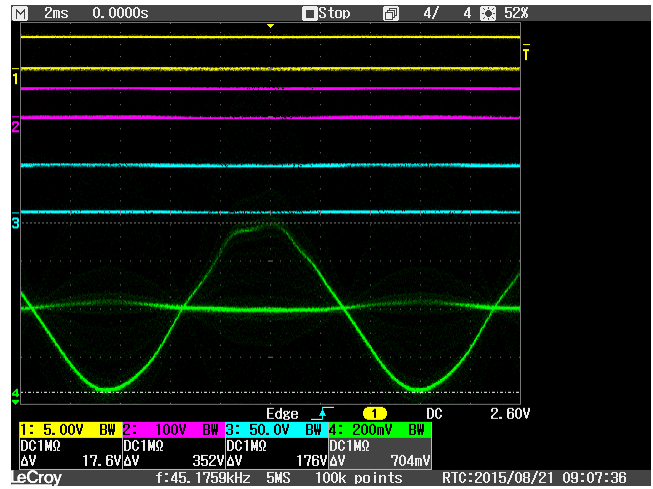


Figure 63 Envelope of motor phase current feedback signal, 1200 RPM, 1.0 N-m load

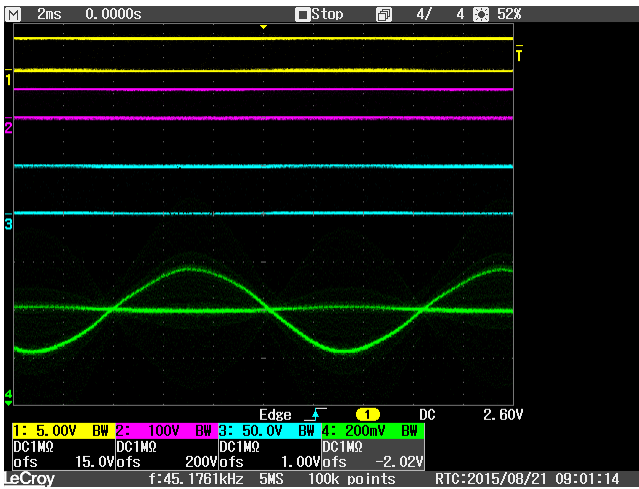


Figure 61 Envelope of motor phase current feedback signal, 1200 RPM, 0.5 N-m load

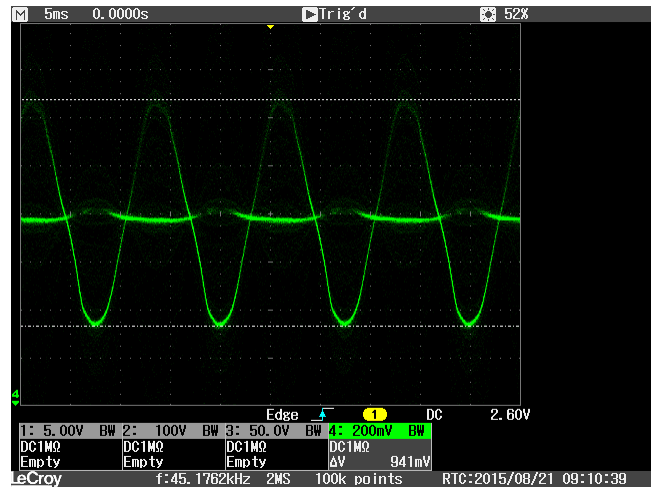


Figure 64 Envelope of motor phase current feedback signal, 1200 RPM, 1.3 N-m load

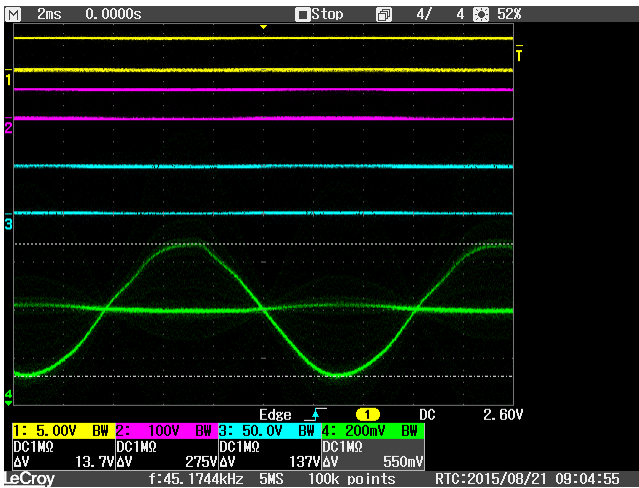


Figure 62 Envelope of motor phase current feedback signal, 1200 RPM, 0.8 N-m load

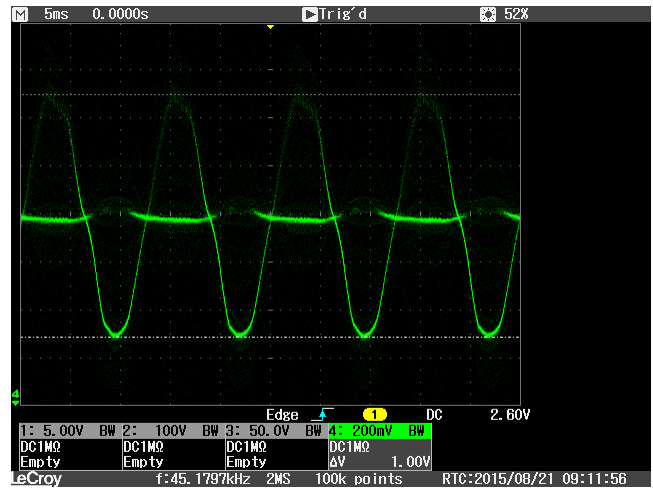


Figure 65 Envelope of motor phase current feedback signal, 1200 RPM, 1.4 N-m load

The current feedback signal (IA_FB) reaches a peak amplitude of about 500 mV (1Vp-p) in Figure 65. The total current from the 48V supply is about 7.3 Amps (rms) for a total electrical power of 350 Watts into the system. The period of the sinusoidal envelope of the current feedback is 5 horizontal divisions, or 12.5 milliseconds, as expected. A summary of these test results is shown in Figure 66 which also shows the electrical power supplied by the 48V supply, and the mechanical power delivered to the load, as measured by the dynamometer.

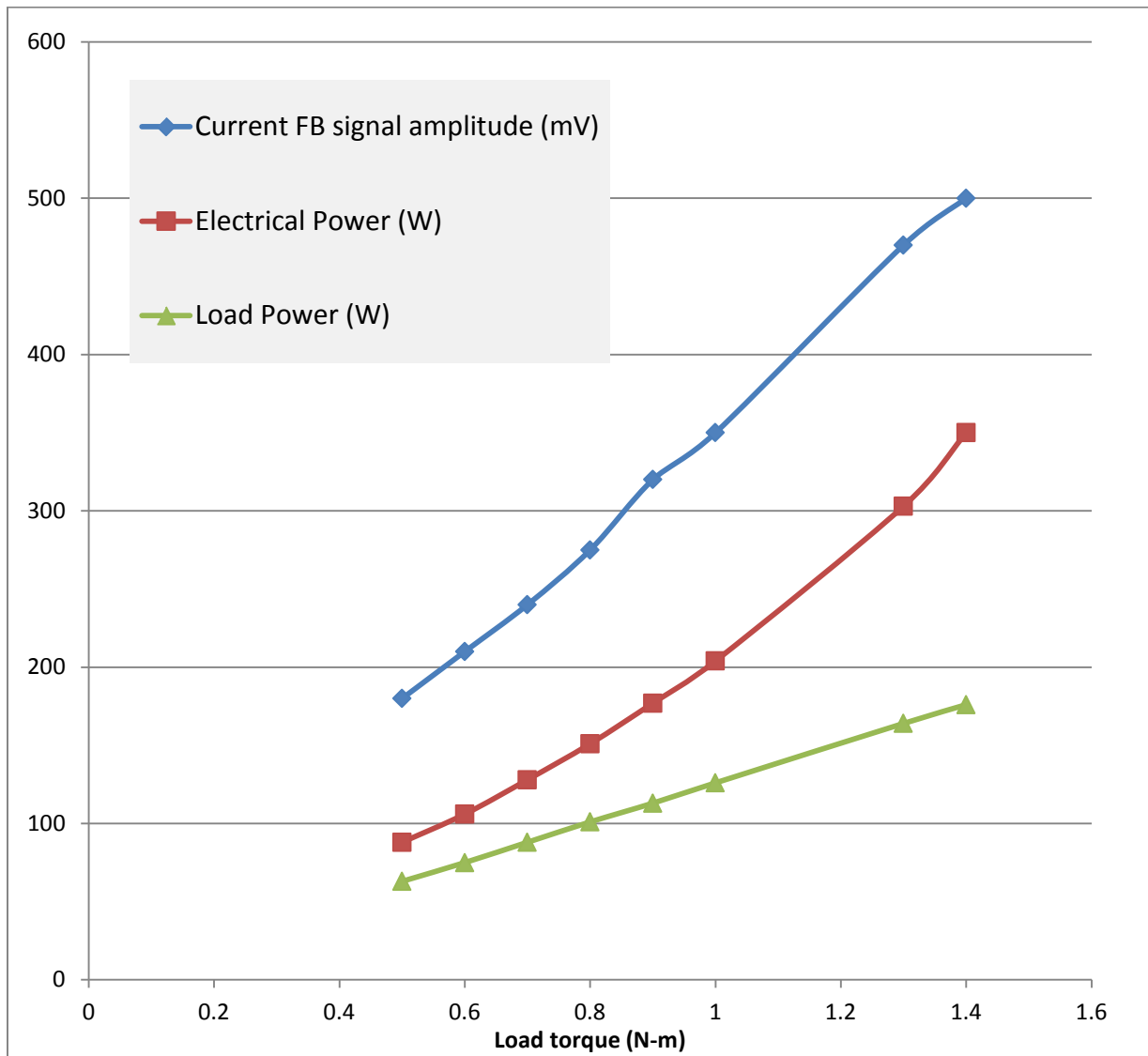


Figure 66 Summary of current feedback measurement results

7.4 Motor Phase Voltages and Feedback Signals

The voltage supplied to each phase of the motor is controlled by the C2000 Real-time microcontroller on the LaunchPad, which sends pulse-width modulated (PWM) signals to each of the UCC27201 gate drivers. The UCC27201 outputs alternately switch the high-side and low-side FETs for each motor phase, supplying the motor phase current needed to create torque in the brushless DC motor.

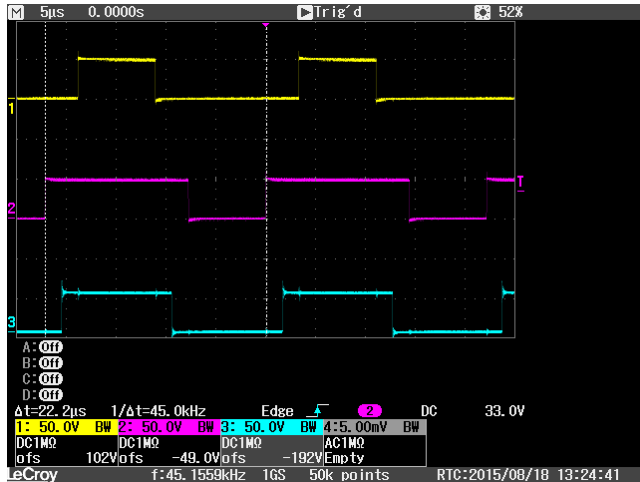


Figure 67 Phase voltages, 1000 RPM, No load

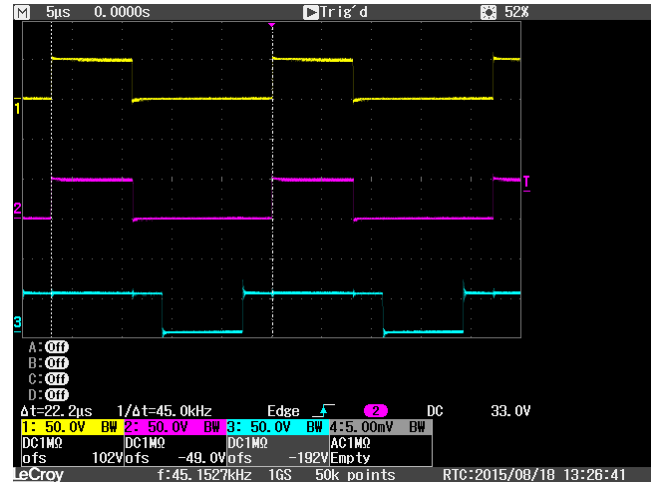


Figure 69 Phase voltages, 1000 RPM, 30% brake

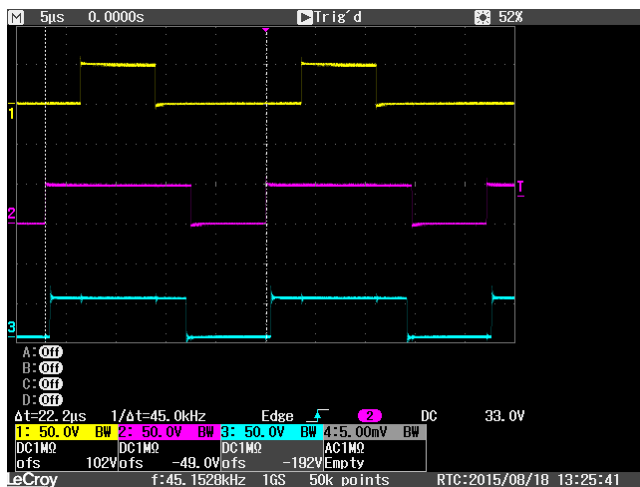


Figure 68 Phase voltages, 1000 RPM, 20% brake

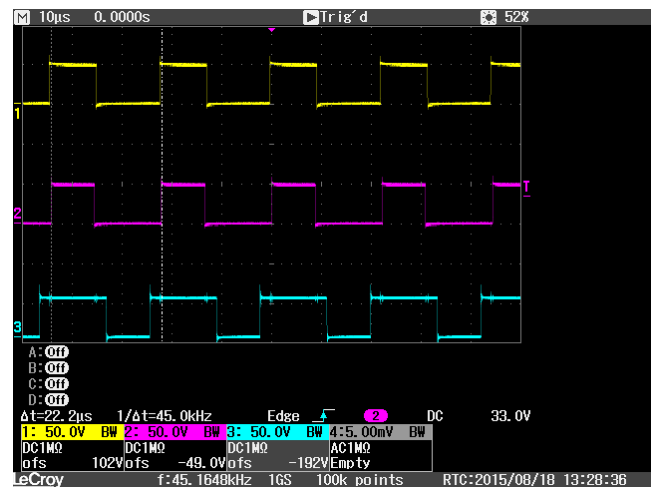


Figure 70 Phase voltages, 1000 RPM, no brake

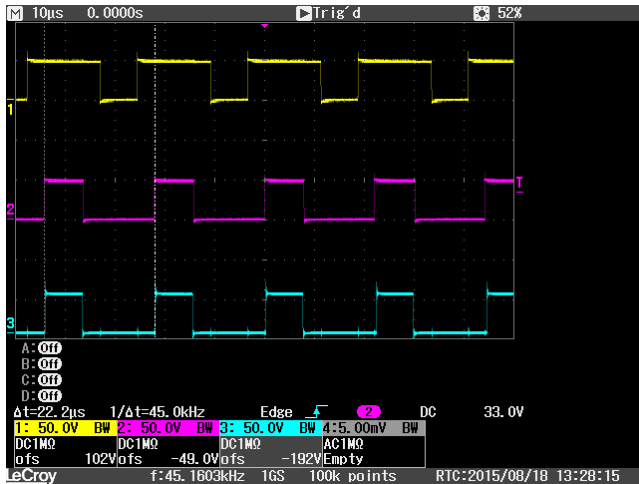


Figure 71 Phase voltages, 1000 RPM, 20% brake

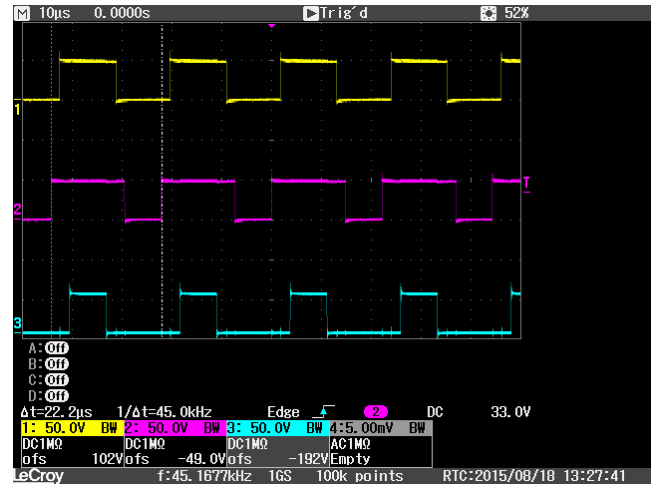


Figure 72 Phase voltages, 1000 RPM, 30% brake

In addition to the PWM signals and motor phase voltages, the feedback signal to the microcontroller is also of interest. The motor commutation algorithm and control loops require information on the present voltage on each of the motor phase windings. The motor phase current is filtered and scaled to fit the 3.3V analog-to-digital converter (ADC) inputs on the C2000, providing a feedback signal for the digital control loop.

In Figure 73 through Figure 81, these signals are captured on oscilloscope plots under various operating conditions. Channel 1 (yellow) is the PWM signal from the C2000 to the UCC27201 high-side gate driver input (PWM_AH). Channel 2 (pink) is the corresponding output from the UCC27201 to the phase A high-side FET gate (GATE_DRIVE_AH). Channel 3 (blue) is the voltage at motor phase A (A_PHASE). Channel 4 (green) is the filtered, shifted, scaled version of the phase signal that is fed back to the C2000 ADC. (VA_FB).

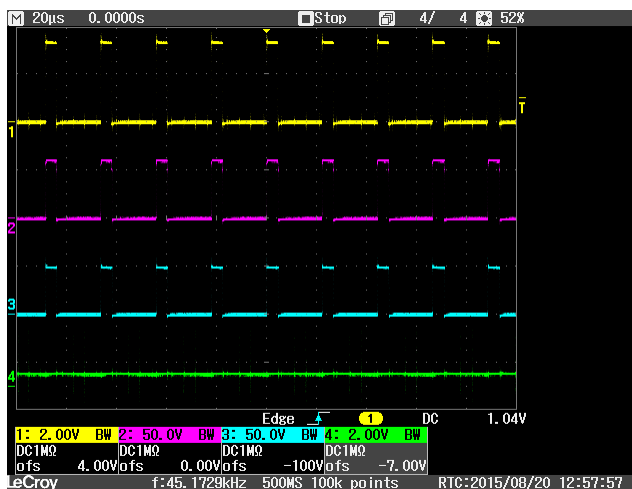


Figure 73 Motor speed 2400 RPM, no load, phase A duty cycle < 50%

In Figure 73, the PWM signal from the microcontroller is high about 25% of the time; this is reflected in Channels 1, 2 and 3. Channel 4 is a filtered version, scaled for the ADC, and represents the average (filtered) version of the PWM phase voltage, about 500 mV.

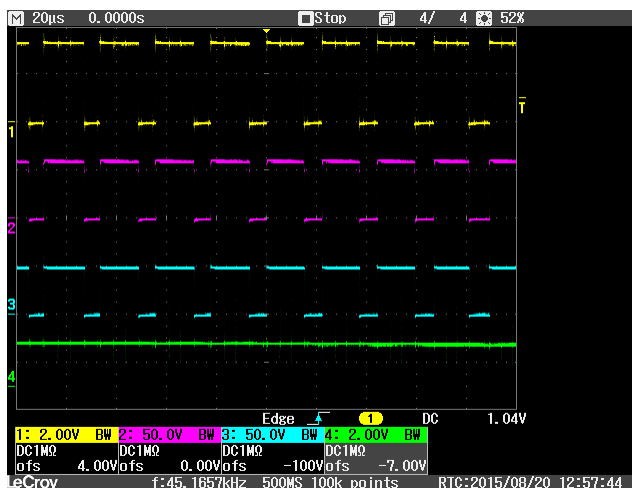


Figure 74 Motor speed 2400 RPM, no load, phase A duty cycle > 50%

In Figure 74, the motor is at a different point in its rotation, and the PWM signal from the microcontroller is high about 75% of the time; this is reflected in Channels 1, 2 and 3. Channel 4 is about 1V.

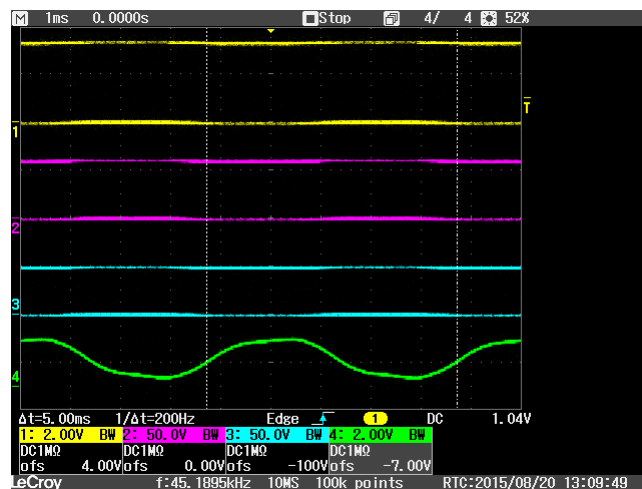


Figure 75 PWM_AH, GATE_DRIVE_AH, A_PHASE and VA_FB with motor speed 3000 RPM, no load, showing Phase A average voltage repeating with a 5 ms period (4 pole-pair motor)

Figure 75 has a longer time scale, such that the individual PWM pulses are no longer distinct on Channels 1, 2 and 3. At this scale, the sinusoidal variation in the filtered feedback signal (VA_FB on Channel 4) can be observed. The peak-to-peak amplitude of the feedback signal is about 2V, which fits well with the 3.3V range of the C2000 ADCs.

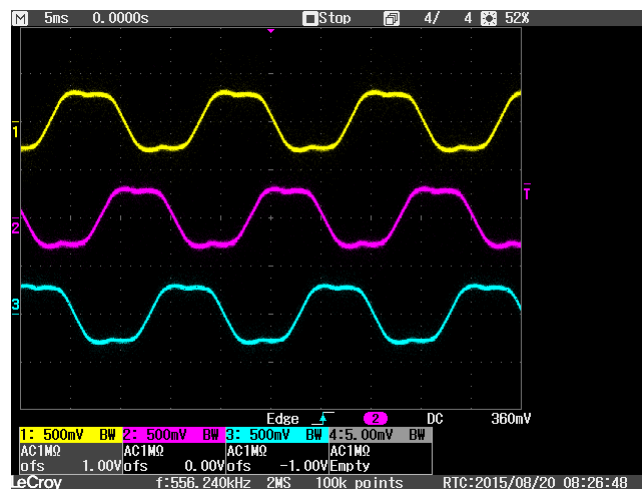


Figure 76 Phase voltage feedback signals, 1000 RPM, no brake, 9.5W electrical power

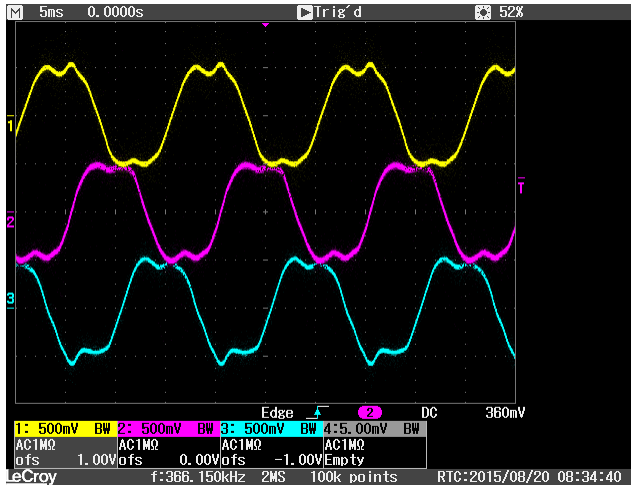


Figure 77 Phase voltage feedback signals, 1000 RPM, 126W (1.2 N-m) load, 225W electrical power

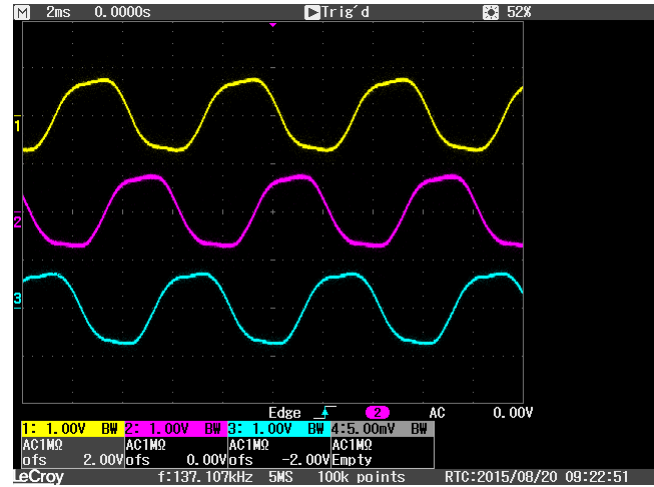


Figure 79 Phase voltage signals, 2500 RPM, 0.3 N-m load, 84W @ dyno, 107W electrical power

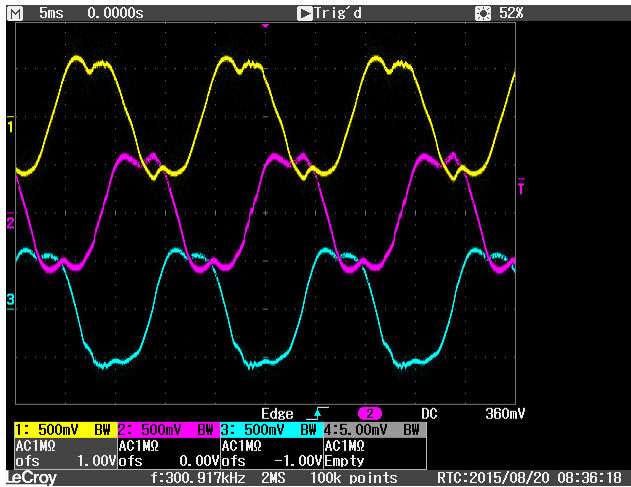


Figure 78 Phase voltage feedback signals, 1000 RPM, 147W (1.x N-m) load, 324W electrical power

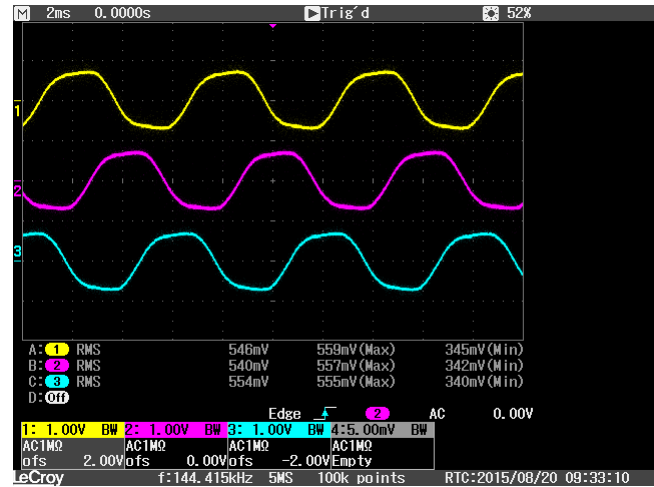


Figure 80 Phase voltage signals, 2500 RPM, 0.19 N-m load, 50W @ dyno, 68W electrical power

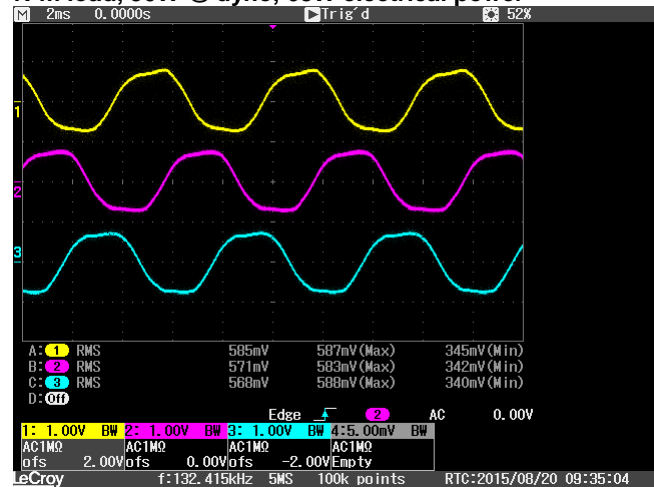


Figure 81 Phase voltage signals, 2500 RPM, 0.4 N-m load, 104W @ dyno, 130W electrical power

7.5 Response to Speed Ramp Commands

One measure of performance for this system is its ability to respond to a change in commanded speed. In this section, the speed command was changed from an initial setting to a final setting. Since the MotorWare software includes a setting for angular acceleration, the change in commanded speed is implemented as a ramp (either increasing or decreasing) with uniform acceleration from the initial angular velocity to the final angular velocity. A dynamometer is used to apply a braking torque load to the system and to measure the actual angular velocity.



Figure 82 Speed ramp increase from 300 RPM to 600 RPM @ 200 RPM/sec, no brake

The actual measured speed in Figure 82 shows a brief overshoot speed error as the motor reaches the final velocity of 600 RPM. The peak speed error is about 15 RPM, which represents a 5% error compared to the step speed increase of 300 RPM.



Figure 84 Speed ramp from 200 RPM to 2000 RPM @ 200 RPM/sec, 0.33 Nm load (77W)

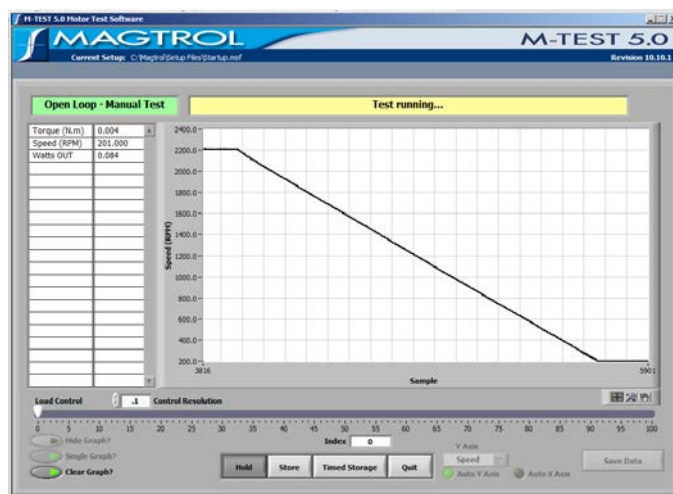


Figure 85 Ramp speed decrease from 2200 RPM to 200 RPM, no load



Figure 83 Speed ramp from 200 RPM to 2000 RPM @ 200 RPM/sec, no brake

In Figure 86 the angular acceleration has been increased to 500 RPM/second. This results in an observably higher overshoot of the final speed as compared to Figure 84, which has similar loading but a lower acceleration rate.

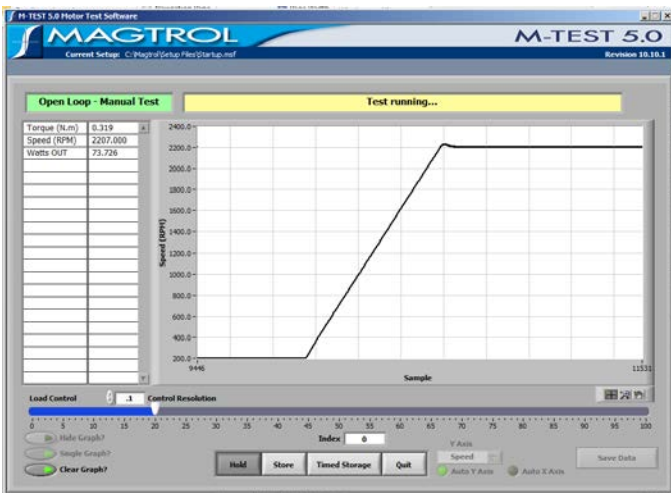


Figure 86 Speed ramp increase from 200 RPM to 2200 RPM @ 500 RPM/sec, 0.32 Nm load

This trend continues in Figure 87, in which the acceleration has been increased to 1000 RPM/second. The speed overshoot has increased to about 50 RPM, which is 2.5% of the commanded increase in speed.

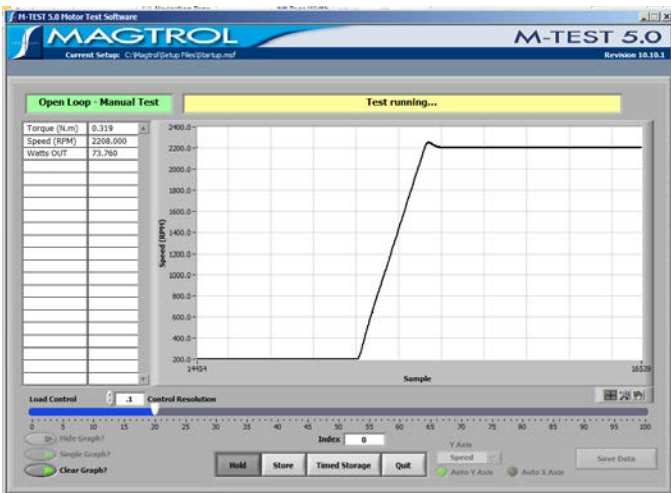


Figure 87 Speed ramp increase from 200 RPM to 2200 RPM @ 1000 RPM/sec, 0.32 Nm load



Figure 88 RP34-313, speed increase from 200 RPM to 2200 RPM @ 500 RPM/sec, no brake

In Figure 88 and Figure 89, the effect of reducing the load torque is illustrated. In these figures, the dynamometer brake was disabled. The maximum overshoot in speed is about 50 RPM, which is very comparable to the overshoot with 0.32 Nm.



Figure 89 RP34-313 motor, 48V, detail of speed increase from 200 RPM to 2200 RPM @ 500 RPM, showing overshoot in speed response

The following figures (Figure 90 - Figure 93) show additional examples of increases and decreases in the commanded speed of the motor. In these figures, the speed error is a function of the motor and load characteristics, as well as the parameters set in the control software. For more information, see the labs on motor control in the MotorWare software package.

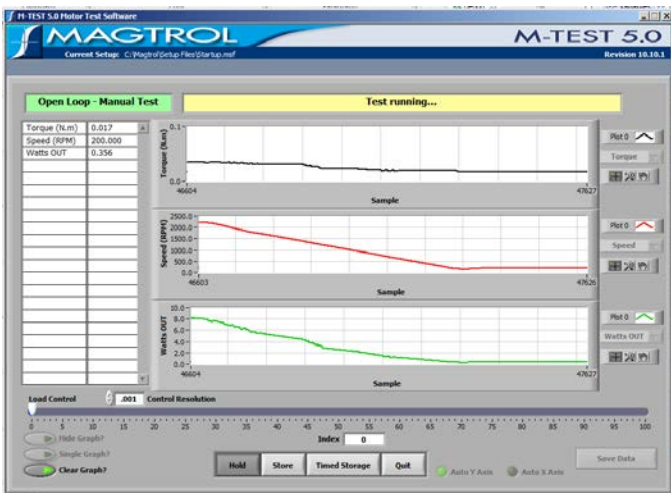


Figure 90 RP34-313, speed decrease from 2200 RPM to 200 RPM @ 500 RPM/sec, no brake



Figure 92 Speed response, RP34-313, 48V, 14% brake load



Figure 91 Detail of speed decrease showing overshoot in speed response

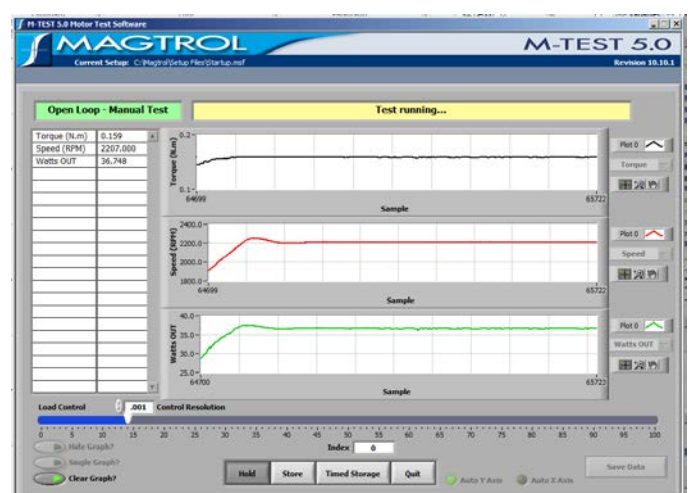


Figure 93 Speed response, RP34-313, 48V, 14% brake load, detail showing overshoot in speed response

7.6 Response to Load Torque Steps

7.6.1 Load Torque Step Test Set-up

The response of the motor control design to step changes in load torque was tested using the dynamometer set-up as described above. Step changes in the load torque were commanded via the M-TEST user interface, by altering the load control setting between two steady-state values. Unless otherwise specified, all tests were performed with a nominal 12V supply and a nominal 48V supply.

7.6.2 Load Torque Step Test Results

In Figure 94 the motor is commanded to spin at a rate of 1000 RPM, with an initial light load of 0.1 N-m. A step increase in the dynamometer braking load is then commanded, increasing the load torque to 1.36 N-m. This is indicated in the

top (black) trace. In this figure, the vertical grid lines represent 100 samples (600 ms @ 6ms/sample) so the torque step transition takes about 300 ms.

The second (red) trace shows the speed of the tachometer, which is firmly coupled to the BLDC motor. From the initial 1000 RPM, the speed momentarily decreases when the braking torque step is applied. In this case, a peak speed error of about 30% is evident. The motor speed returns to the commanded 1000 RPM after about 500 milliseconds.

The third (green) trace shows the power measured at the tachometer, and is the product of the measured torque and rotational speed. Note that with the 1.36 N-m load applied at 1000 RPM, the power delivered to the tachometer is about 143 Watts.

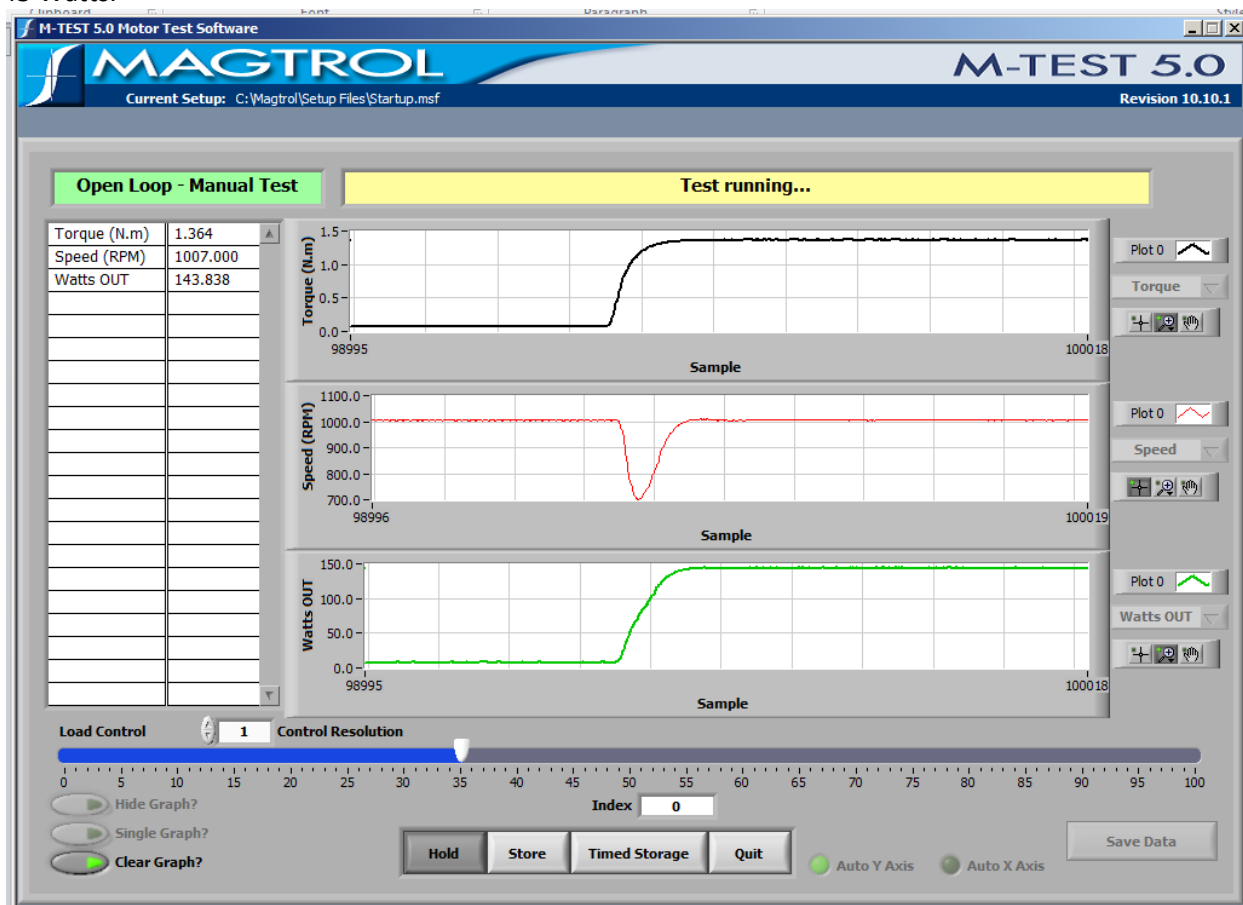


Figure 94 Response to a positive increase in load torque

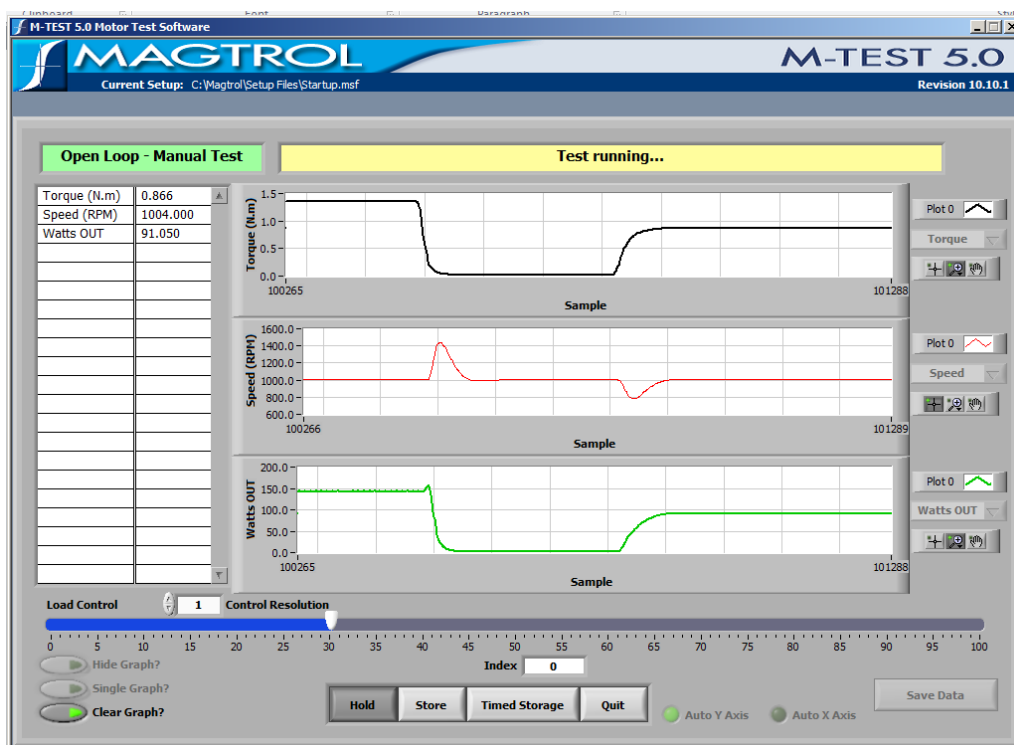


Figure 95 Response to decrease then increase in load torque, 1000 RPM, 150W to no brake then 90W load

Note that in Figure 95 the maximum speed error during the decrease in load torque is about 45%, and the maximum speed error during the increase in load torque is about 20%, corresponding to the amplitude change of the load torque.

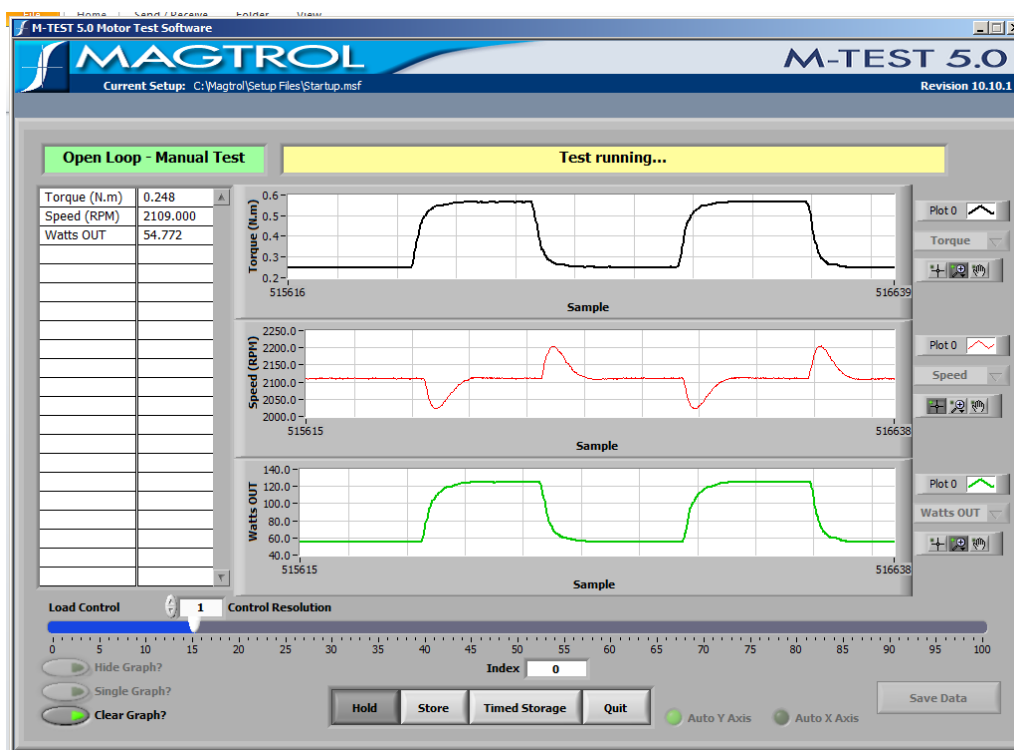


Figure 96 Repeated torque steps between 0.25 N-m and 0.55 N-m, with motor speed 2100 RPM

In Figure 96 the load torque applied by the dynamometer is repetitively cycled between 0.25 N-m and 0.55 N-m, with the motor commanded to a constant 2100 RPM speed. This represents a load power that alternates between about 55W and 125W. As the load varies in a stepwise fashion, the speed changes from the set-point of 2100 RPM and then recovers as the control loop compensates for the change in load.

7.7 Dead-time Settings and PWM Signals

The pulse-width modulation signals from the LaunchPad's C2000 Real-time microcontroller to the UCC27201 gate driver must incorporate sufficient "dead-time" (or deadband) such that the high-side FETs and low-side FETs for any motor phase are never on at the same time. This would cause a short-circuit between the 48V supply and ground through the high-side and low-side FETs.

The dead-time on the rising and falling edges of the PWM signal can be independently set, by altering the code in the hardware abstraction layer file, hal.h, as shown in Figure 97 below. Note that the unit of time is system clock periods, which for the TMS320F28027F LaunchPad is 16.7 nanoseconds (the reciprocal of the 60 MHz system clock frequency). Integer multiples of the clock period are valid settings for these parameters.

```

115
116 /// \brief Defines the PWM deadband falling edge delay count (system clocks)
117 ///
118 #define HAL_PWM_DBFED_CNT      1      // originally was 4
119
120
121 /// \brief Defines the PWM deadband rising edge delay count (system clocks)
122 ///
123 #define HAL_PWM_DBRED_CNT      1      // originally was 4
124

```

Figure 97 Code fragment in hal.h, allowing setting the PWM dead-time parameters

In part due to the precise timing specifications of the UCC27201A-Q1, the dead-time for this design can be reduced below the default value of 4 system clock cycles (67 nanoseconds). Figure 98 and Figure 99 show the two PWM signals associated with motor phase A, and illustrate the adjustability of the dead-time parameter, in this case for the falling edge. Note that in both plots, the measured dead-time between transitions is as expected.

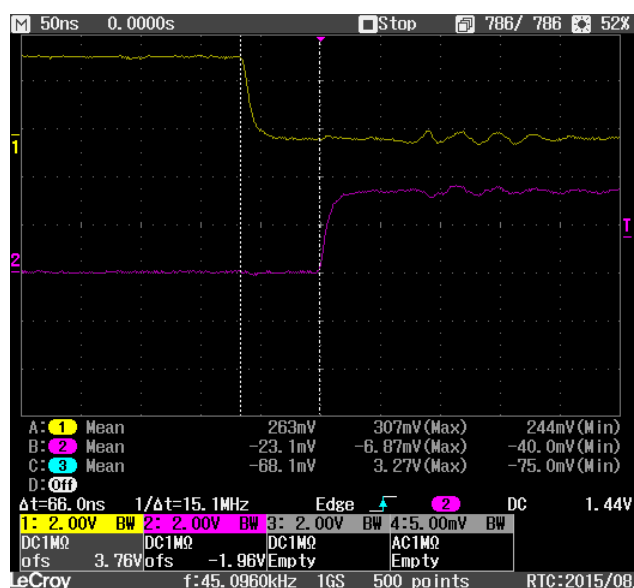


Figure 98 PWM phase A HI (yellow) and low (pink) with deadband = 4

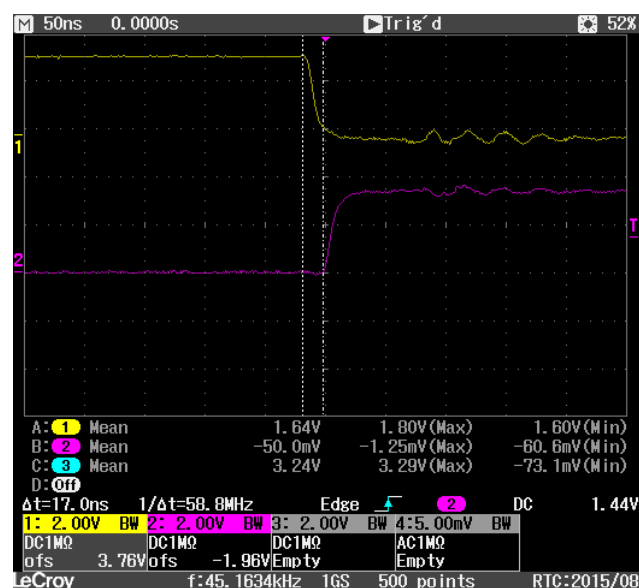


Figure 99 PWM phase A HI (yellow) and low (pink) with deadband = 1

Figure 100 and Figure 101 show the effect of changing the dead-time parameter on the waveforms of the motor drive stage. In these oscilloscope plots, channel 1 (yellow) is the gate drive signal from the UCC27201A-Q1 to the high-side FET gate, and channel 2 (pink) is the gate drive signal to the low-side FET. Although it is difficult to discern the initiation of the rising edge due to the shape of the waveform, it is evident that even with only 1 system clock period of dead-time, there is no overlap in the high-side FET and low-side FET “on” times.

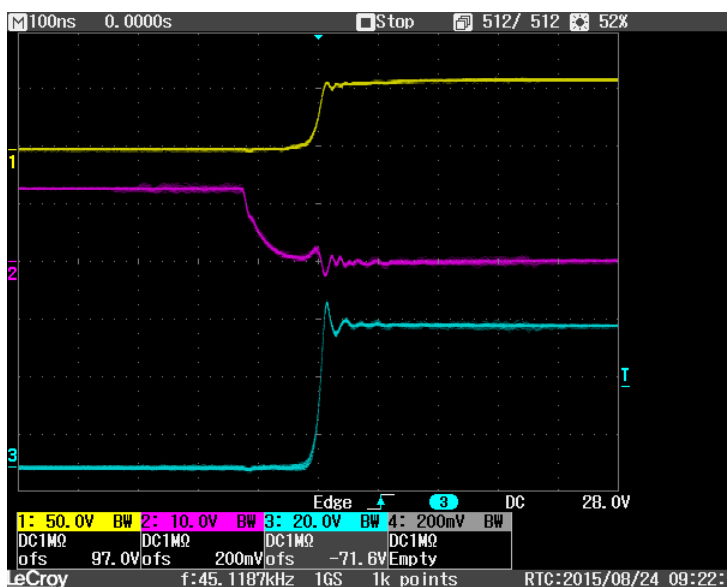


Figure 100 PWM signal GATE_DRIVE_BH (yellow) and GATE_DRIVE_BL (pink) with 4 pu dead-time, blue channel is Phase B motor voltage

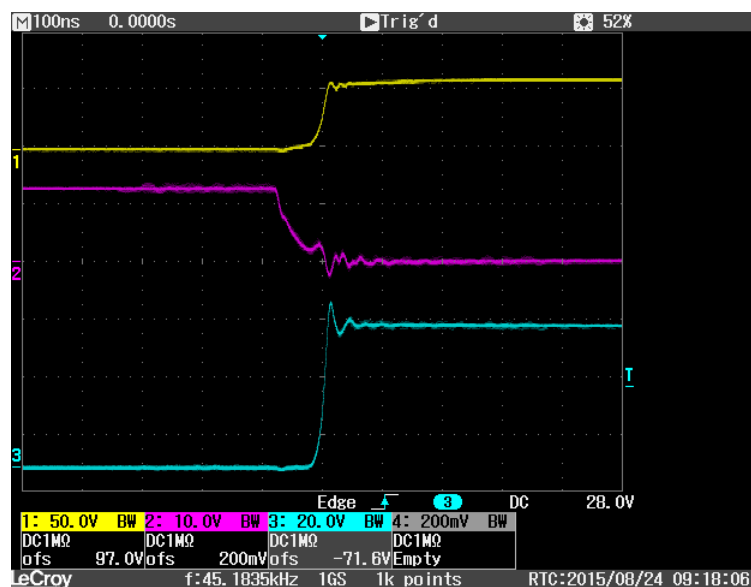


Figure 101 PWM signal GATE_DRIVE_BH (yellow) and GATE_DRIVE_BL (pink) with 1 pu dead-time, blue channel is Phase B motor voltage

Figure 102 shows the effect of varying one of the “tuning” components around the motor drive stage. In this case, the capacitor which couples high-frequency ringing through the RCD clamp circuit (C73 in Figure 22) has been changed from the default value of 1 nF to a new value of 10 nF. Compare the amplitude of overshoot on the channel 3 waveform (A_PHASE) to the previous plot in Figure 101.

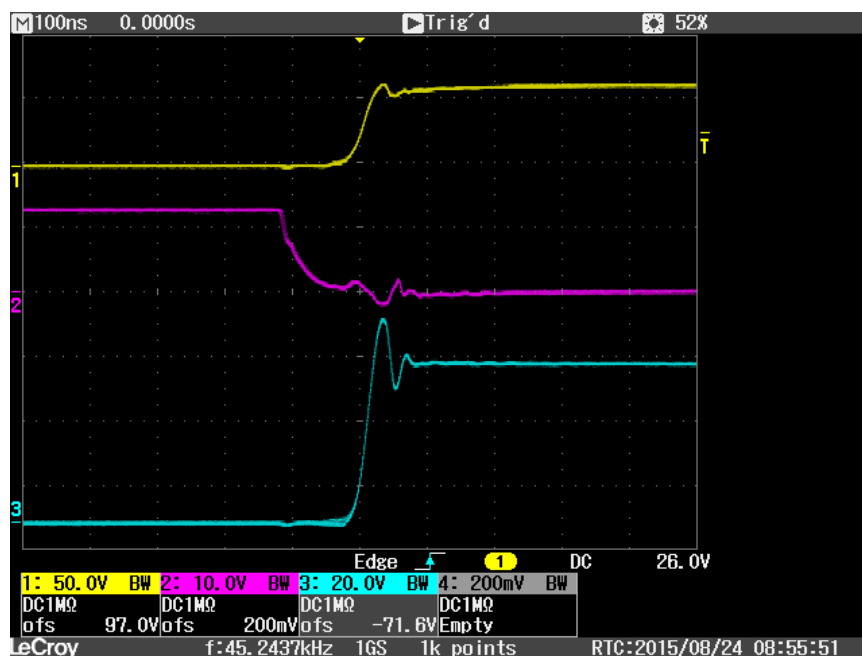


Figure 102 PWM gate drive phase A HI (yellow) and low (pink) with 1 pu deadband, blue channel is Phase A motor voltage, C73 = 10 nF

7.8 Motor Identification Algorithm Testing

One of the features of InstaSPIN-FOC is the ability to identify the parameters of the BLDC motor automatically. The InstaSPIN FOC Motor Identification algorithm measures all the required electrical motor parameters of an unloaded motor in under 2 minutes (typical). The motor identification is based on measures of the current and voltage for the motor phases, as illustrated in Figure 103. Note that these measurements are also the basis for sensorless commutation, as the FAST estimator calculates the motor flux, angle, speed, and torque.

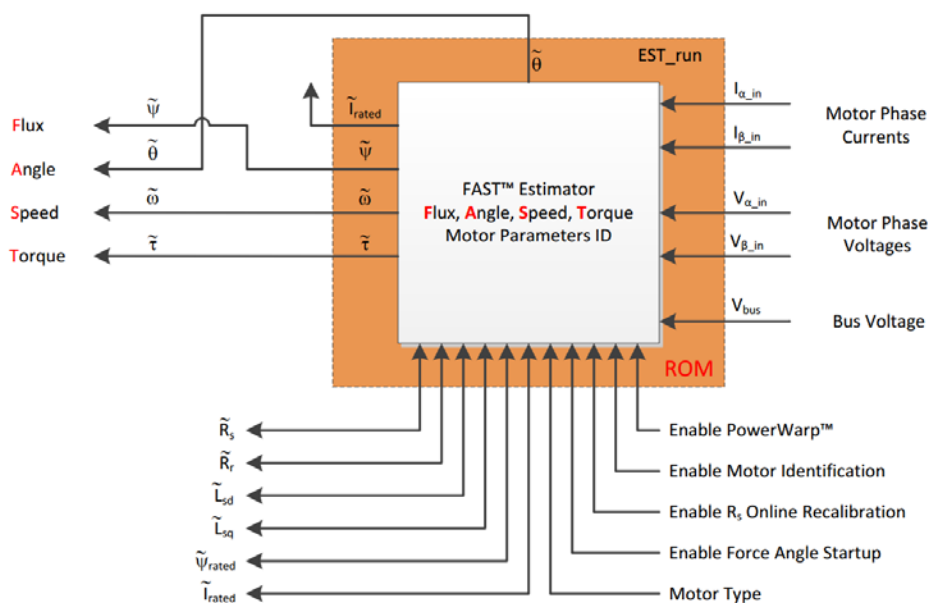


Figure 103 Automatic motor identification using InstaSPIN

For the testing below, the nominal conditions of 48V supply, and motor with no dynamometer brake load were used. Figure 104 and Figure 105 show the results of repeated runs of motor identification, and illustrate the repeatable nature of the identification process.

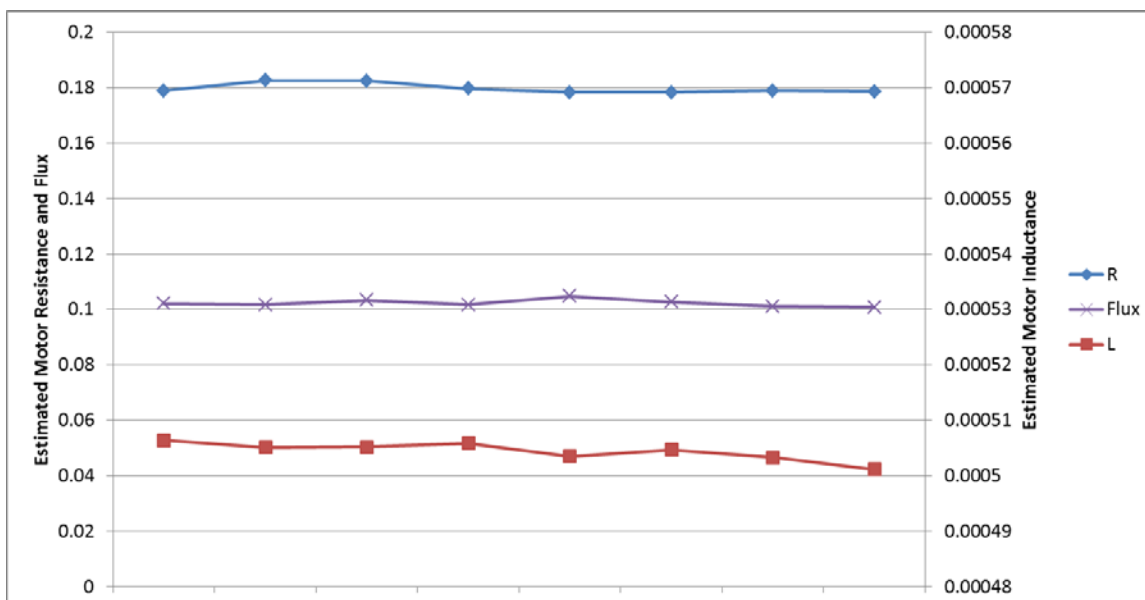


Figure 104 Results of repeated motor identification (specialty motor)

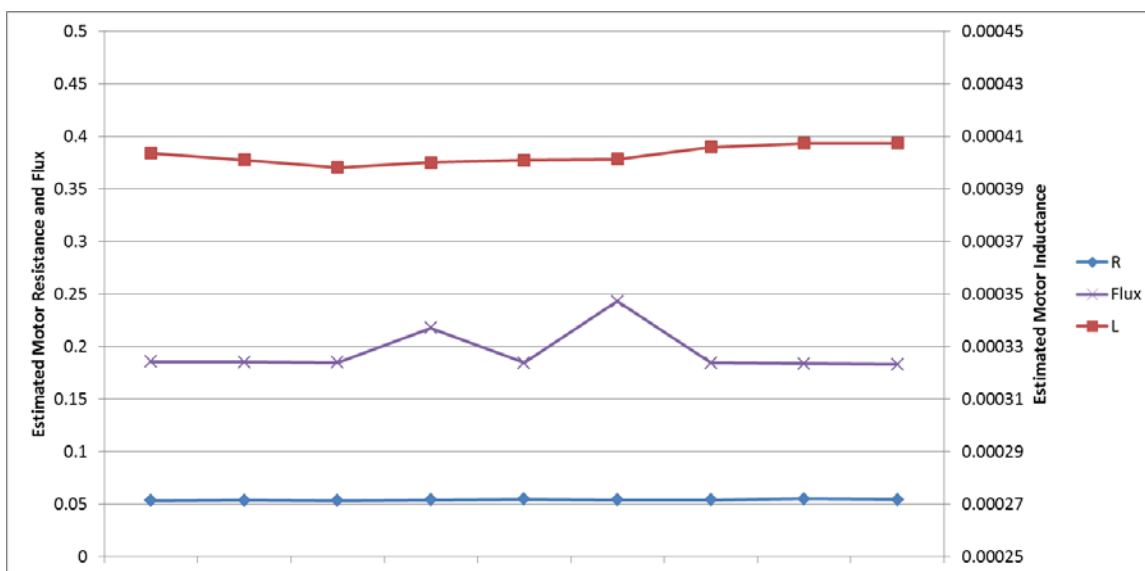


Figure 105 Results of repeated motor identification (EC motor)

7.9 CAN transceiver

The isolated CAN transceiver circuit (refer to Figure 30) was tested to determine data latency through the chain of components, signal timing distortion, and effect of the transceiver switching on the stability of the 5V supply generated by the flyback circuit.

7.9.1 CAN transceiver test set-up

In the following oscilloscope plots, the input to the CAN differential transmitter (uC_CAN_TX) is driven by a signal generator at J4-1. The differential CAN bus signals (CAN_EXT_H and CAN_EXT_L) are monitored on J3-1 and J3-2. Thus

any contributions to latency or signal distortion by the CAN transceiver, protection circuits, or digital isolator are included in the results.

For the CAN receiver tests, a separate SN65HVD255D evaluation module (SN65HVD255DEVM) was used to generate the differential bus signals (CAN_H and CAN_L) from a signal generator output. The differential signals were connected to J3-1 (CAN_EXT_L) and J3-2 (CAN_EXT_H) as inputs to the CAN receiver circuit. The isolated received signal was monitored on J4-3 (uc_CAN_RX). As with the transmitter tests, any contributions to latency or signal distortion by the CAN receiver, protection circuits, or digital isolator are included in the results.

7.9.2 CAN transmitter test results

Figure 106 shows the CAN signals with a 250 kHz square wave as input to the differential transmitter, for an effective bit rate of 500 kbps, typical of automotive CAN networks. Channel 1 (dark blue) is the CAN_TX signal, channel 2 (light blue) is the CAN_H signal, and channel 3 (purple) is the CAN_L signal. There is negligible propagation delay through the digital isolator and the transmitter. With an input duty cycle of approximately 50%, the outputs exhibit less than 1% duty cycle distortion, which indicates the impact of timing tolerances through the digital isolation channel and transmitter is negligible.

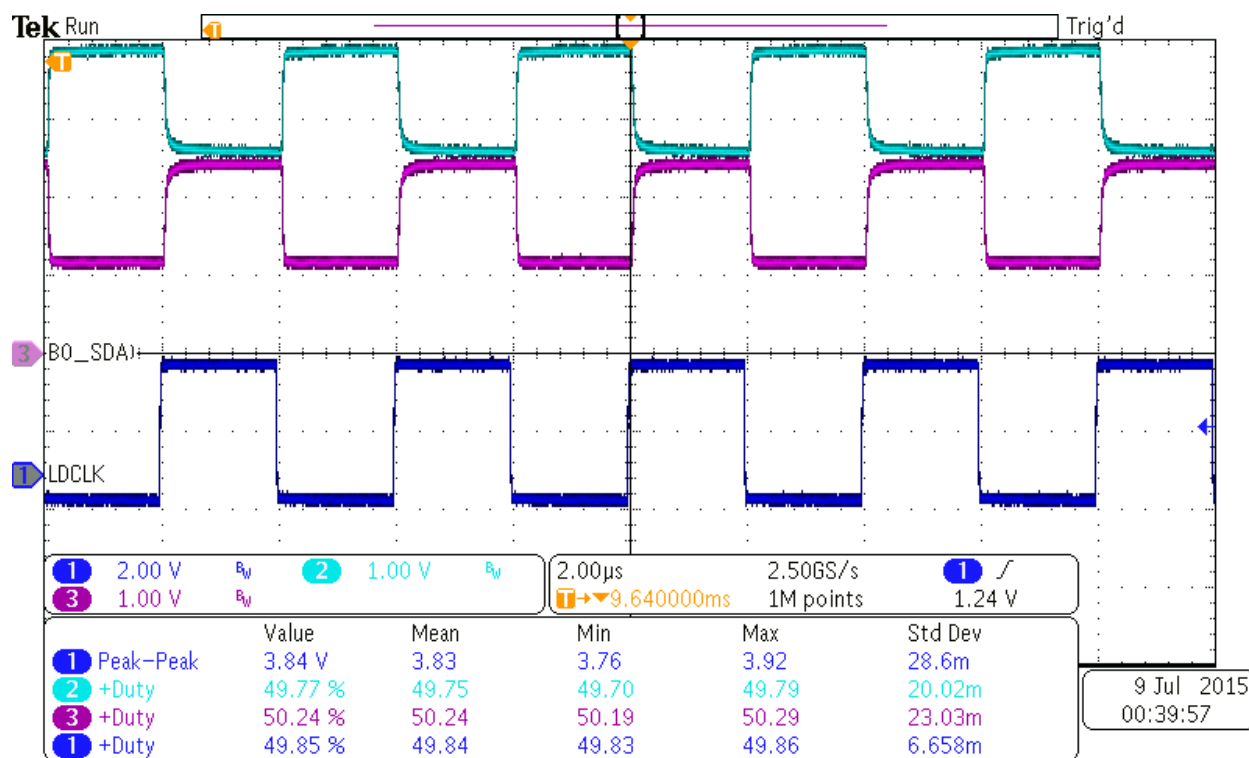


Figure 106 CAN transmitter signals showing negligible propagation delay and minimal duty cycle distortion

Figure 107 illustrates the stability of the 5V supply (derived from the auxiliary winding on the flyback converter) during the transitions between CAN transmitter dominant and recessive states. When the transmitter is in recessive mode, there is only a small bias current drawn from the 5V_CAN_A supply. When in dominant mode, the transmitter creates a differential output voltage of about 2.8V across the 120 Ohm termination load (R15 and R17), increasing the current by about 23 mA. As shown, there is no significant variation of the 5V supply, which is represented on channel 3 (purple). For completeness, Figure 108 shows the stability of the 12V_A supply during similar CAN transmitter transitions.

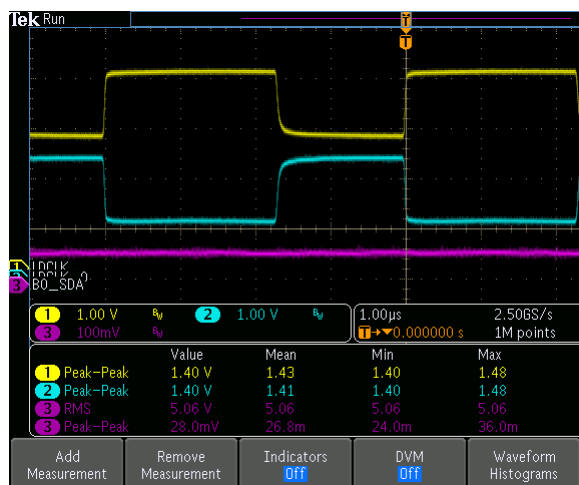


Figure 107 5V supply voltage response when transmitting

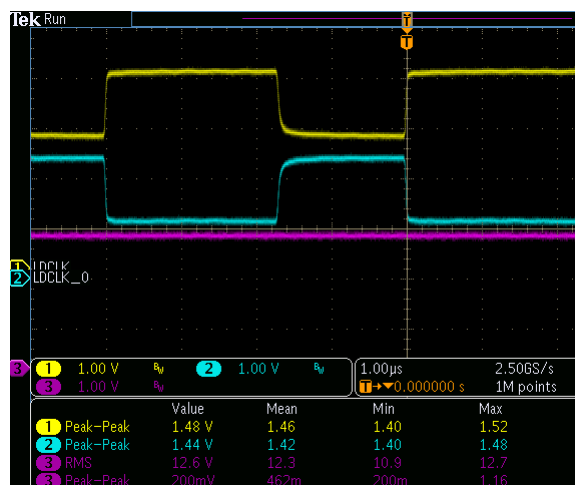


Figure 108 12V_A flyback response when transmitting

7.9.3 CAN receiver test results

Figure 109 shows the performance of the HVDA553-Q1's differential receiver in response to valid signals on the CAN bus inputs. In this oscilloscope plot, the 500 kbps inputs are on channel 1 (yellow CAN_EXT_H) and channel 2 (light blue CAN_EXT_L), and the received uC_CAN_RX is on channel 3 (purple). Note that there is a small amount of propagation delay between the input differential transitions and the output single-ended transitions. The delay is less than 200 nanoseconds, (one minor horizontal division) which is consistent with the specified delays for the HVDA553-Q1 and the ISO7331. Therefore the protection devices such as L4, C33 and C41 do not add significant delay to the signal chain.

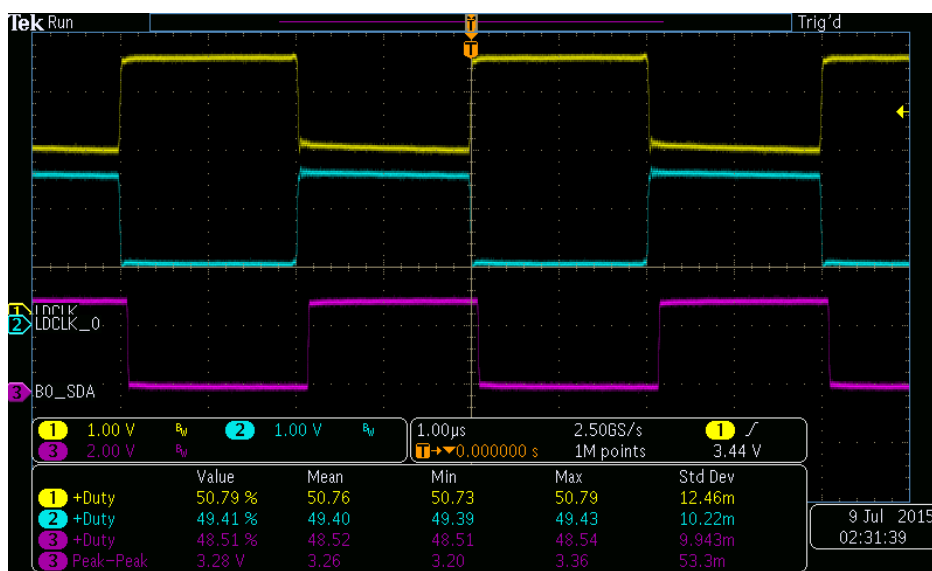


Figure 109 CAN receiver test showing propagation delay and duty cycle distortion

Note also that the incoming duty cycle is within 1% of a square wave (50% duty cycle) on both CAN_EXT_H and CAN_EXT_L. The outgoing received signal uC_CAN_RX has slightly more duty cycle distortion, but the contribution from the receiver and isolator is less than 2%.

7.10 Thermal images

In the following thermal images, the surface temperature of the various components is visible. Each of the images represents a different level of total system power, set by varying the motor speed and brake load of the dynamometer attached to the motor. Note that due to the auto-ranging feature of the Fluke Ti-110 thermal imaging camera, the various colors in each image represent varying temperature levels. The background (ambient) temperature in each case was room temperature.

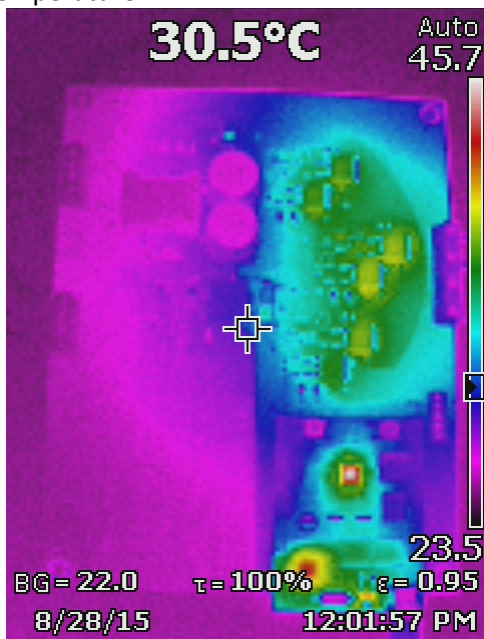


Figure 110 Thermal image - no dynamometer brake, 100 RPM

Figure 110 shows the temperature profile of the board with the LaunchPad processor running, and the unloaded motor running at 100 RPM. Note that the hottest part of the image is the C2000 Piccolo real-time microcontroller; the motor drive stages are not dissipating any significant amount of power.

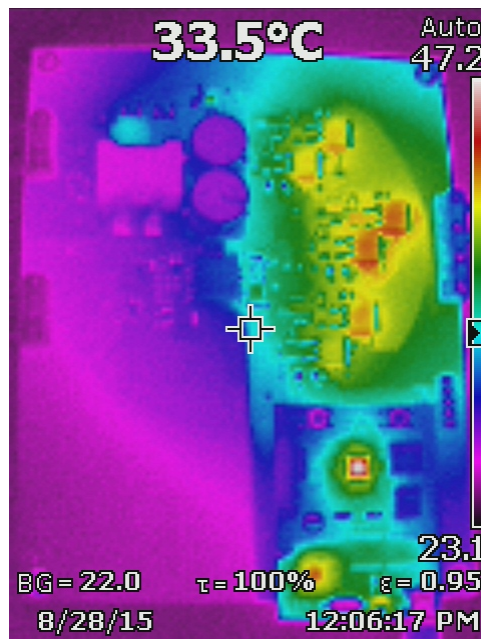


Figure 111 Thermal image - 0.5 Nm load, 1000 RPM (75W/52W)

In Figure 111, the dynamometer brake load is 0.5 N-m, with the motor running at 1000 RPM. The electrical power from the 48V supply is 75 Watts, and the mechanical power delivered to the dynamometer is 52 Watts. The motor drive FETs have increased in temperature, while the microcontroller is about the same temperature, and is still the hottest component in the image. The maximum temperature in the image has increased slightly to 47.2 degrees Centigrade.

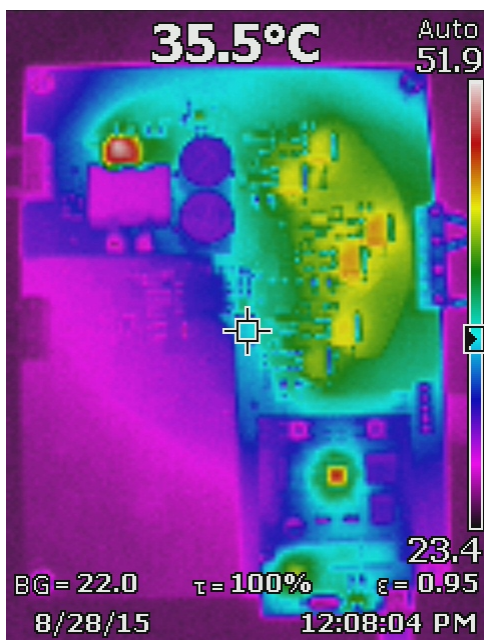


Figure 112 Thermal image - 1 Nm brake, 1000 RPM, (170W/105W)

In Figure 112 the dynamometer brake load has been increased to 1 N-m, and the motor speed is still 1000 RPM. This gives a mechanical power delivered of 105W, and the electrical power from the 48V supply is 170W. Under these conditions, Q10, one of the FETs which supplies the 48V power to the drive stage, is the warmest component in the image.



Figure 113 Thermal image - 1 Nm load, 1500 RPM, (233W/158W)

In Figure 113 the dynamometer brake load is still 1 N-m, and the motor speed has been increased to 1500 RPM. This gives a mechanical power delivered of 158W, and the electrical power from the 48V supply is 233W. Q10 is again the hottest component in the image, with a surface temperature of about 66 degrees Centigrade.

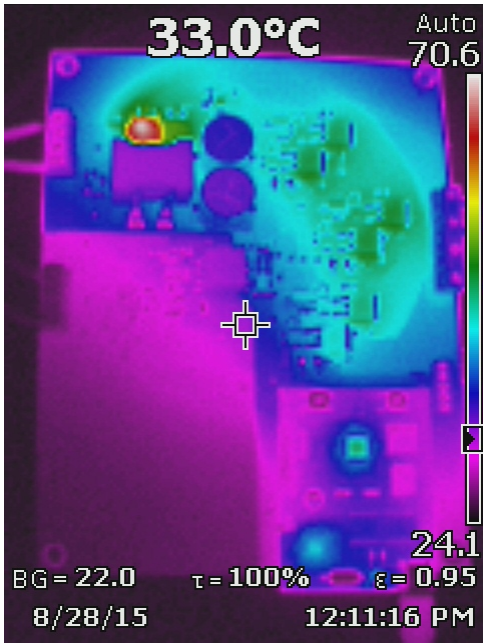


Figure 114 Thermal image - 1 Nm load, 1700 RPM, (257W/179W)

In Figure 114 the dynamometer brake load is still 1 N-m, and the motor speed has been increased to 1700 RPM. This gives a mechanical power delivered of 179W, and the electrical power from the 48V supply is 257W. Q10 is the hottest component in the image, with a surface temperature of about 71 degrees Centigrade. Note that Q2 (next to Q10) shares the 48V current, and about the same temperature (based on its color) as the drive FETs in the motor phase drive circuits.

8 Design Files

8.1 Electrical Schematics

To download the electrical schematics for each board, see the design files at <http://www.ti.com/tool/tida-00281>

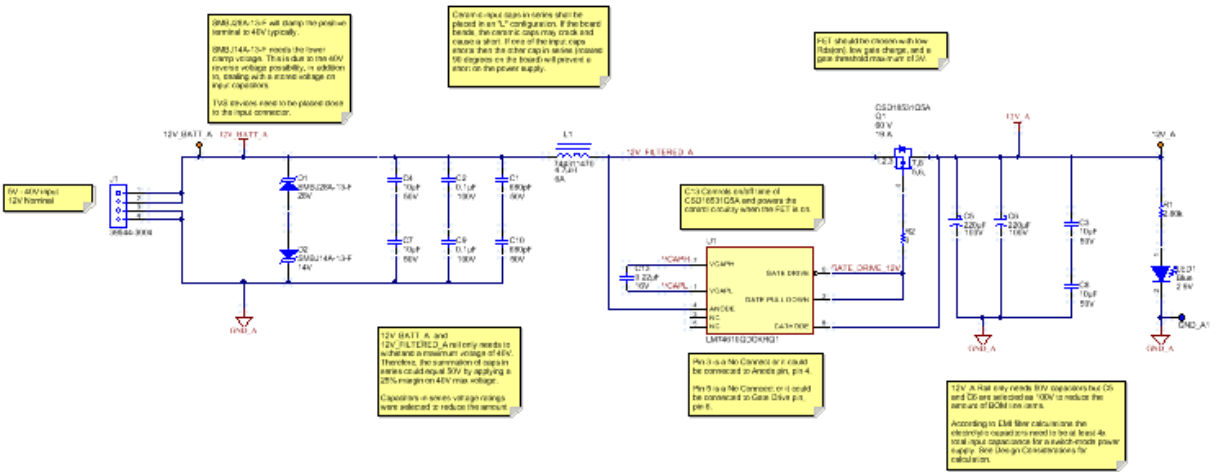


Figure 115: 12V Input Circuit Schematics

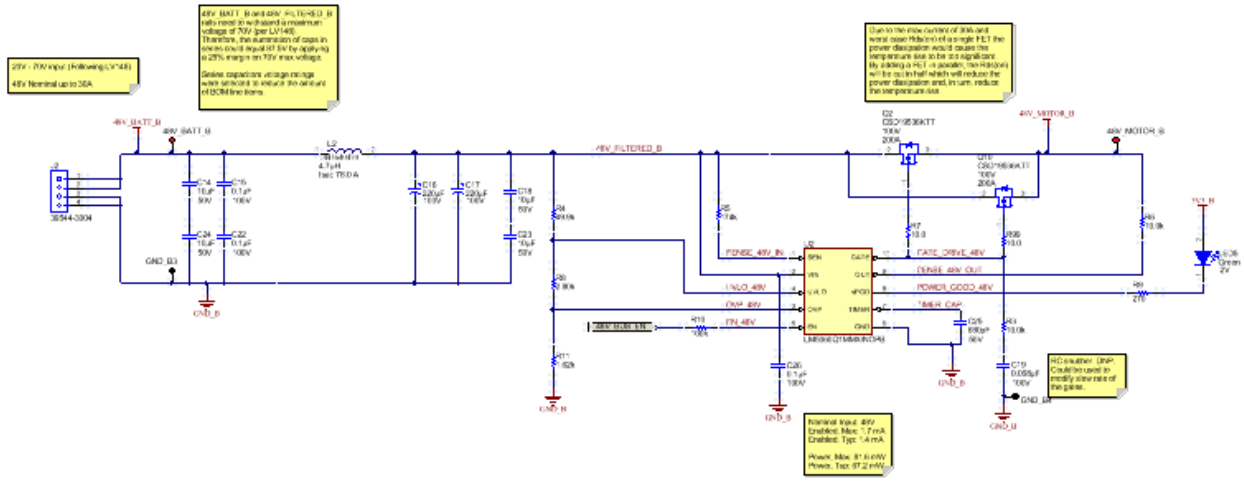


Figure 116: 48V Input Circuit Schematics

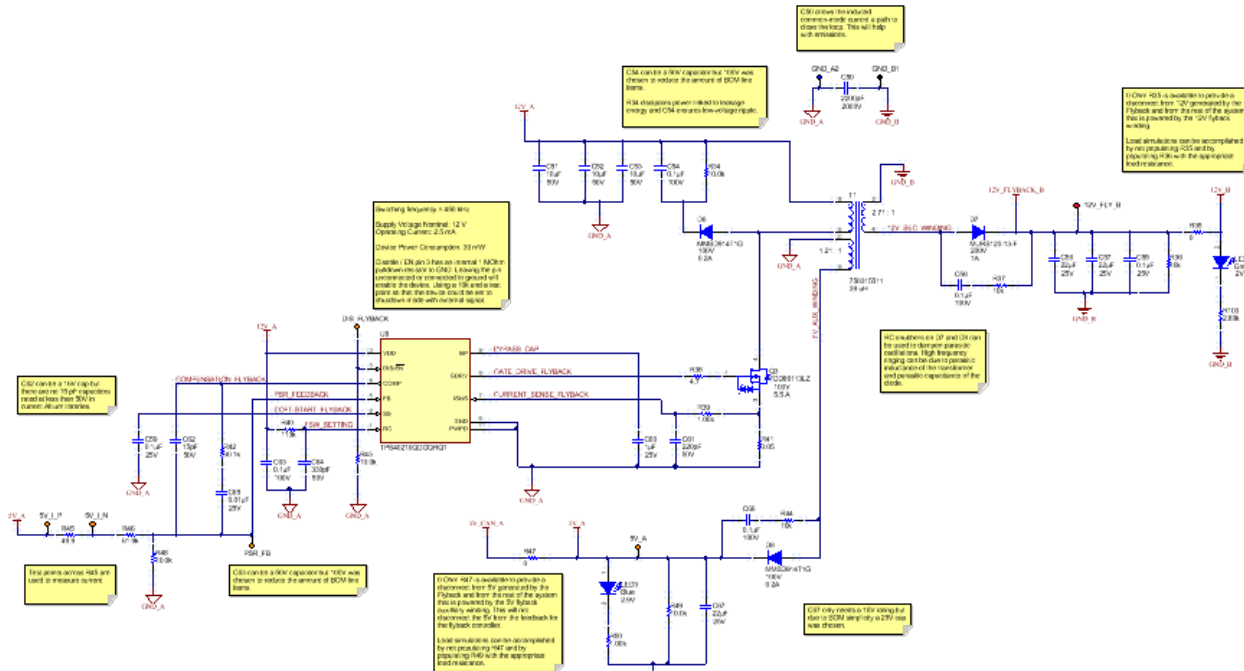


Figure 117: Flyback Converter Circuit Schematics

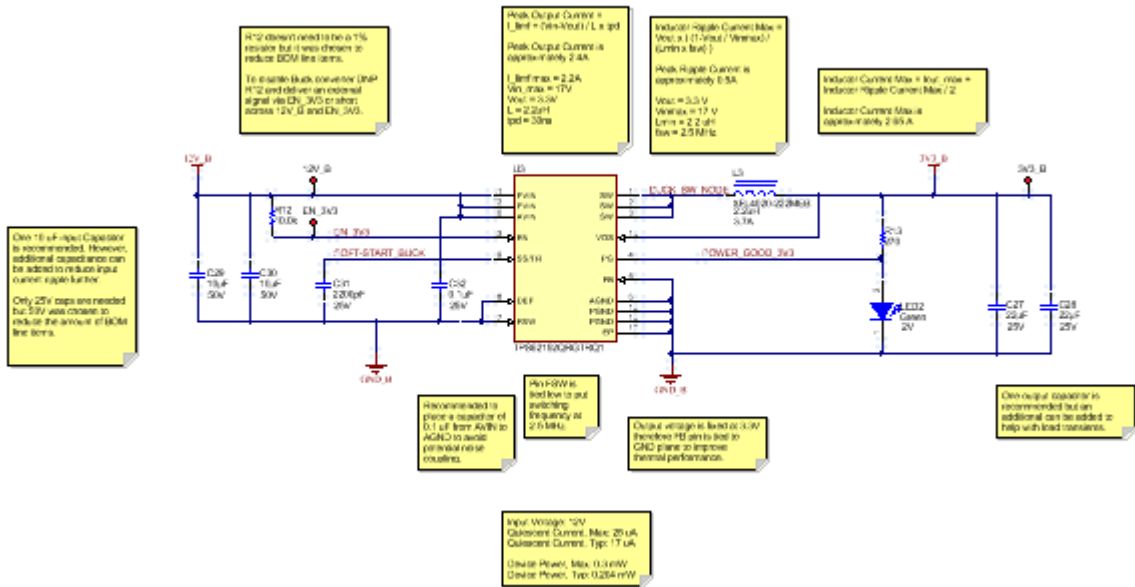


Figure 118: Buck Regulator Circuit Schematics

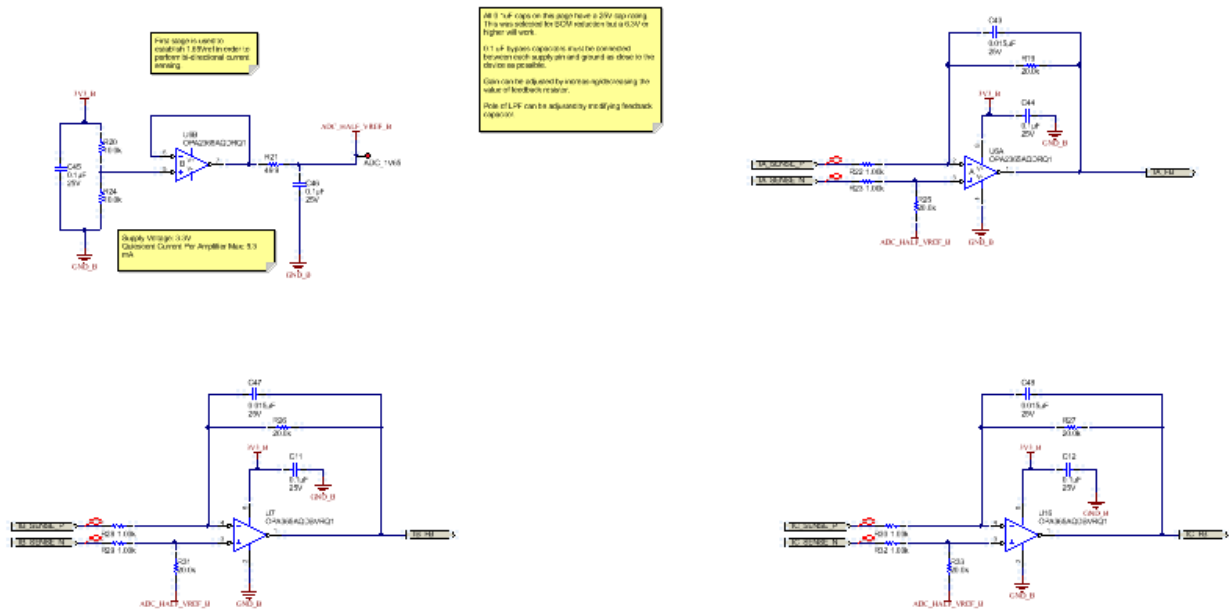


Figure 120 Current Sense Circuit Schematics

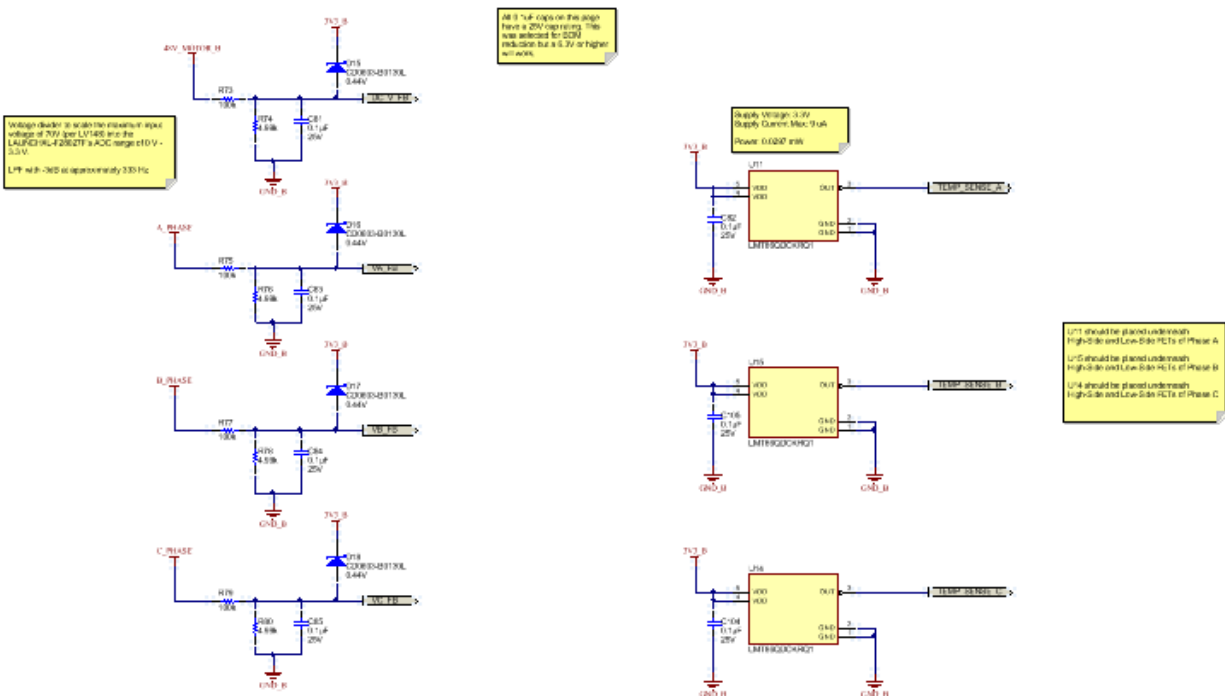


Figure 121 Voltage and Temperature Feedback Circuit Schematics

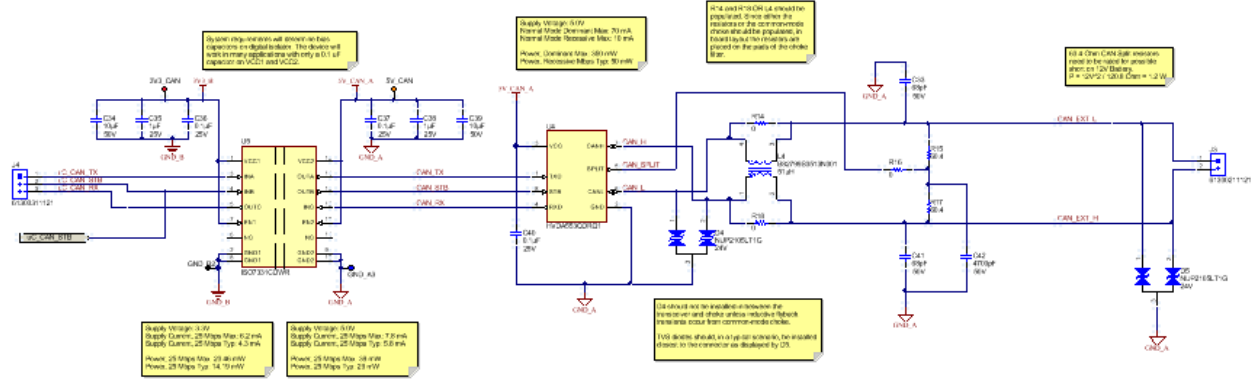


Figure 122 Isolated CAN Circuit Schematics

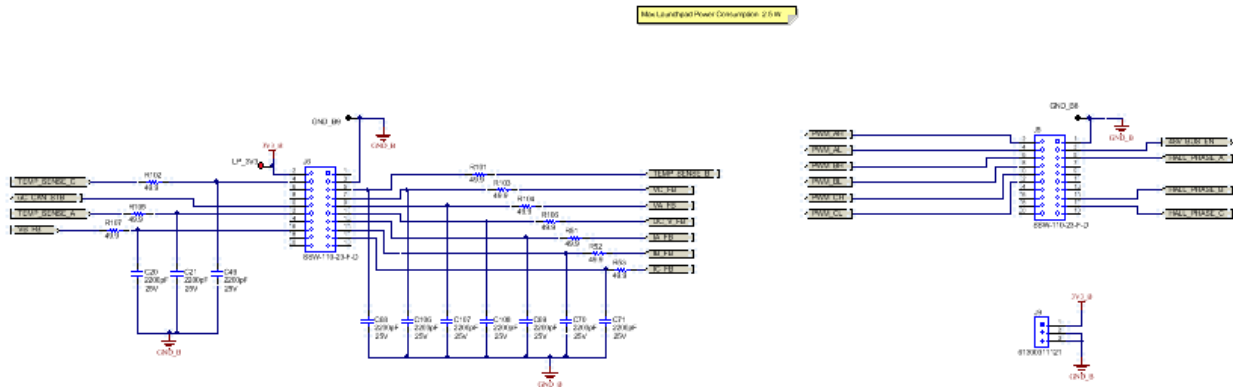


Figure 123 LaunchPad Interface Circuit Schematics

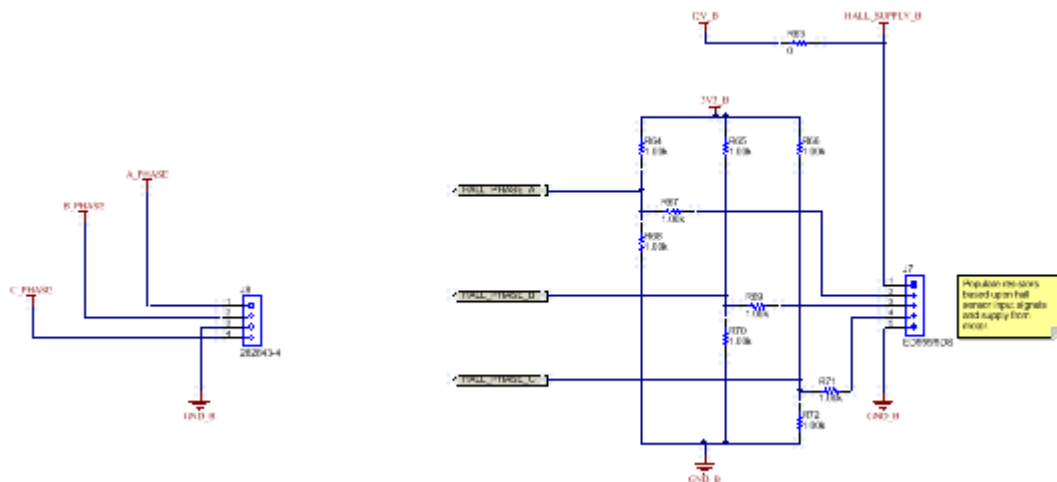


Figure 124 Motor Interface Circuit Schematics

8.2 Bill of Materials

The bill of materials below is for reference; to download the latest complete bill of materials for this design, see the design files at <http://www.ti.com/tool/tida-00281>

Table 2: TIDA-00281 BOM

Item #	Designator	Quantity	Value	Part Number	Manufacturer	Description
1	!PCB1	1		TIDA-00281	Any	Printed Circuit Board
2	3V3_B, 3V3_CAN, 12V_B, 12V_FLY_B, 48V_BATT_B, 48V_MOTOR_B, A_CURRENT, ADC_1V65, B_CURRENT, C_CURRENT, EN_3V3, LP_3V3, PHASE_A, PHASE_B, PHASE_C	15	Red	5000	Keystone	Test Point, Miniature, Red, TH
3	5V_A, 5V_CAN, 5V_I_N, 5V_I_P, 12V_A, 12V_BATT_A, DIS_FLYBACK, PSR_FB	8	Orange	5003	Keystone	Test Point, Miniature, Orange, TH
4	C1, C10	2	680pF	C0603C681K5RACTU	Kemet	CAP, CERM, 680 pF, 50 V, +/- 10%, X7R, 0603
5	C2, C9, C15, C22, C26, C54, C63, C76, C90, C99	10	0.1uF	C2012X7R2A104K	TDK	CAP, CERM, 0.1 μF, 100 V, +/- 10%, X7R, 0805
6	C3, C4, C7, C8, C14, C18, C23, C24, C29, C30, C34, C39, C51, C52, C53, C79, C93, C102	18	10uF	GRM32ER71H106KA12L	MuRata	CAP, CERM, 10uF, 50V, +/-10%, X7R, 1210
7	C5, C16, C17	3	220uF	EEV-FK2A221M	Panasonic	CAP, AL, 220 μF, 100 V, +/- 20%, 0.153 ohm, SMD
8	C11, C12, C32, C36, C37, C40, C44, C45, C46, C55, C59, C75, C78, C80, C81, C82, C83, C84, C85, C89, C92, C94, C98, C101, C103, C104, C105	27	0.1uF	C1608X7R1E104K	TDK	CAP, CERM, 0.1 μF, 25 V, +/- 10%, X7R, 0603
9	C13	1	0.22uF	0805YC224KAT2A	AVX	CAP, CERM, 0.22 μF, 16 V, +/- 10%, X7R, 0805
10	C20, C21, C31, C49, C68, C69, C70, C71, C106, C107, C108	11	2200pF	GRM155R71E222KA01D	MuRata	CAP, CERM, 2200 pF, 25 V, +/- 10%, X7R, 0402

Item #	Designator	Quantity	Value	Part Number	Manufacturer	Description
11	C25	1	0.068uF	GRM188R71C683KA01D	MuRata	CAP, CERM, 0.068 μ F, 16 V, +/- 10%, X7R, 0603
12	C27, C28, C56, C57, C67	5	22uF	GRM32ER71E226KE15L	MuRata	CAP, CERM, 22 μ F, 25 V, +/- 10%, X7R, 1210
13	C33, C41	2	68pF	C1608COG1H680J	TDK	CAP, CERM, 68 pF, 50 V, +/- 5%, COG/NPO, 0603
14	C35, C38, C60, C74, C88, C97	6	1uF	C1608X7R1E105K080AB	TDK	CAP, CERM, 1 μ F, 25 V, +/- 10%, X7R, 0603
15	C42	1	4700pF	C1005X7R1H472K	TDK	CAP, CERM, 4700 pF, 50 V, +/- 10%, X7R, 0402
16	C43, C47, C48	3	0.015uF	GRM188R71E153KA01D	MuRata	CAP, CERM, 0.015 μ F, 25 V, +/- 10%, X7R, 0603
17	C50	1	2200pF	C4532X7R3D222K	TDK	CAP, CERM, 2200 pF, 2000 V, +/- 10%, X7R, 1812
18	C61	1	220pF	C0603C221K5RACTU	Kemet	CAP, CERM, 220 pF, 50 V, +/- 10%, X7R, 0603
19	C62	1	15pF	C1608COG1H150J	TDK	CAP, CERM, 15 pF, 50 V, +/- 5%, COG/NPO, 0603
20	C64	1	330pF	C0603C331K5RACTU	Kemet	CAP, CERM, 330 pF, 50 V, +/- 10%, X7R, 0603
21	C65	1	0.01uF	C1005X7R1E103K	TDK	CAP, CERM, 0.01 μ F, 25 V, +/- 10%, X7R, 0402
22	C72, C86, C95	3	2.2uF	GRM32ER72A225KA35L	MuRata	CAP, CERM, 2.2 μ F, 100 V, +/- 10%, X7R, 1210
23	C73, C77, C87, C91, C96, C100	6	1000pF	C2012X7R2A102K	TDK	CAP, CERM, 1000 pF, 100 V, +/- 10%, X7R, 0805
24	D1	1	28V	SMBJ28A-13-F	Diodes Inc.	Diode, TVS, Uni, 28 V, 600 W, SMB
25	D2, D11, D14, D21, D24, D27, D30	7	14V	SMBJ14A-13-F	Diodes Inc.	Diode, TVS, Uni, 14 V, 600 W, SMB
26	D5	1	24V	NUP2105LT1G	ON Semiconductor	Diode, TVS, Bi, 24 V, 350 W, SOT-23
27	D6, D8	2	100V	MMSD914T1G	ON Semiconductor	Diode, Switching, 100 V, 0.2 A, SOD-123
28	D7	1	200V	MURS120-13-F	Diodes Inc.	Diode, Superfast Rectifier, 200 V, 1 A, SMB
29	D9, D10, D12, D13, D19, D20, D22, D23, D25, D26,	12	100V	DFLS1100-7	Diodes Inc.	Diode, Schottky, 100 V, 1 A, PowerDI123

Item #	Designator	Quantity	Value	Part Number	Manufacturer	Description
	D28, D29					
30	D15, D16, D17, D18	4	0.44V	CD0603-B0130L	Bourns	Diode, Schottky, 35V, 0.1A, 0603 Diode
31	GND_A1, GND_A2, GND_A3	3	Blue	5117	Keystone	Test Point, Miniature, Blue, TH
32	GND_B1, GND_B2, GND_B3, GND_B4, GND_B5, GND_B6, GND_B7, GND_B8, GND_B9	9	Black	5001	Keystone	Test Point, Miniature, Black, TH
33	H1, H2, H3, H4	4		NY PMS 440 0025 PH	B&F Fastener Supply	Machine Screw, Round, #4-40 x 1/4, Nylon, Philips panhead
34	H5, H6, H7, H8	4		1902E	Keystone	Standoff, Hex, 1"L #4-40 Nylon
35	J1, J2	2		39544-3004	Molex	Terminal Block, 4x1, 5.08mm, TH
36	J3	1		61300211121	Würth Elektronik	Header, 2.54 mm, 2x1, Gold, TH
37	J4, J9	2		61300311121	Würth Elektronik	Header, 2.54 mm, 3x1, Gold, TH
38	J5, J6	2		SSW-110-23-F-D	Samtec	Connector, Receptacle, 100mil, 10x2, Gold plated, TH
39	J7	1		ED555/5DS	On-Shore Technology	Terminal Block, 6A, 3.5mm Pitch, 5-Pos, TH
40	J8	1		282843-4	TE Connectivity	Terminal Block, 10.16mm, 4x1, Tin, TH
41	L1	1	4.7uH	744311470	Würth Elektronik	Inductor, Shielded Drum Core, Superflux, 4.7 μ H, 6 A, 0.02 ohm, SMD
42	L2	1				SMD High Current Inductor WE-HCF, L=4.7 μ H
43	L3	1	2.2uH	XFL4020-222MEB	Coilcraft	Inductor, Shielded, Composite, 2.2 μ H, 3.7 A, 0.02 ohm, SMD
44	L4	1	51uH	B82799S0513N001	TDK	Coupled inductor, 51 μ H, A, 0.25 ohm, +/- 30%, SMD
45	LED1, LED3	2	Blue	SMLP12BC7TT86	Rohm	LED, Blue, SMD

Item #	Designator	Quantity	Value	Part Number	Manufacturer	Description
46	LED2, LED4, LED5	3	Green	150060VS75000	Würth Elektronik	LED, Green, SMD
47	Q1	1	60V	CSD18531Q5A	Texas Instruments	MOSFET, N-CH, 60 V, 19 A, SON 5x6mm
48	Q2, Q10	2	100V	CSD19536KTT	Texas Instruments	MOSFET, N-CH, 100 V, 200 A,
49	Q3	1	100V	FDD86113LZ	Fairchild Semiconductor	MOSFET, N/P-CH, 100 V, 5.5 A, DPAK
50	Q4, Q5, Q6, Q7, Q8, Q9	6	100V	CSD19535KTT	Texas Instruments	MOSFET, N-CH, 100 V, 197 A,
51	R1, R8, R100	3	2.80k	CRCW04022K80FKED	Vishay-Dale	RES, 2.80 k, 1%, 0.063 W, 0402
52	R2, R16, R35, R47, R63	5	0	CRCW08050000Z0EA	Vishay-Dale	RES, 0, 5%, 0.125 W, 0805
53	R4	1	49.9k	CRCW080549K9FKEA	Vishay-Dale	RES, 49.9 k, 1%, 0.125 W, 0805
54	R5	1	174k	CRCW0603174KFKEA	Vishay-Dale	RES, 174 k, 1%, 0.1 W, 0603
55	R6, R12, R20, R24, R34, R43, R48, R56, R59, R83, R86, R92, R95	13	10.0k	CRCW080510K0FKEA	Vishay-Dale	RES, 10.0 k, 1%, 0.125 W, 0805
56	R7, R54, R55, R57, R58, R60, R62, R81, R82, R84, R85, R87, R89, R90, R91, R93, R94, R96, R98, R99	20	10.0	CRCW060310R0FKEA	Vishay-Dale	RES, 10.0, 1%, 0.1 W, 0603
57	R9, R13	2	270	CRCW0402270RJNED	Vishay-Dale	RES, 270, 5%, 0.063 W, 0402
58	R10, R73, R75, R77, R79	5	100k	CRCW0402100KFKEA	Vishay-Dale	RES, 100 k, 1%, 0.063 W, 0402
59	R11	1	1.62k	CRCW04021K62FKED	Vishay-Dale	RES, 1.62 k, 1%, 0.063 W, 0402
60	R15, R17	2	60.4	CRCW251260R4FKEG	Vishay-Dale	RES, 60.4, 1%, 1 W, 2512
61	R19, R25, R26, R27, R31, R33	6	20.0k	CRCW060320K0FKEA	Vishay-Dale	RES, 20.0 k, 1%, 0.1 W, 0603
62	R21, R45, R51, R52, R53, R101, R102, R103, R104, R105, R106, R107	12	49.9	CRCW040249R9FKED	Vishay-Dale	RES, 49.9, 1%, 0.063 W, 0402
63	R22, R23, R28, R29, R30, R32, R39, R50	8	1.00k	CRCW06031K00FKEA	Vishay-Dale	RES, 1.00k ohm, 1%, 0.1W, 0603
64	R38	1	4.7	CRCW06034R70JNEA	Vishay-Dale	RES, 4.7, 5%, 0.1 W, 0603
65	R40	1	113k	CRCW0603113KFKEA	Vishay-Dale	RES, 113 k, 1%, 0.1 W, 0603
66	R41	1	0.05	CRM1206-FZ-R050ELF	Bourns	RES, 0.05, 1%, 0.5 W, 1206
67	R42	1	30.1k	CRCW060330K1FKEA	Vishay-Dale	RES, 30.1 k, 1%, 0.1 W, 0603

Item #	Designator	Quantity	Value	Part Number	Manufacturer	Description
68	R46	1	61.9k	CRCW080561K9FKEA	Vishay-Dale	RES, 61.9 k, 1%, 0.125 W, 0805
69	R61, R88, R97	3	0.001	CSNL2512FT1L00	Panasonic	RES, 0.001 ohm, 1%, 2W, 2512
70	R74, R76, R78, R80	4	4.99k	CRCW06034K99FKEA	Vishay-Dale	RES, 4.99k ohm, 1%, 0.1W, 0603
71	T1	1	39 uH	750315511	Würth Elektronik	Transformer, 39 uH, SMT
72	U1	1		LM74610QDGKRQ1	Texas Instruments	Smart Diode Controller, DGK0008A
73	U2	1		LM5060Q1MMX/NOPB	Texas Instruments	High-Side Protection Controller with Low Quiescent Current, 10-pin MSOP, Pb-Free
74	U3	1		TPS62152QRGTRQ1	Texas Instruments	3 to 17-V 1-A Step-Down Converter in 3x3-mm QFN Package, RGT0016C
75	U4	1		HVDA553QDRQ1	Texas Instruments	5-V CAN TRANSCEIVER WITH I/O LEVEL ADAPTING AND LOW-POWER-MODE SUPPLY OPTIMIZATION, D0008A
76	U5	1		ISO7331CDWR	Texas Instruments	Robust EMC, Low Power, Triple-Channel Digital Isolators, DW0016B
77	U6	1		OPA2365AQDRQ1	Texas Instruments	50-MHz Low-Distortion High-CMRR Rail-to-Rail I/O, Single-Supply Operational Amplifier, D0008A
78	U7, U16	2		OPA365AQDBVRQ1	Texas Instruments	Automotive Catalog, 50 MHz, Low-Noise, Single-Supply Rail-to-Rail Operational Amplifier, 2.2 to 5.5 V, -40 to 125 degC, 5-pin SOT23 (DBV0005A), Green (RoHS & no Sb/Br)

Item #	Designator	Quantity	Value	Part Number	Manufacturer	Description
79	U8	1		TPS40210QDQQRQ1	Texas Instruments	4.5-V TO 52-V INPUT CURRENT MODE BOOST CONTROLLER, DGQ0010D
80	U10, U12, U13	3		UCC27201AQDDARQ1	Texas Instruments	120-V, 3-A Peak, High-Frequency, High-Side/Low-Side Driver, DDA0008G
81	U11, U14, U15	3		LMT86QDCKRQ1	Texas Instruments	SC70 Analog Temperature Sensor with Class-AB Output, DCK0005A
82	C6	0	220uF	EEV-FK2A221M	Panasonic	CAP, AL, 220 μ F, 100 V, +/- 20%, 0.153 ohm, SMD
83	C19	0	0.068uF	C0805C683K1RACTU	Kemet	CAP, CERM, 0.068 μ F, 100 V, +/- 10%, X7R, 0805
84	C58, C66	0	0.1uF	C2012X7R2A104K	TDK	CAP, CERM, 0.1 μ F, 100 V, +/- 10%, X7R, 0805
85	D4	0	24V	NUP2105LT1G	ON Semiconductor	Diode, TVS, Bi, 24 V, 350 W, SOT-23
86	FID1, FID2, FID3	0		N/A	N/A	Fiducial mark. There is nothing to buy or mount.
87	R3, R49	0	10.0k	CRCW080510K0FKEA	Vishay-Dale	RES, 10.0 k, 1%, 0.125 W, 0805
88	R14, R18	0	0	CRCW08050000Z0EA	Vishay-Dale	RES, 0, 5%, 0.125 W, 0805
89	R36, R37, R44	0	10k	CRCW080510K0JNEA	Vishay-Dale	RES, 10 k, 5%, 0.125 W, 0805
90	R64, R65, R66, R67, R68, R69, R70, R71, R72	0	1.00k	CRCW06031K00FKEA	Vishay-Dale	RES, 1.00k ohm, 1%, 0.1W, 0603

8.3 PCB Layout Recommendations

8.3.1 General Notes on Noise Sensitive Traces and Components

- Route voltage feedback traces away from other noisy traces or components, like clock lines. Avoid routing things under the switch node of a power inductor altogether if possible.
- Feedback nodes are generally high impedance lines which are quite sensitive to disturbances. The switch node can radiate a significant amount of energy and could couple noise into FB traces or other sensitive lines. Placing these traces on the other side of the board (with ground planes between them) helps mitigate ill effects as well.
- It is critical that analog/control loop components be placed such that their trace lengths back to the IC are minimized. Below is an example of the feedback and compensation components for the TPS62152 DC-DC converter:

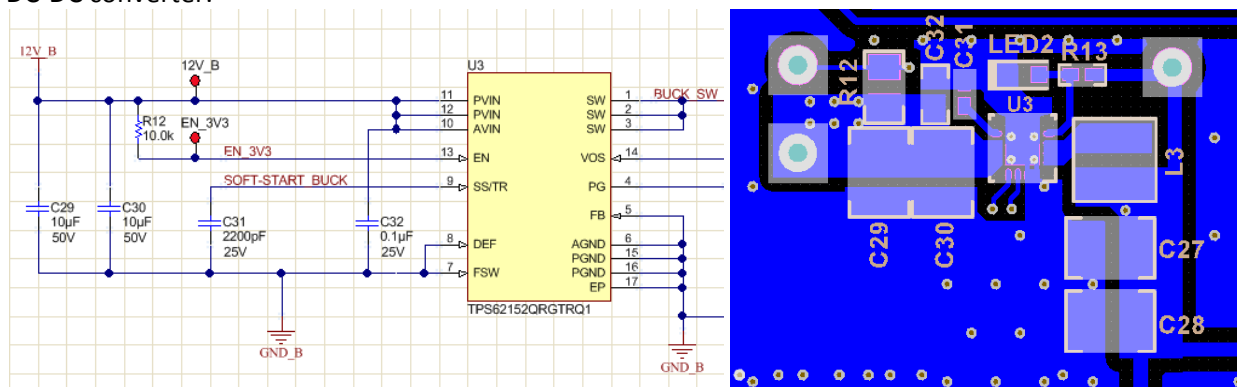
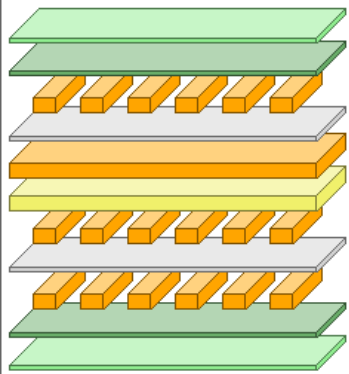


Figure 125: Compensation/Feedback components placed close to IC

The feedback and compensation nodes are especially high impedance and thus susceptible to picking up. As these are critical in the operation of the devices control loop, poor placement and routing of these components/traces can affect the performance of the device by introducing unwanted parasitic inductances and capacitances.

8.3.2 PCB Layering recommendations

This design uses a 6-layer board, with an internal ground plane to shield the bottom signal layer from the switch nodes found on the top layer. Figure 126 shows the layer stack-up used in this board.



Layer Name	Type	Material	Thickness (mil)	Dielectric Material	Dielectric Constant
Top Overlay	Overlay				
Top Solder	Solder Mask/Coverlay	Surface Material	0.4	Solder Resist	3.5
Top Layer	Signal	Copper	2.8		
Dielectric1	Dielectric	Prepreg	14	FR-4	4.2
Internal Plane 1	Internal Plane	Copper	2.8		
Dielectric 3	Dielectric	Core	22	FR-4	4.2
Signal Layer 3	Signal	Copper	2.8		
Dielectric 2	Dielectric	Prepreg	14	FR-4	4.2
Bottom Layer	Signal	Copper	2.8		
Bottom Solder	Solder Mask/Coverlay	Surface Material	0.4	Solder Resist	3.5
Bottom Overlay	Overlay				

Figure 126: Layer stack up, GND plane separating top layer power circuits from bottom layer signals

- Wherever practical, keep power traces/pours on the same layer. This isn't always possible due to routing requirements. This will minimize the inductance of the path (by using as few vias as possible) by keeping individual power traces on the same layer, and reduce any noise coupling between planes by reducing overlap. Unfortunately, due to the number of different rails in this design, and the routing requirements needed to get them to the EVM connectors, this wasn't totally possible on this board.

8.3.3 General Power Supply Considerations

- Input capacitors should be placed as close to the IC as possible to reduce the parasitic series inductance from the capacitor to the device it is supplying. This is especially important for DCDC converters as the inductance from the capacitor to the high-side switching FET can cause high voltage spikes and ringing on the switch node, which can be damaging to components and cause problems for EMI.
- Place the **input** capacitors in order of descending size/value, with the smallest being closest to the device input pin. Contrastingly, place the **output** capacitors in order of descending size/value, with the largest being closest to the device's output pins/power inductor.

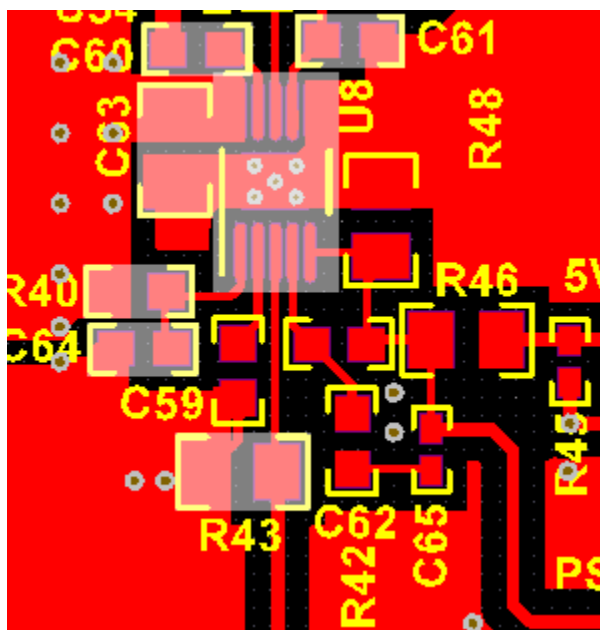


Figure 127: Input/output Capacitor placement in DC/DC Converter

- Use wide copper areas/traces for routing outputs of the converters to the connectors or loads. This reduces the I^2R drop along the power path and thus improves load regulation:

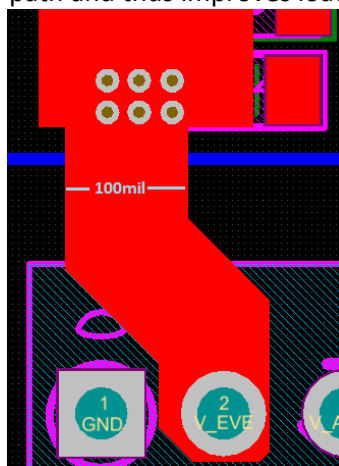


Figure 128: Wide traces for power path

- The resistivity of a trace drops as the width of the trace increases ($R \propto \frac{1}{W}$). If not using DCDC/linear converters capable of differential remote sensing, care must be taken that the voltage drop from the location of regulation (close to the converter) to the load is not significant. While there isn't really a maximum limit on this, there is a minimum. PCB traces, like wires, are rated for current ranges based on their cross-sectional area. This depends not only on the width but also on the thickness/height of the trace. Calculators are available online for calculating minimum trace width.

- Minimize the loop area and series path inductance of the switching return current in a DCDC converter. It is preferable that this be on the same layer and can be achieved by careful placement of the components.
- Since it is not always convenient to guarantee a good return path on the same layer, we can drop ground vias to an internal plane which is not broken up providing a more direct return path. The figure below shows the use of these ground vias where it was not possible to create a small loop on the top layer.
- The power inductors should be close to the switch node pins of the ICs, minimizing the distance from the pin to the inductor, but maintaining large area as much as possible. The goal is to minimize both the parasitic inductance, as well as reduce the radiated emissions from the node:

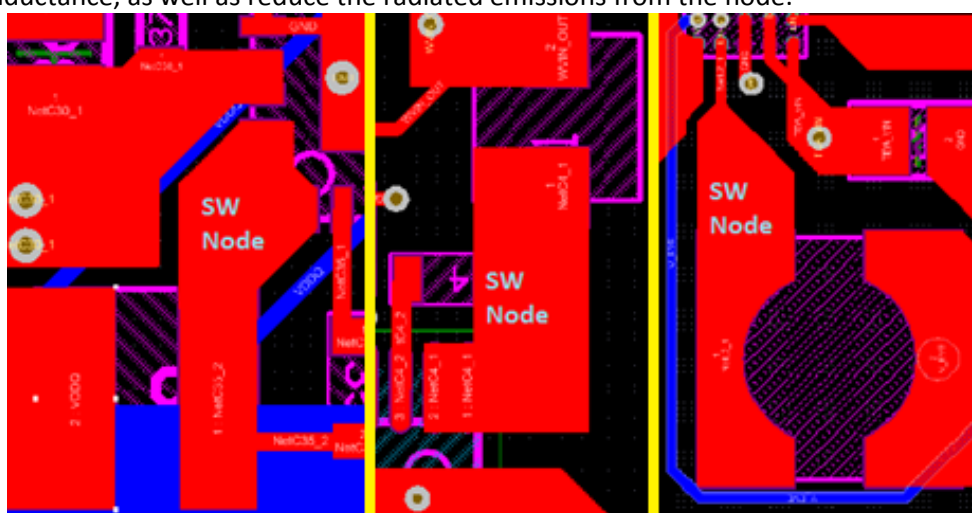


Figure 129: SW nodes, minimizing length of trace from IC to inductor

- If a bootstrap capacitor is used, place this component as close to the power inductor as practical.

8.3.4 12V Protection Circuitry

- Place input protection circuitry as close to the battery terminal inputs as possible, rather than close to the downstream circuit it is protecting, to reduce the inductance of the path. First of all, this means that the TVS diodes will be as quick as possible to react to any transients. Second of all, in the event of a reverse polarity event, the FET controlled by the LM74610-Q1 will shut off quickly and this could cause inductive kicks due to the interrupted current flow – the severity of this kick is a function of the inductance (and therefore the length/width) of the power path. Lastly, this provides a close, tight loop for the current/return path back to the battery terminals while the TVS diodes shunt a transient.

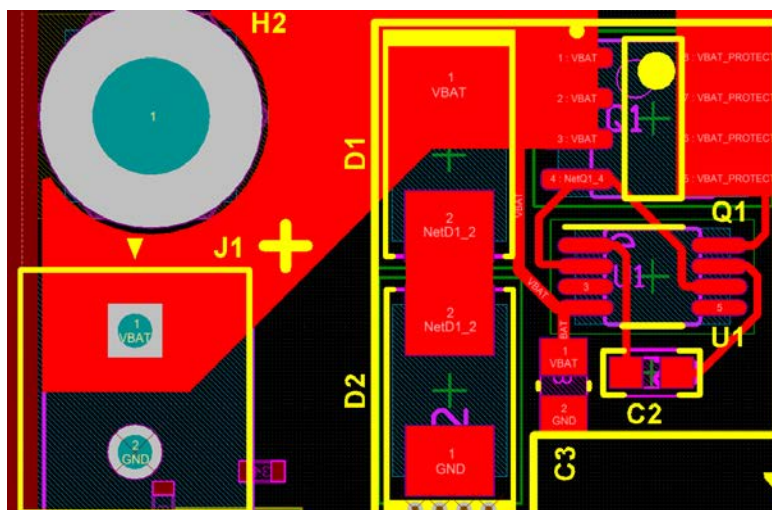


Figure 130: TVS diodes and reverse battery protection

8.3.5 Separation of 12V and 48V power

To avoid creating ground loops between the 12V battery system and the 48V battery system, this design maintains isolation between the two grounds. GND_A is part of the 12V battery system, and is isolated physically and electrically from GND_B, which is part of the 48V battery system.

This is illustrated in Figure 131 and Figure 132 where the physical separation of the A (12V battery) ground and B (48V battery) ground is easily observed.

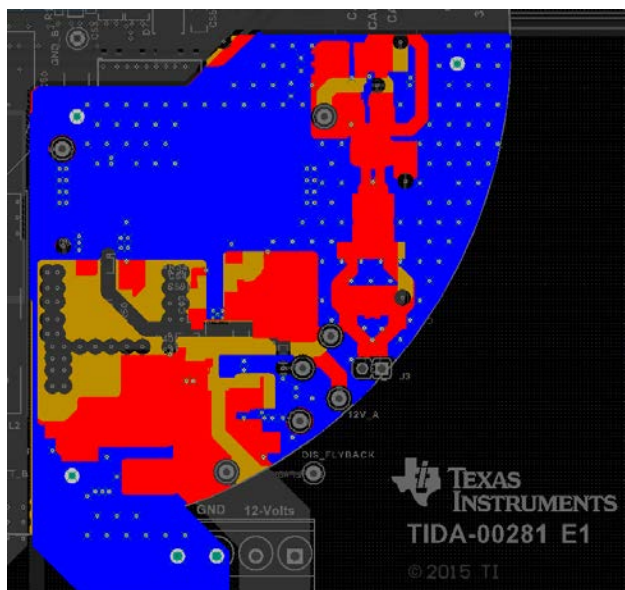


Figure 131 GND_A traces highlighted



Figure 132 GND_B traces highlighted

8.3.6 48V power protection

The filtering and protection circuitry for the 48V power (refer to Figure 20 and Figure 21) consists of relatively large components due to the high current involved. These components should be located near the 48V input connector, in order to remove unwanted transients before these can propagate through the rest of the board.

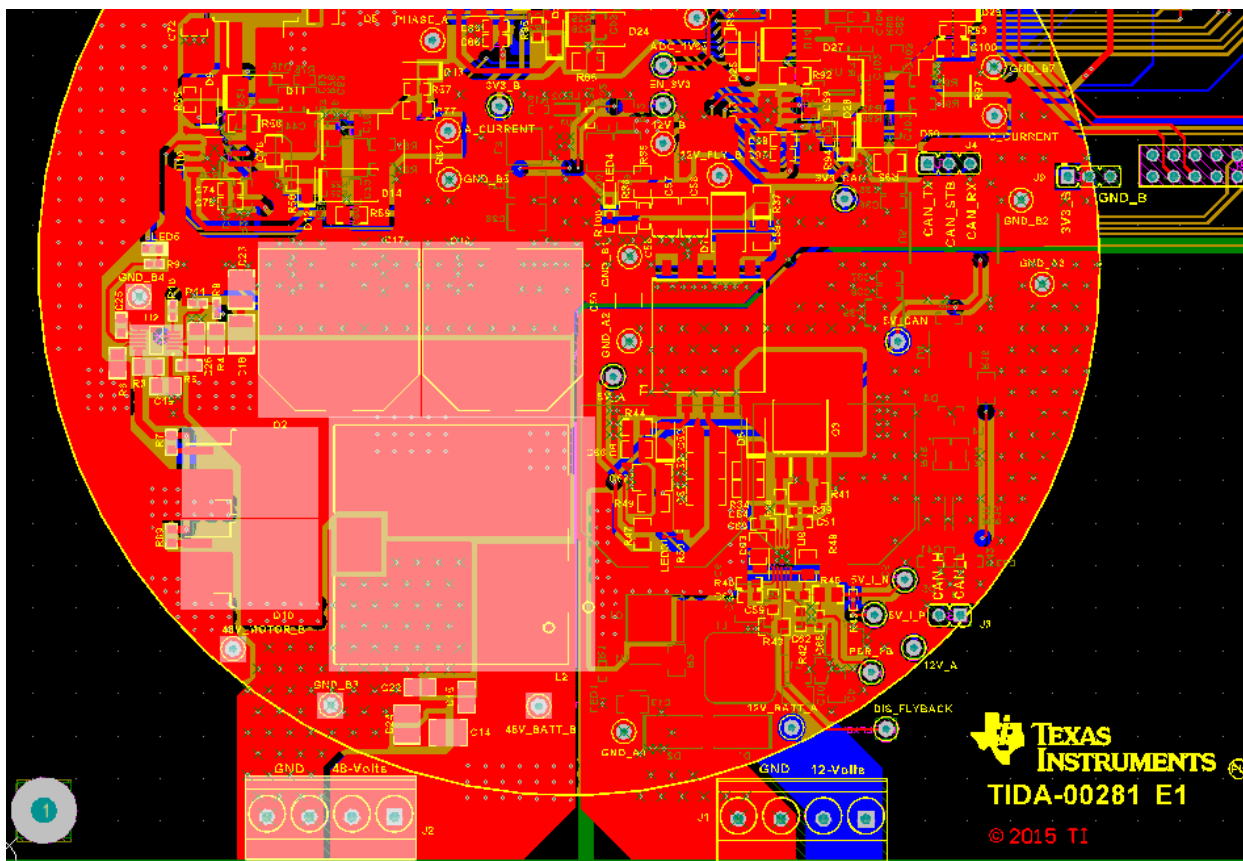


Figure 133 Layout with 48V protection highlighted

8.3.7 48V Power Routing

The 48V power supplies power to the drive stage for the motor, and must be capable of delivering high currents, as much as 30A. Large areas are used for routing this current through the board and components which carry the high 48V current. In Figure 134, the routing for the 48V power is shown in three views of the board.

On the left is the polygon for 48V_BATT_B, from the input connector to the large filter inductor L2, as well as the filtering capacitors. Note that while the red (top) layer is visible, this polygon shape is also found on the bottom (blue) layer, with vias to connect the two layers.

The middle image shows the 48V_FILTERED_B polygon, which connects the output of the filter inductor (L2) to the 48V switching circuit. Again the polygon is copied on the bottom layer, with numerous vias to connect the top and bottom layers. The right image shows the polygon for 48V_MOTOR_B, which goes from the 48V

switching circuit to the three high-side driver FETs of the motor drive circuit. In this view, the bottom (blue) layer is highlighted, with some edges of the similar top (red) layer visible.

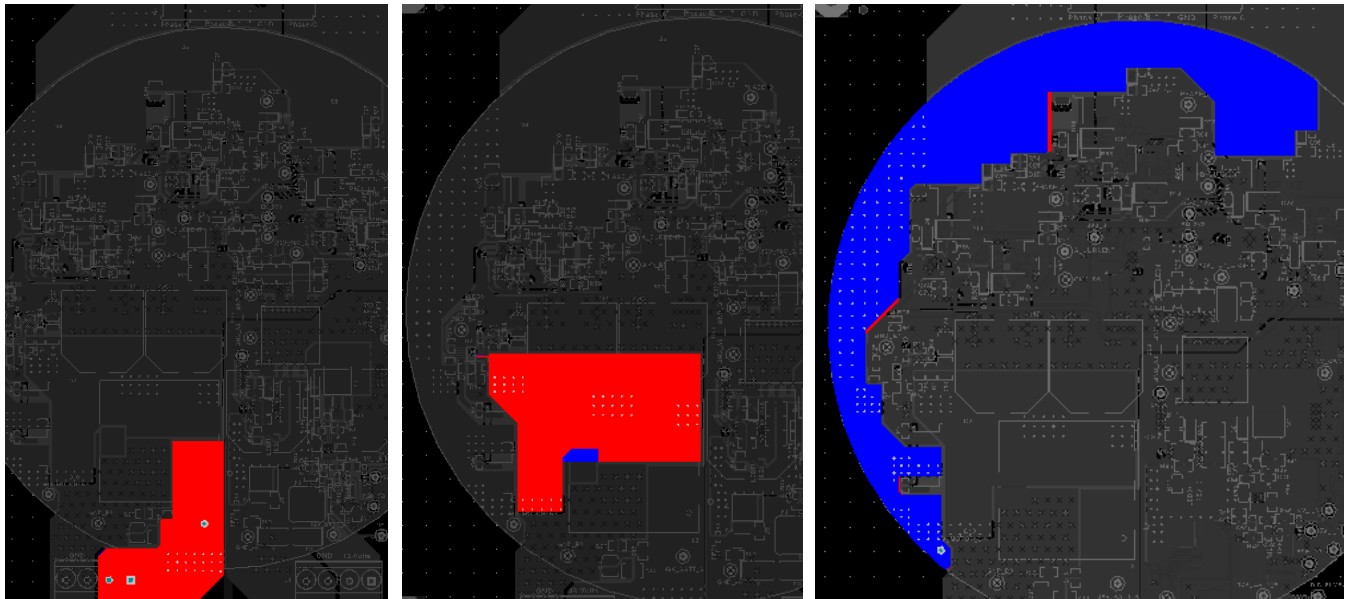


Figure 134 Polygons for 48V supply to motor drive stages

8.3.8 Motor Drive Circuit

The components related to the drive stage for each phase of the motor are grouped together, and the layout of each of the phases is similar. The power FETs (Q4 and Q5 in Figure 135) and associated components are located on the top side of the board, as is the UCC27201A gate driver (U10). The two power FETs are located in close proximity, and such that the shared output node PHASE_A connects them with solid current path.

C72 provides a low-inductance reservoir of charge near the high-side FET

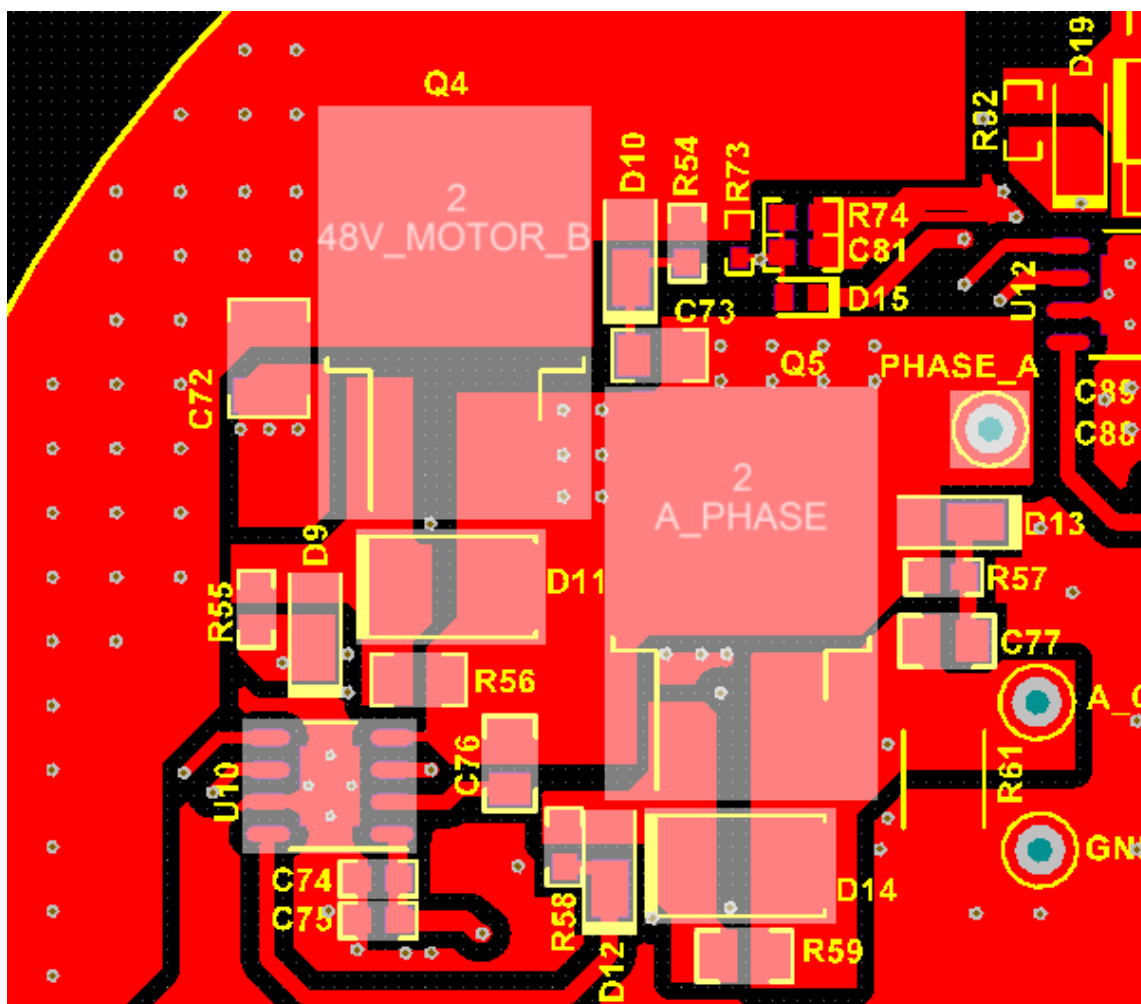


Figure 135 Layout of Motor Drive Stage for Phase A

8.3.9 Differential Signals

In the case of differential signals, such as the motor current feedback across the current sense resistors, use symmetry to ensure that any noise picked up on one line is also picked up approximately equally on the other line.

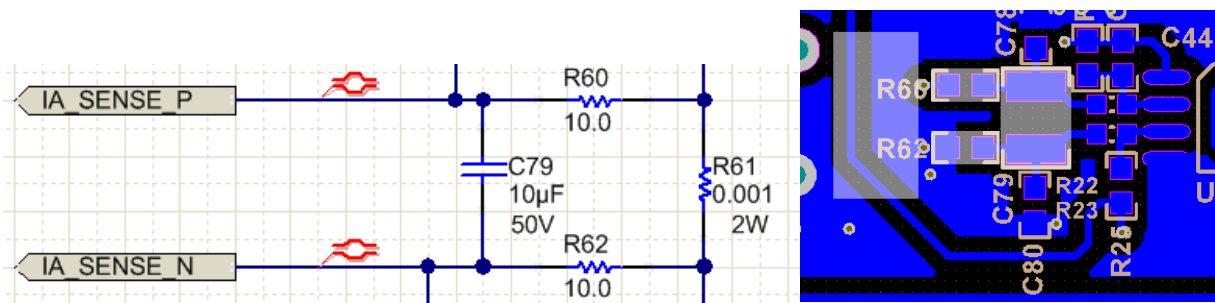


Figure 136 Layout symmetry used to reduce differential-mode noise on analog signal

8.4 Layout Prints

The following figures are for reference; to download the layout prints for each board, see the design files at <http://www.ti.com/tool/tida-00281>.

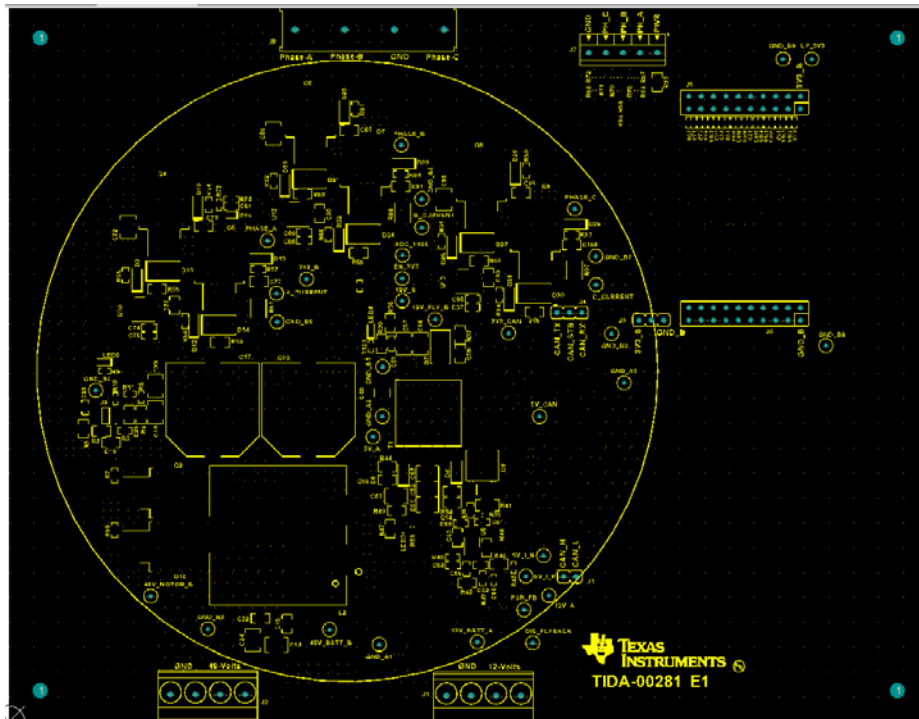


Figure 137: Top Silkscreen



Figure 138: Top Solder Mask

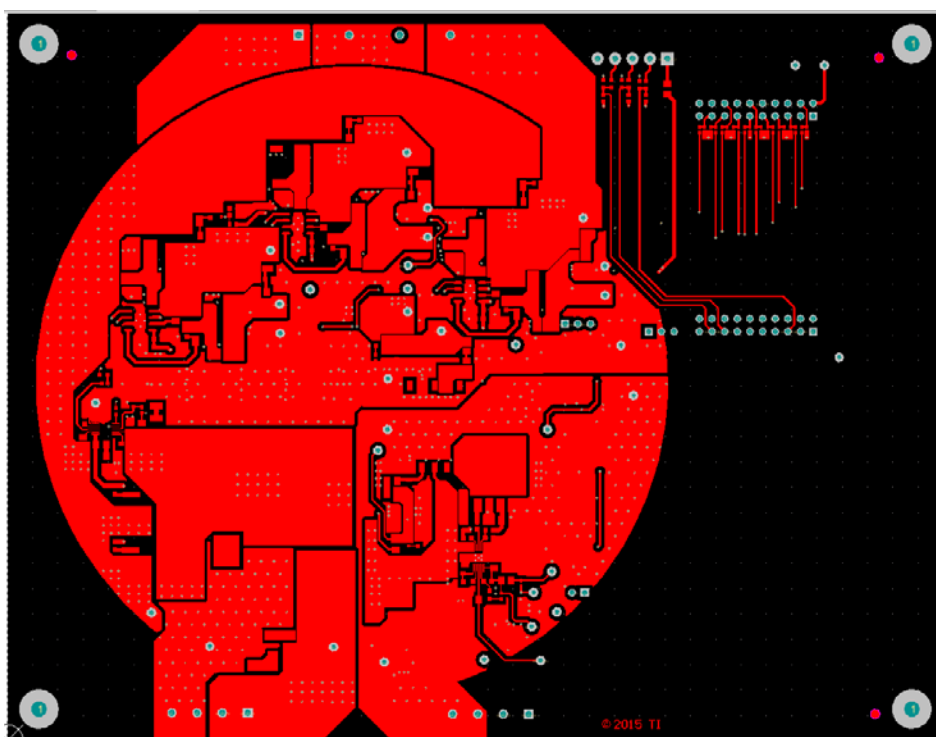


Figure 139: Top Layer

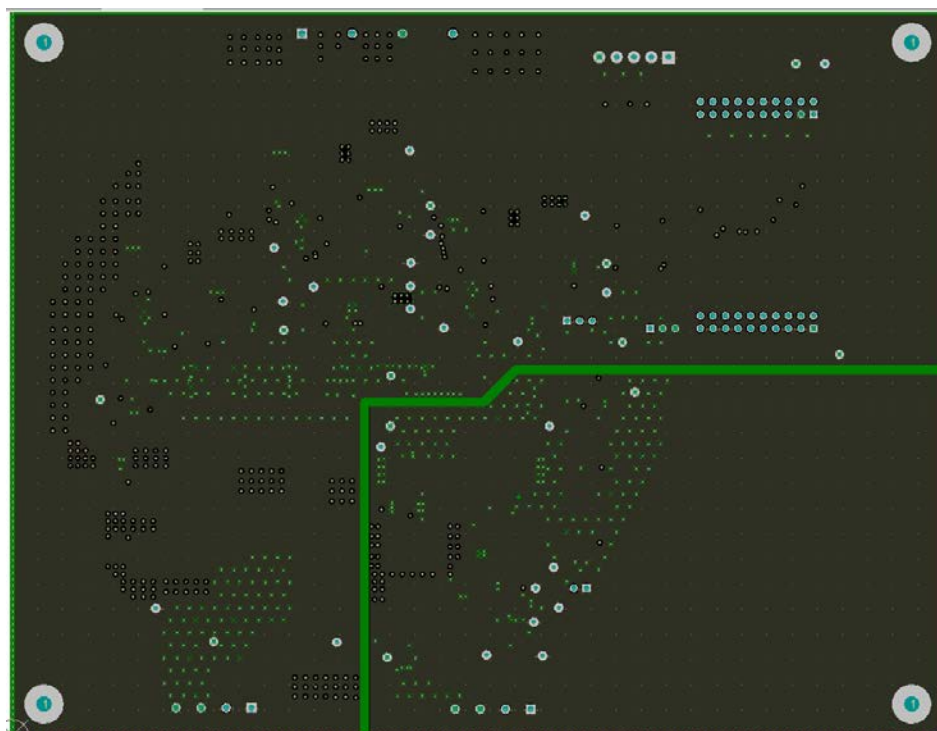


Figure 140: Layer 2 - Ground

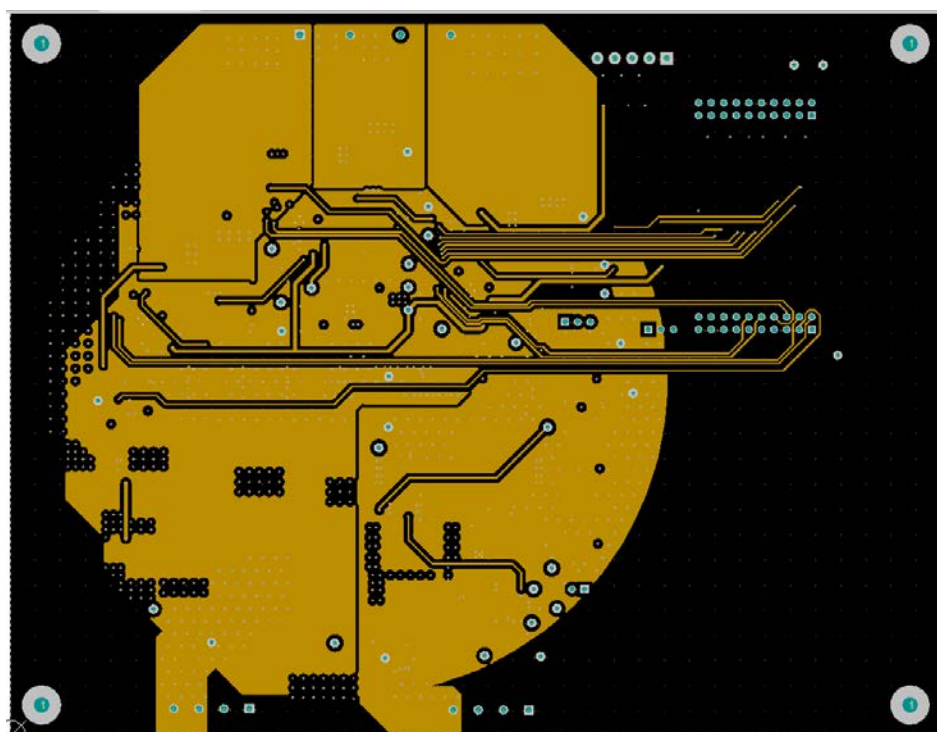


Figure 141: Layer 3 - Power

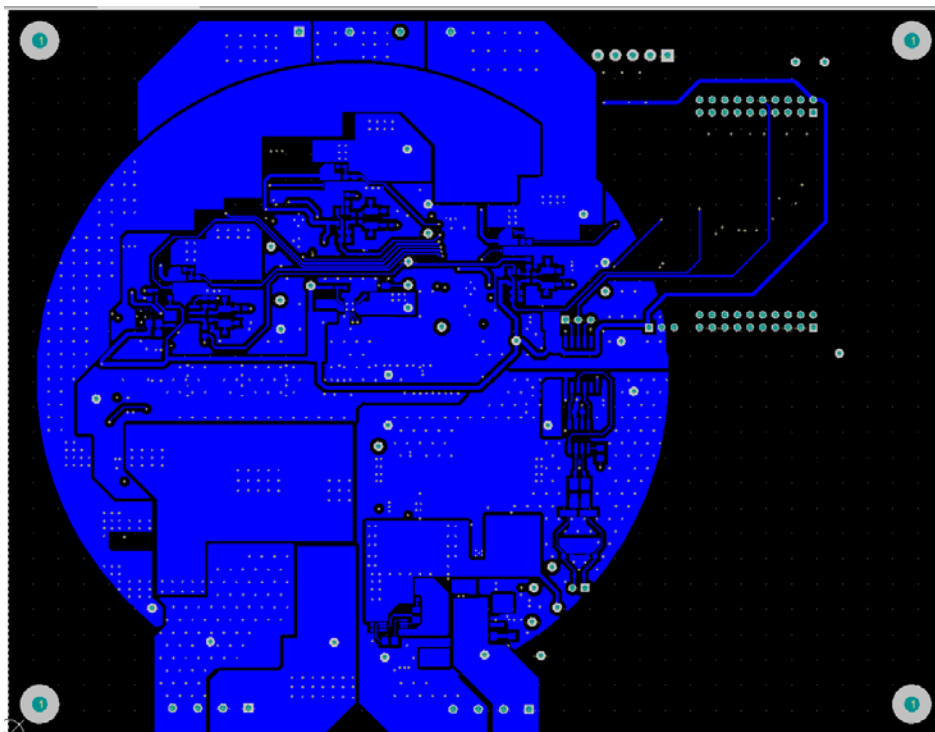


Figure 142: Bottom Layer

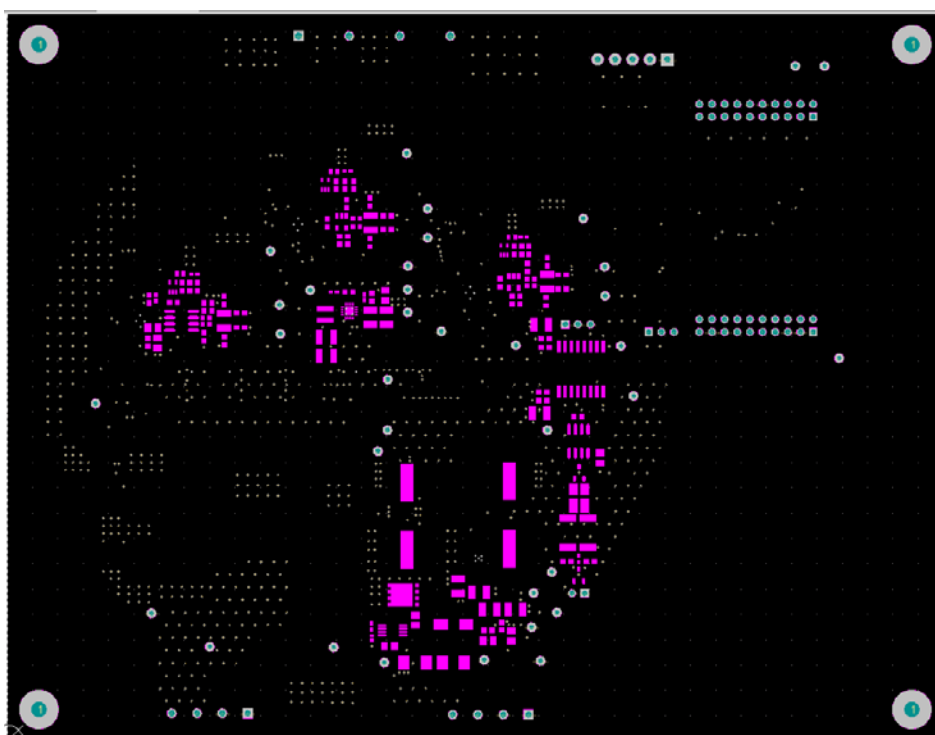


Figure 143: Bottom Solder

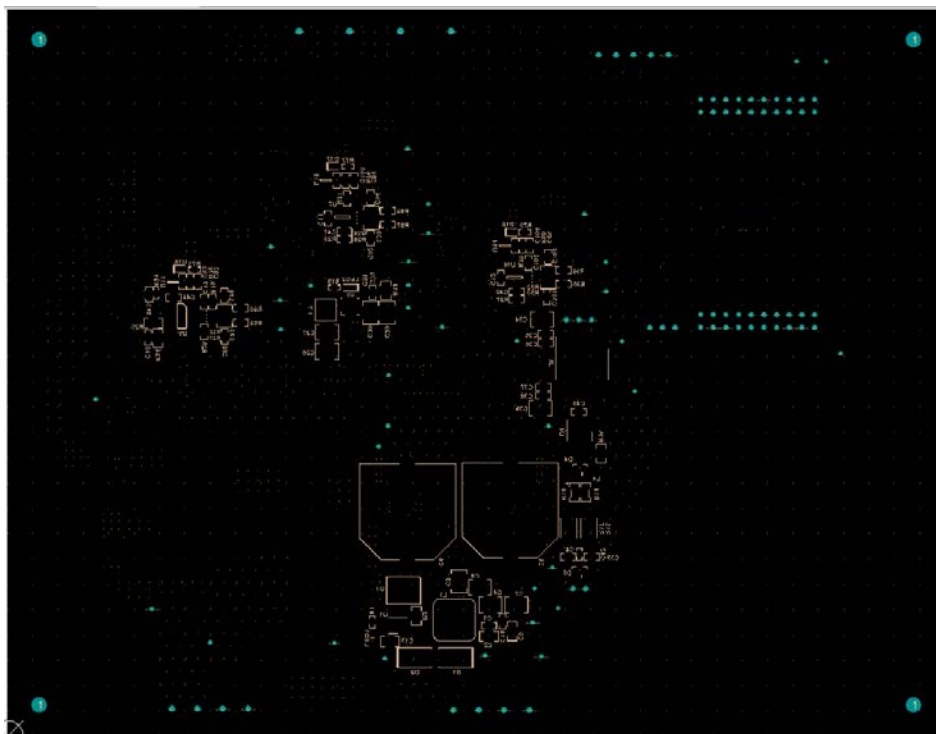


Figure 144: Bottom silkscreen

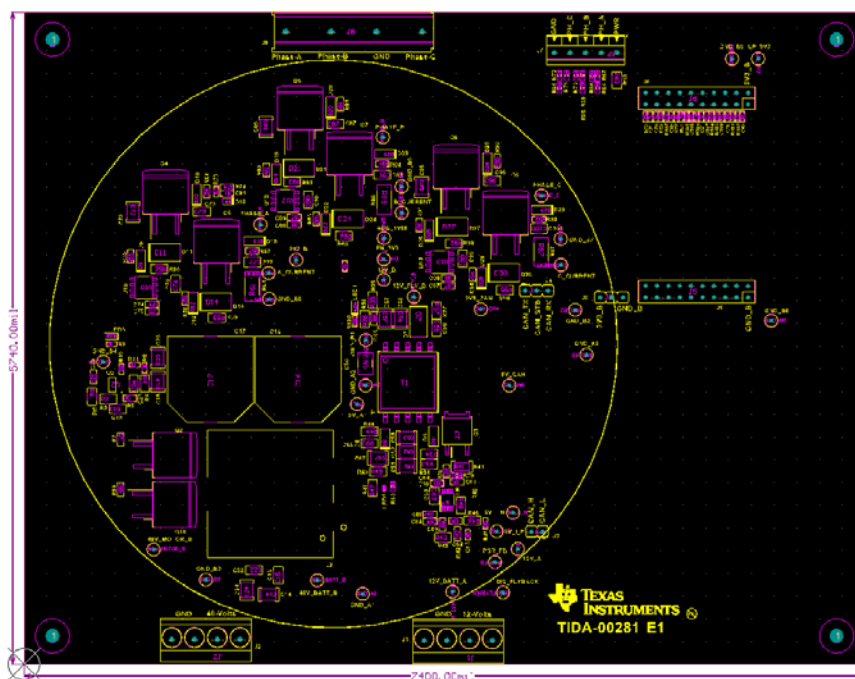


Figure 23: Mechanical Dimensions

8.5 Altium Project & Gerber files

To download the Altium project & Gerber files for each board, see the design files at:

<http://www.ti.com/tool/tida-00281>

9 Software Files

To download the Code Composer Studio Integrated Development Environment:

<http://www.ti.com/tool/CCSTUDIO>

To download the MotorWare Software package:

<http://www.ti.com/tool/MOTORWARE>

To download the TIDA-00281 hardware-specific files:

<http://www.ti.com/tool/tida-00281>

10 References

1. UCC27201A-Q1 datasheet <http://www.ti.com/product/ucc27201a-q1>
2. TPS40210-Q1 datasheet <http://www.ti.com/product/tps40210-q1>
3. TPS62152-Q1 datasheet <http://www.ti.com/product/tps62152-q1>
4. LM5060-Q1 datasheet <http://www.ti.com/product/lm5060-q1>
5. LM76410-Q1 datasheet <http://www.ti.com/product/lm76410-q1>
6. HVDA553-Q1 datasheet <http://www.ti.com/product/hvda553-q1>
7. OPA365-Q1 datasheet <http://www.ti.com/product/opa365-q1>
8. OPA2365-Q1 datasheet <http://www.ti.com/product/opa2365-q1>
9. LMT86-Q1 datasheet <http://www.ti.com/product/lmt86-q1>
10. ISO7331 datasheet <http://www.ti.com/product/iso7331>
11. TMS320F28026F, TMS320F28027F InstaSPIN-FOC Software Technical Reference Manual
<http://www.ti.com/lit/ug/spruhp4/spruhp4.pdf>
12. ISO 11898-2:2003 Road vehicles – Controller area network (CAN) – Part 2: High-speed medium access unit
13. ISO 7637-2:2004 Road vehicles – Electrical disturbances from conduction and coupling – Part 2: Electrical transient conduction along supply lines only, section 5.6

11 Terminology

ADC	analog-to-digital converter
BOM	bill of materials
Buck	step-down switching-mode voltage converter
CAN	Controller Area Network
CCS	Code Composer Studio
EMC	electromagnetic compatibility
EMF	electromotive force
FET	field effect transistor
FOC	field oriented control
GND	ground
MOSFET	metal oxide semiconductor field effect transistor
OEM	original equipment manufacturer
PCB	printed circuit board
RC	resistor capacitor
RCD	resistor capacitor diode
SPICE	Simulation Program with Integrated Circuit Emphasis
TIDA	Texas Instruments Design

12 About the Authors

Trenton Reed is an Applications Engineer at Texas Instruments. As a member of the Automotive Systems Engineering team, Trent focuses on powertrain end-equipments, creating reference designs for top automotive OEM and Tier 1 manufacturers. He brings to this role experience in power electronics and motor drive systems design. Trenton earned his Bachelor of Science in Electrical Engineering from the University of Central Florida in Orlando, FL.

Clark Kinnaird is a Systems Applications Engineer at Texas Instruments. As a member of the Automotive Systems Engineering team, Clark works on various types of motor drive end-equipment, creating reference designs for automotive manufacturers. Clark earned his Bachelor of Science and Master of Science in Engineering from the University of Florida, and his Ph.D. in Electrical Engineering from Southern Methodist University.

13 Appendix

13.1 TINA Simulation Models

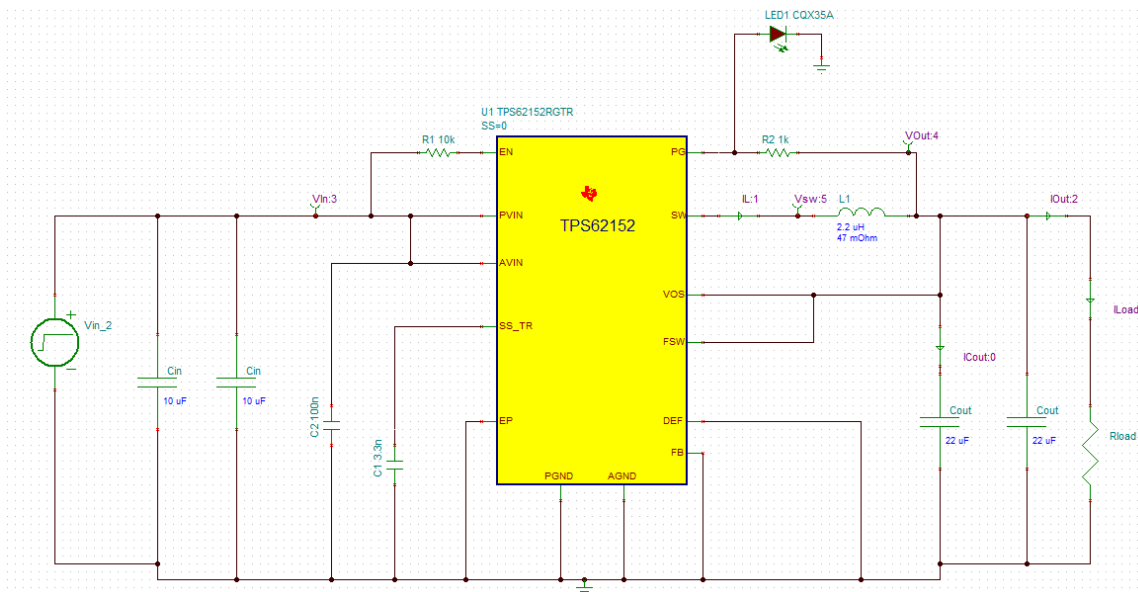


Figure 145 TINA simulation schematic for TPS62152 buck converter circuit

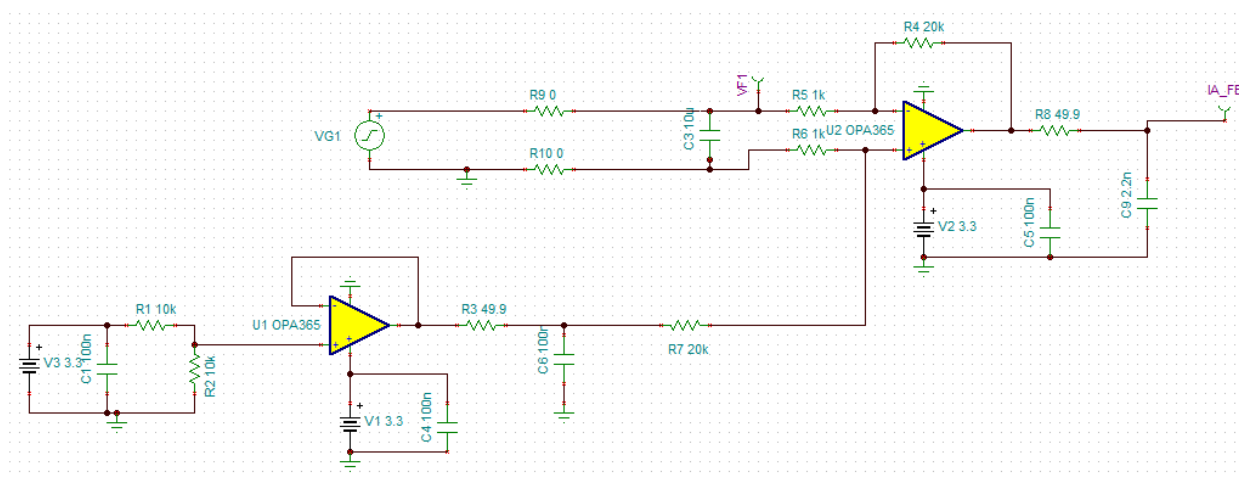


Figure 146 TINA simulation schematic for motor current feedback circuit

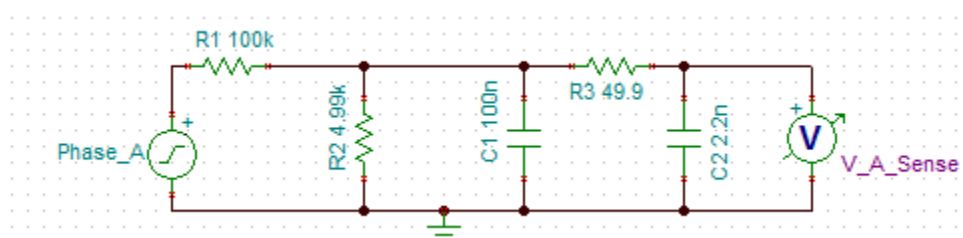


Figure 147 TINA simulation schematic for motor voltage feedback circuit

Motor Specifications

Parameter	Units	BLY344S-48V-3200 ¹	RP34-313V24-100	Specialty
Vendor		Anaheim Automation	ElectroCraft	Custom
Rated Voltage	V	48	24	60
Rated Speed	RPM	3200	2400	4000
Rated Power	W	660	545	
Back EMF Constant	V/kRPM	9.07	10.2	14.8
Electrical Poles		8	4	8
Phase Resistance	Ohms	0.07	0.2	0.410
Phase Inductance	mH	0.1	1	0.812 (D) 1.25 (Q)
Stall torque	N-m		221	
Peak torque	N-m		773	
Electrical time constant	msec		6	
Rotor inertia	in-oz-sec ²	0.03399	0.0385	
Motor efficiency	%	84		
Weight	kg	4.0	4.1	

¹ The Hall Effect sensors were swapped with the automotive-qualified DRV5013ADELPGMQ1.



Figure 148 Specialty motor

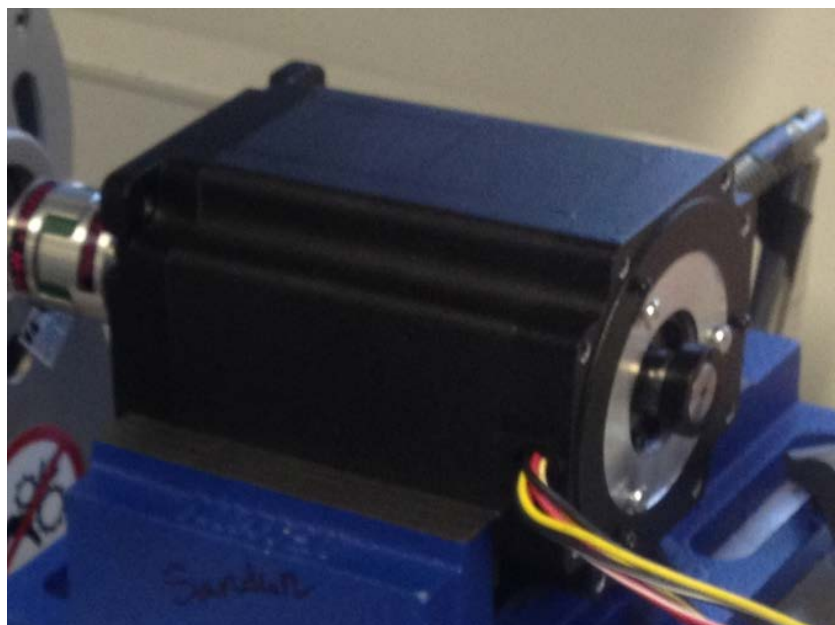


Figure 149 BLY344 motor

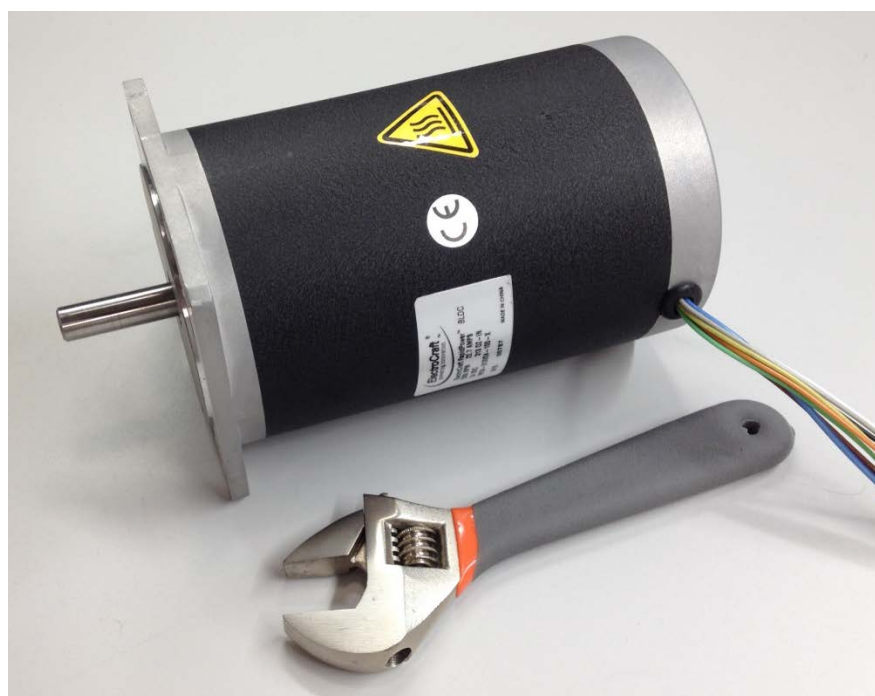


Figure 150 RP34-313V24-100 Motor

IMPORTANT NOTICE FOR TI REFERENCE DESIGNS

Texas Instruments Incorporated ("TI") reference designs are solely intended to assist designers ("Buyers") who are developing systems that incorporate TI semiconductor products (also referred to herein as "components"). Buyer understands and agrees that Buyer remains responsible for using its independent analysis, evaluation and judgment in designing Buyer's systems and products.

TI reference designs have been created using standard laboratory conditions and engineering practices. **TI has not conducted any testing other than that specifically described in the published documentation for a particular reference design.** TI may make corrections, enhancements, improvements and other changes to its reference designs.

Buyers are authorized to use TI reference designs with the TI component(s) identified in each particular reference design and to modify the reference design in the development of their end products. HOWEVER, NO OTHER LICENSE, EXPRESS OR IMPLIED, BY ESTOPPEL OR OTHERWISE TO ANY OTHER TI INTELLECTUAL PROPERTY RIGHT, AND NO LICENSE TO ANY THIRD PARTY TECHNOLOGY OR INTELLECTUAL PROPERTY RIGHT, IS GRANTED HEREIN, including but not limited to any patent right, copyright, mask work right, or other intellectual property right relating to any combination, machine, or process in which TI components or services are used. Information published by TI regarding third-party products or services does not constitute a license to use such products or services, or a warranty or endorsement thereof. Use of such information may require a license from a third party under the patents or other intellectual property of the third party, or a license from TI under the patents or other intellectual property of TI.

TI REFERENCE DESIGNS ARE PROVIDED "AS IS". TI MAKES NO WARRANTIES OR REPRESENTATIONS WITH REGARD TO THE REFERENCE DESIGNS OR USE OF THE REFERENCE DESIGNS, EXPRESS, IMPLIED OR STATUTORY, INCLUDING ACCURACY OR COMPLETENESS. TI DISCLAIMS ANY WARRANTY OF TITLE AND ANY IMPLIED WARRANTIES OF MERCHANTABILITY, FITNESS FOR A PARTICULAR PURPOSE, QUIET ENJOYMENT, QUIET POSSESSION, AND NON-INFRINGEMENT OF ANY THIRD PARTY INTELLECTUAL PROPERTY RIGHTS WITH REGARD TO TI REFERENCE DESIGNS OR USE THEREOF. TI SHALL NOT BE LIABLE FOR AND SHALL NOT DEFEND OR INDEMNIFY BUYERS AGAINST ANY THIRD PARTY INFRINGEMENT CLAIM THAT RELATES TO OR IS BASED ON A COMBINATION OF COMPONENTS PROVIDED IN A TI REFERENCE DESIGN. IN NO EVENT SHALL TI BE LIABLE FOR ANY ACTUAL, SPECIAL, INCIDENTAL, CONSEQUENTIAL OR INDIRECT DAMAGES, HOWEVER CAUSED, ON ANY THEORY OF LIABILITY AND WHETHER OR NOT TI HAS BEEN ADVISED OF THE POSSIBILITY OF SUCH DAMAGES, ARISING IN ANY WAY OUT OF TI REFERENCE DESIGNS OR BUYER'S USE OF TI REFERENCE DESIGNS.

TI reserves the right to make corrections, enhancements, improvements and other changes to its semiconductor products and services per JESD46, latest issue, and to discontinue any product or service per JESD48, latest issue. Buyers should obtain the latest relevant information before placing orders and should verify that such information is current and complete. All semiconductor products are sold subject to TI's terms and conditions of sale supplied at the time of order acknowledgment.

TI warrants performance of its components to the specifications applicable at the time of sale, in accordance with the warranty in TI's terms and conditions of sale of semiconductor products. Testing and other quality control techniques for TI components are used to the extent TI deems necessary to support this warranty. Except where mandated by applicable law, testing of all parameters of each component is not necessarily performed.

TI assumes no liability for applications assistance or the design of Buyers' products. Buyers are responsible for their products and applications using TI components. To minimize the risks associated with Buyers' products and applications, Buyers should provide adequate design and operating safeguards.

Reproduction of significant portions of TI information in TI data books, data sheets or reference designs is permissible only if reproduction is without alteration and is accompanied by all associated warranties, conditions, limitations, and notices. TI is not responsible or liable for such altered documentation. Information of third parties may be subject to additional restrictions.

Buyer acknowledges and agrees that it is solely responsible for compliance with all legal, regulatory and safety-related requirements concerning its products, and any use of TI components in its applications, notwithstanding any applications-related information or support that may be provided by TI. Buyer represents and agrees that it has all the necessary expertise to create and implement safeguards that anticipate dangerous failures, monitor failures and their consequences, lessen the likelihood of dangerous failures and take appropriate remedial actions. Buyer will fully indemnify TI and its representatives against any damages arising out of the use of any TI components in Buyer's safety-critical applications.

In some cases, TI components may be promoted specifically to facilitate safety-related applications. With such components, TI's goal is to help enable customers to design and create their own end-product solutions that meet applicable functional safety standards and requirements. Nonetheless, such components are subject to these terms.

No TI components are authorized for use in FDA Class III (or similar life-critical medical equipment) unless authorized officers of the parties have executed an agreement specifically governing such use.

Only those TI components that TI has specifically designated as military grade or "enhanced plastic" are designed and intended for use in military/aerospace applications or environments. Buyer acknowledges and agrees that any military or aerospace use of TI components that have **not** been so designated is solely at Buyer's risk, and Buyer is solely responsible for compliance with all legal and regulatory requirements in connection with such use.

TI has specifically designated certain components as meeting ISO/TS16949 requirements, mainly for automotive use. In any case of use of non-designated products, TI will not be responsible for any failure to meet ISO/TS16949.